

CERN-PH-EP-2014-121

Submitted to: JHEP

arXiv:1407.0350v2 [hep-ex] 22 Oct 2014

Search for the direct production of charginos, neutralinos and staus in final states with at least two hadronically decaying taus and missing transverse momentum in pp collisions at $\sqrt{s} = 8$ TeV with the ATLAS detector

The ATLAS Collaboration

Abstract

Results of a search for the electroweak associated production of charginos and next-to-lightest neutralinos, pairs of charginos or pairs of tau sleptons are presented. These processes are characterised by final states with at least two hadronically decaying tau leptons, missing transverse momentum and low jet activity. The analysis is based on an integrated luminosity of 20.3 fb^{-1} of proton–proton collisions at $\sqrt{s} = 8$ TeV recorded with the ATLAS experiment at the Large Hadron Collider. No significant excess is observed with respect to the predictions from Standard Model processes. Limits are set at 95% confidence level on the masses of the lighter chargino and next-to-lightest neutralino for various hypotheses for the lightest neutralino mass in simplified models. In the scenario of direct production of chargino pairs, with each chargino decaying into the lightest neutralino via an intermediate tau slepton, chargino masses up to 345 GeV are excluded for a massless lightest neutralino. For associated production of mass-degenerate charginos and next-to-lightest neutralinos, both decaying into the lightest neutralino via an intermediate tau slepton, masses up to 410 GeV are excluded for a massless lightest neutralino.

Search for the direct production of charginos, neutralinos and staus in final states with at least two hadronically decaying taus and missing transverse momentum in pp collisions at $\sqrt{s} = 8$ TeV with the ATLAS detector

The ATLAS Collaboration

ABSTRACT: Results of a search for the electroweak associated production of charginos and next-to-lightest neutralinos, pairs of charginos or pairs of tau sleptons are presented. These processes are characterised by final states with at least two hadronically decaying tau leptons, missing transverse momentum and low jet activity. The analysis is based on an integrated luminosity of 20.3 fb^{-1} of proton–proton collisions at $\sqrt{s} = 8$ TeV recorded with the ATLAS experiment at the Large Hadron Collider. No significant excess is observed with respect to the predictions from Standard Model processes. Limits are set at 95% confidence level on the masses of the lighter chargino and next-to-lightest neutralino for various hypotheses for the lightest neutralino mass in simplified models. In the scenario of direct production of chargino pairs, with each chargino decaying into the lightest neutralino via an intermediate tau slepton, chargino masses up to 345 GeV are excluded for a massless lightest neutralino. For associated production of mass-degenerate charginos and next-to-lightest neutralinos, both decaying into the lightest neutralino via an intermediate tau slepton, masses up to 410 GeV are excluded for a massless lightest neutralino.

Contents

1	Introduction	1
2	SUSY scenarios	2
3	The ATLAS detector	4
4	Data sample	4
5	Monte Carlo simulation	4
5.1	Standard Model processes	5
5.2	SUSY processes	5
6	Event reconstruction	7
7	Event selection	9
8	Standard Model background estimation	11
8.1	Multi-jet background estimation	12
8.2	W +jets background estimation	13
8.3	Estimation of irreducible backgrounds	15
8.4	Fitting procedure	19
9	Systematic uncertainties	20
10	Results	23
11	Interpretation	25
11.1	Simplified models: chargino–neutralino and chargino–chargino production	26
11.2	Direct stau production	26
11.3	The pMSSM model	27
12	Conclusion	29
13	Acknowledgements	29

1 Introduction

Supersymmetry (SUSY) [1–9] is a promising extension of the Standard Model (SM) of particle physics. For each SM particle supersymmetry predicts the existence of a super-partner (also referred to as a ‘sparticle’), whose spin differs by one half unit from the corresponding

SM partner. Supersymmetric theories provide elegant solutions to unanswered questions of the SM, such as the hierarchy problem [10–13]. In R -parity-conserving SUSY models [14–18], SUSY particles are always produced in pairs and the lightest supersymmetric particle (LSP) provides a dark matter candidate [19–21].

In SUSY models, the mass eigenstates formed from the linear superpositions of the SUSY partners of the charged and neutral Higgs bosons and electroweak gauge bosons, the charginos ($\tilde{\chi}_i^\pm$, $i = 1, 2$) and neutralinos ($\tilde{\chi}_j^0$, $j = 1, 2, 3, 4$ in the order of increasing masses), as well as the sleptons (superpartners of the leptons,¹ $\tilde{\ell}$ and $\tilde{\nu}$) can be sufficiently light to be produced at the Large Hadron Collider (LHC) [22]. Naturalness arguments suggest that the lightest third-generation sparticles, charginos and neutralinos should have masses of a few hundred GeV to protect the Higgs boson mass from quadratically divergent quantum corrections [23, 24]. Furthermore, light sleptons could play a role in the co-annihilation of neutralinos, leading to a dark matter relic density consistent with cosmological observations [25, 26], and their mass is expected to be in the $\mathcal{O}(100 \text{ GeV})$ range in gauge-mediated [27–32] and anomaly-mediated [33, 34] SUSY breaking scenarios. Models with light tau sleptons (the staus, labelled as $\tilde{\tau}$ in the following) are consistent with current dark matter searches [35].

This paper presents a search for electroweak production of charginos, next-to-lightest neutralinos and staus in events with at least two hadronically decaying tau leptons, missing transverse momentum and low jet activity, using the 2012 dataset of $\sqrt{s} = 8 \text{ TeV}$ proton–proton collisions collected with the ATLAS detector. Previous searches from the ATLAS collaboration cover electroweak production of supersymmetric particles in final states with electrons and muons [36] using signal models where the neutralinos and charginos decay with equal probability to all lepton flavours, and final states with exactly three leptons of any flavour (electrons, muons, and hadronically decaying taus) [37] using models similar to those described in this paper. A search for associated production of charginos and next-to-lightest neutralinos in stau dominated scenarios has recently been published by the CMS collaboration [38]. The combined LEP limits on the stau and chargino masses are $m_{\tilde{\tau}} > 87\text{--}93 \text{ GeV}$ (depending on the $\tilde{\chi}_1^0$ mass) and $m_{\tilde{\chi}_1^\pm} > 103.5 \text{ GeV}$ [39–42]. It should be noted that the stau mass limit from LEP assumes gaugino mass unification, which is not assumed in the results presented here.

2 SUSY scenarios

SUSY scenarios characterised by the presence of light charginos, next-to-lightest neutralinos and sleptons can be realised in the general framework of the phenomenological Minimal Supersymmetric Standard Model (pMSSM) [43–45]. The dominant processes are the electroweak production of $\tilde{\chi}_1^\pm \tilde{\chi}_2^0$ and $\tilde{\chi}_1^\pm \tilde{\chi}_1^\mp$, such as $q\bar{q} \rightarrow (Z/\gamma)^* \rightarrow \tilde{\chi}_1^+ \tilde{\chi}_1^-$ and $q\bar{q}' \rightarrow W^{\pm*} \rightarrow \tilde{\chi}_1^\pm \tilde{\chi}_2^0$. The chargino and neutralino decay properties depend on the Minimal Supersymmetric Standard Model (MSSM) parameters M_1 and M_2 (the gaugino masses), $\tan\beta$ (the ratio of the vacuum expectation values of the two Higgs doublets), and μ (the

¹ The sleptons are referred to as left- or right-handed ($\tilde{\ell}_L$ or $\tilde{\ell}_R$), depending on the helicity of their SM partners. The slepton mass eigenstates are a mixture of $\tilde{\ell}_L$ and $\tilde{\ell}_R$ and labelled as $\tilde{\ell}_1$ and $\tilde{\ell}_2$.

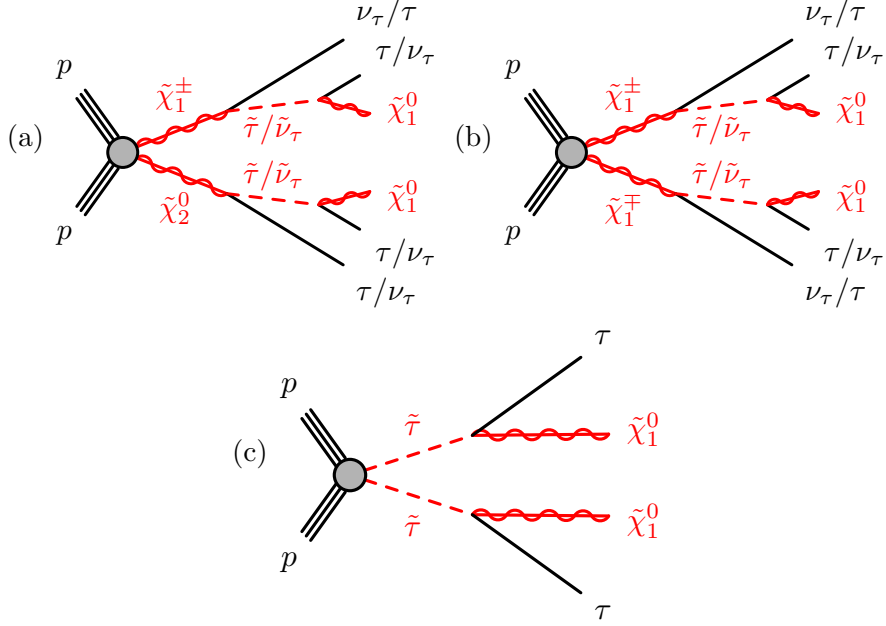


Figure 1. Representative diagrams for the electroweak production processes of supersymmetric particles considered in this work: (a) $\tilde{\chi}_1^\pm \tilde{\chi}_2^0$, (b) $\tilde{\chi}_1^\pm \tilde{\chi}_1^\mp$, and (c) $\tilde{\tau} \tilde{\tau}$ production.

higgsino-mixing mass term). In this paper we study two pMSSM model implementations with large $\tan\beta$ and where the only light slepton is the stau partner of the right-handed tau ($\tilde{\tau}_R$). More details of the considered models are given in section 5.2.

“Simplified models” [46, 47] characterised by $\tilde{\chi}_1^\pm \tilde{\chi}_2^0$ and $\tilde{\chi}_1^\pm \tilde{\chi}_1^\mp$ production, where the charginos and neutralinos decay with 100% branching fraction to final states with taus, are also considered. In both simplified models the lightest neutralino is the LSP, and the only light slepton is the stau partner of the left-handed tau ($\tilde{\tau}_L$). If the stau and the superpartner of the tau neutrino (the tau sneutrino, labelled as $\tilde{\nu}_\tau$) are lighter than the $\tilde{\chi}_1^\pm$ and $\tilde{\chi}_2^0$, the following decay processes can occur: $\tilde{\chi}_2^0 \rightarrow \tilde{\tau}_L \tau \rightarrow \tau \tau \tilde{\chi}_1^0$, and $\tilde{\chi}_1^\pm \rightarrow \tilde{\tau}_L \nu(\tilde{\nu}_\tau \tau) \rightarrow \tau \nu \tilde{\chi}_1^0$. Figures 1(a) and 1(b) show diagrams of associated $\tilde{\chi}_1^\pm \tilde{\chi}_2^0$ and $\tilde{\chi}_1^\pm \tilde{\chi}_1^\mp$ production.

If charginos and next-to-lightest neutralinos are too heavy to be produced at the LHC, direct production of stau pairs [48] might become the dominant electroweak production process in the pMSSM. The production of stau pairs is studied in this paper, and the relevant process is depicted in figure 1(c).

The studied final state contains at least two taus with opposite electric charge (opposite-sign, OS), low jet activity and large missing transverse momentum due to the escaping neutrinos and LSPs. Only final states containing hadronically decaying taus are considered in this search.

3 The ATLAS detector

The ATLAS detector [49] is a multi-purpose particle physics detector with forward-backward symmetric cylindrical geometry, and nearly 4π coverage in solid angle.² It features an inner tracking detector (ID) surrounded by a 2 T superconducting solenoid, electromagnetic and hadronic calorimeters, and a muon spectrometer (MS). The ID covers the pseudorapidity region $|\eta| < 2.5$ and consists of a silicon pixel detector, a silicon microstrip detector (SCT), and a transition radiation tracker (TRT). The calorimeters are composed of high-granularity liquid-argon (LAr) electromagnetic calorimeters with lead, copper, or tungsten absorbers (in the pseudorapidity region $|\eta| < 3.2$) and an iron-scintillator hadronic calorimeter (over $|\eta| < 1.7$). The end-cap and forward regions, spanning $1.5 < |\eta| < 4.9$, are instrumented with LAr calorimeters for both the electromagnetic and hadronic measurements. The MS surrounds the calorimeters and consists of three large superconducting air-core toroid magnets, each with eight coils, a system of precision tracking chambers ($|\eta| < 2.7$), and detectors for triggering ($|\eta| < 2.4$). Events are selected by a three-level trigger system.

4 Data sample

The analysed dataset, after the application of beam, detector and data quality requirements, corresponds to an integrated luminosity of $20.3 \pm 0.6 \text{ fb}^{-1}$. The luminosity is measured using techniques similar to those described in ref. [50] with a preliminary calibration of the luminosity scale derived from beam-overlap scans performed in November 2012. The average number of inelastic interactions per bunch crossing (pile-up) varied from 5.9 to 36.5.

The events used in this analysis are recorded using a di-tau trigger, which requires identification of two hadronically decaying tau candidates with transverse momenta (p_{T}) exceeding a set of thresholds, similar to those described in ref. [51]. Trigger efficiency measurements using a sample of $Z \rightarrow \tau\tau$ events where one tau decays hadronically and the other leptonically into a muon and two neutrinos, show that the di-tau trigger reaches constant efficiency ($\sim 65\%$) when the leading tau has $p_{\text{T}} > 40 \text{ GeV}$ and the next-to-leading tau has $p_{\text{T}} > 25 \text{ GeV}$.

5 Monte Carlo simulation

Monte Carlo (MC) simulated event samples are used to estimate the SUSY signal yields and to aid in evaluating the SM backgrounds. MC samples are processed through a detailed detector simulation [52] based on GEANT4 [53] and reconstructed using the same algorithms

²ATLAS uses a right-handed coordinate system with its origin at the nominal interaction point (IP) in the centre of the detector, and the z -axis along the beam line. The x -axis points from the IP to the centre of the LHC ring, and the y -axis points upwards. Cylindrical coordinates (r, ϕ) are used in the transverse plane, ϕ being the azimuthal angle around the z -axis. Observables labelled “transverse” refer to the projection into the x - y plane. The pseudorapidity is defined in terms of the polar angle θ by $\eta = -\ln \tan(\theta/2)$.

as the data. The effect of multiple proton–proton collisions in the same or nearby bunch crossings is also taken into account.

5.1 Standard Model processes

The main sources of SM background to final states with at least two hadronically decaying taus are multi-jet, W +jets and diboson events. They are estimated with methods using simulation samples and data as described in section 8. MC samples are used to estimate the SM background contributions from processes leading to at least one tau from prompt boson decays in the final state, such as diboson production (WW , WZ , ZZ), processes including a top quark pair or single top quark (in association with jets or W/Z bosons), and Z boson production in association with jets. Production of the SM Higgs boson with a mass of 125 GeV is also considered.

The diboson samples are generated with SHERPA v1.4.1 [54], with additional gluon–gluon contributions simulated with gg2WW v3.1.2 [55]. The production of top quark pairs is also simulated with the SHERPA v1.4.1 generator. Samples of $t\bar{t}+V$ ($V = W, Z$) are generated with the leading-order (LO) generator MadGraph 5 v1.3.33 [56] interfaced to PYTHIA v8.165 [57, 58]. Single-top production is simulated with MC@NLO v4.06 (Wt - and s -channel) [59–61] and AcerMC v3.8 (t -channel) [62]. In all samples the top quark mass is set to 172.5 GeV. Events with $Z/\gamma^* \rightarrow \ell\ell$ and $W \rightarrow \ell\nu$ produced with accompanying jets (including light and heavy flavours) are generated with ALPGEN v2.14 [63] interfaced to PYTHIA 6. The gluon fusion and vector-boson fusion production modes of the SM Higgs are simulated with POWHEG-BOX v1.0 [64], and the associated production (WH and ZH) with PYTHIA v8.165.

The simulation parameters are tuned to describe the soft component of the hadronic final state [65, 66]. The next-to-leading-order (NLO) CT10 [67] parton distribution function (PDF) set is used for SHERPA and MC@NLO. The CTEQ6L1 [68] set is used for MadGraph, AcerMC, PYTHIA, and ALPGEN.

All SM background production cross sections are normalised to the results of higher-order calculations when available. The inclusive W and Z production cross sections are calculated to next-to-next-to-leading order (NNLO) in the strong coupling constant with DYNLLO [69] using the MSTW2008NNLO PDF set [70]. The $t\bar{t}$ cross section is normalised to a NNLO calculation including resummation of next-to-next-to-leading logarithmic (NNLL) soft gluon terms obtained with Top++ v2.0 [71]. The diboson production cross section is normalised to NLO using MCFM v6.2 [72, 73]. The production of $t\bar{t}$ in association with W/Z is normalised to the NLO cross section [74, 75].

5.2 SUSY processes

Simulated signal samples are generated with Herwig++ v2.5.2 [76] and the CTEQ6L1 PDF set. Signal production cross sections are calculated to NLO using PROSPIN02 [77]. They are in agreement with the NLO calculations matched to resummation at the next-to-leading-logarithmic accuracy (NLO+NLL) within $\sim 2\%$ [78–80].

The results of this search are interpreted in the context of two pMSSM models with the following specifications. The masses of squarks, gluinos and sleptons other than the

stau partner of the right-handed taus are set to 3 TeV, and $\tan\beta$ is set to 50. In the first (second) pMSSM model, M_1 is set to 50 (75) GeV and M_2 and μ are varied between 100 and 500 (600) GeV. The mass of the lighter stau, $\tilde{\tau}_1 = \tilde{\tau}_R$, is set to 95 GeV in the first pMSSM model, whereas in the second pMSSM model it is set halfway between those of the $\tilde{\chi}_2^0$ and the $\tilde{\chi}_1^0$. In the first pMSSM scenario (with fixed stau mass), the dominant processes are the associated production of charginos and neutralinos ($\tilde{\chi}_1^\pm \tilde{\chi}_2^0$), or pair production of charginos ($\tilde{\chi}_1^\pm \tilde{\chi}_1^\mp$) or staus ($\tilde{\tau}\tilde{\tau}$), depending on the values of M_2 and μ . The cross section of direct stau production is 163 fb over the whole set of models, while the production cross sections of chargino–neutralino and chargino–chargino vary from $5 \cdot 10^{-3}$ to 40 pb and from 0.01 to 16 pb, respectively. In the second pMSSM scenario (with variable stau mass), the dominant processes are $\tilde{\chi}_1^\pm \tilde{\chi}_2^0$ and $\tilde{\chi}_1^\pm \tilde{\chi}_1^\mp$ production. The cross section of direct stau production varies from 0.4 to 42 fb, while the production cross sections of chargino–neutralino and chargino–chargino vary from $5 \cdot 10^{-4}$ to 1.2 pb and $8 \cdot 10^{-4}$ to 0.9 pb, respectively.

Two simplified models characterised by $\tilde{\chi}_1^\pm \tilde{\chi}_2^0$ and $\tilde{\chi}_1^\pm \tilde{\chi}_1^\mp$ production are also considered. In these models, all sparticles other than $\tilde{\chi}_1^\pm$, $\tilde{\chi}_2^0$, $\tilde{\chi}_1^0$, $\tilde{\tau}_L$ and $\tilde{\nu}_\tau$ are assumed to be heavy (masses of order of 2 TeV). The neutralinos and charginos decay via intermediate staus and tau sneutrinos. The stau and tau sneutrino are assumed to be mass-degenerate, which happens to be often the case in pMSSM scenarios with large mass splitting between $\tilde{\chi}_1^\pm$ and $\tilde{\chi}_1^0$. The mass of the $\tilde{\tau}_L$ state is set to be halfway between those of the $\tilde{\chi}_1^\pm$ and the $\tilde{\chi}_1^0$. Furthermore, $\tilde{\chi}_1^\pm$ and $\tilde{\chi}_2^0$ are assumed to be pure wino and mass-degenerate, while the $\tilde{\chi}_1^0$ is purely bino. The $\tilde{\chi}_1^\pm$ ($\tilde{\chi}_2^0$) mass is varied between 100 and 500 GeV, and the $\tilde{\chi}_1^0$ mass is varied between zero and 350 GeV. The cross section for electroweak production of supersymmetric particles ranges from 0.01 to 2 pb in the considered models.

Direct stau production is studied in the context of the pMSSM model described in ref. [81]. The masses of all charginos and neutralinos apart from the $\tilde{\chi}_1^0$ are set to 2.5 TeV. The model contains $\tilde{\tau}_R$ and $\tilde{\tau}_L$, but no tau sneutrinos. The stau mixing is set such that $\tilde{\tau}_1 = \tilde{\tau}_R$ and $\tilde{\tau}_2 = \tilde{\tau}_L$. The stau masses are generated in the range from 90 to 300 GeV and the mass of the bino-like $\tilde{\chi}_1^0$ is varied by scanning the gaugino mass parameter M_1 in the range from zero to 200 GeV. The cross section for direct stau pair production in this scenario decreases from 176 to 1.4 fb for $\tilde{\tau}_L$, and from 70 to 0.6 fb for $\tilde{\tau}_R$ as the stau mass increases from 90 to 300 GeV.

Three reference points are used throughout this paper to illustrate the typical features of the SUSY models to which this analysis is sensitive:

- Ref. point 1: simplified model for chargino–neutralino production with mass of $\tilde{\chi}_1^\pm$ ($\tilde{\chi}_2^0$) equal to 250 GeV, and mass of $\tilde{\chi}_1^0$ equal to 100 GeV;
- Ref. point 2: simplified model for chargino–chargino production with mass of $\tilde{\chi}_1^\pm$ equal to 250 GeV, and mass of $\tilde{\chi}_1^0$ equal to 50 GeV;
- Ref. point 3: direct stau production with mass of the $\tilde{\tau}_R$ ($\tilde{\tau}_L$) equal to 127 (129) GeV, and massless $\tilde{\chi}_1^0$.

6 Event reconstruction

Events with at least one reconstructed primary vertex are selected. A primary vertex must have at least five associated charged-particle tracks with $p_T > 400$ MeV and be consistent with the beam spot envelope. If there are multiple primary vertices in an event, the one with the largest $\sum p_T^2$ of the associated tracks is chosen.

Jets are reconstructed from three-dimensional calorimeter energy clusters using the anti- k_t algorithm [82, 83] with a radius parameter of 0.4. Jet energies are corrected for detector inhomogeneities, the non-compensating nature of the calorimeter, and the impact of pile-up, using factors derived from test beam, cosmic ray, and pp collision data, and from a detailed GEANT4 detector simulation [84]. The impact of pile-up is accounted for by using a technique, based on jet areas, that provides an event-by-event and jet-by-jet correction [85]. Events containing jets that are likely to have arisen from detector noise or cosmic rays are removed. For this analysis jets are required to have $p_T > 20$ GeV and $|\eta| < 4.5$.

Electron candidates are reconstructed by matching clusters in the electromagnetic calorimeter with charged particle tracks in the inner detector. Electrons are required to have $p_T > 10$ GeV, $|\eta| < 2.47$, and to satisfy the “medium” shower-shape and track-selection criteria defined in ref. [86], updated for the 2012 operating conditions. Muon candidates are identified by matching an extrapolated inner detector track and one or more track segments in the muon spectrometer [87]. Muons are required to have $p_T > 10$ GeV and $|\eta| < 2.4$. Events with muons compatible with cosmic rays are rejected.

The reconstruction of hadronically decaying taus is based on the information from tracking in the ID and three-dimensional clusters in the electromagnetic and hadronic calorimeters. The tau reconstruction algorithm is seeded by jets reconstructed as described above but with $p_T > 10$ GeV and $|\eta| < 2.47$. Tracks are subsequently associated with the tau jet within a cone of size $\Delta R = \sqrt{(\Delta\eta)^2 + (\Delta\phi)^2} = 0.2$ around the axis of the tau cluster. The reconstructed energies of the hadronically decaying tau candidates are corrected to the tau energy scale, which is calibrated independently of the jet energy scale, by a MC-based procedure [88]. Tau neutrinos from the tau lepton decay are not taken into account in the reconstruction and calibration of the tau energy and momentum. Since taus decay mostly to either one or three charged pions, together with a neutrino and often additional neutral pions, tau candidates are required to have one or three associated charged particle tracks (prongs) and the total electric charge of those tracks must be ± 1 times the electron charge. To improve the discrimination between hadronically decaying taus and jets, electrons, or muons, multivariate algorithms are used [89]. The tau identification algorithm used in this analysis is based on the Boosted Decision Tree (BDT) method. The BDT algorithms use as input various track and cluster variables for particle discrimination. A “jet BDT” is used to discriminate taus from jets, and an “electron BDT” to discriminate between electrons and taus. Based on the jet BDT result, three tau identification criteria corresponding to “loose”, “medium”, and “tight” quality can be defined. For 1-prong (3-prong) taus the signal efficiencies are 70%, 60% and 40% (65%, 55% and 35%) for the loose, medium and tight working points, respectively. Background rejection factors ranging from 10 to 40 for signal efficiencies of 70% are achieved, increasing to 500 for 35% signal efficiency.

In the following, tau candidates are required to pass the “medium” identification criteria for jet discrimination, while for the final signal region selections both the “tight” and “medium” criteria are used. For electron discrimination, the “loose” quality selection is applied to 1-prong taus only. This requirement has about 95% efficiency, and a rejection factor from 10 to 50 depending on the η range. In addition, a dedicated muon veto is applied to remove tau candidates generated by muons associated with anomalous energy deposits in the calorimeter. The resulting signal efficiency is better than 96%, with a reduction of muons misidentified as taus of around 40%. Tau candidates are required to have $p_T > 20$ GeV and $|\eta| < 2.47$.

The measurement of the missing transverse momentum two-vector, $\mathbf{p}_T^{\text{miss}}$, and its magnitude, E_T^{miss} , is based on the vectorial sum of the \mathbf{p}_T of reconstructed objects (jets, taus, electrons, photons, muons) as well as calorimeter energy clusters (with $|\eta| < 4.9$) not associated with reconstructed objects [90]. Since different requirements on the tau identification (loose, medium, and tight jet BDT quality requirements) are used throughout this analysis, taus are calibrated at the jet energy scale for the calculation of $\mathbf{p}_T^{\text{miss}}$.

The possible double counting of reconstructed objects is resolved in the following order. If two electron candidates are found within a distance $\Delta R = 0.05$, the electron candidate with lower momentum is discarded. Jet candidates are removed if they lie within a distance $\Delta R = 0.2$ of a tau or an electron. Any tau candidate lying within a distance $\Delta R = 0.2$ of any remaining electron or muon is discarded. Any muon candidate within $\Delta R = 0.4$ of a jet is removed. The remaining electrons are rejected if they lie within $0.2 < \Delta R < 0.4$ of a jet. Electron and muon candidates within a distance $\Delta R = 0.1$, or muon candidates within a distance $\Delta R = 0.05$, are rejected. To remove low-mass resonances, electron or muon pairs with opposite electrical charge are rejected if their invariant mass is less than 12 GeV.

Jets are further classified as jets containing a b -quark (b -jets), light-parton jets, and forward jets. A b -tagging algorithm [91], which exploits the long lifetime of b -hadrons, is used to identify jets containing a b -quark. The mean nominal b -tagging efficiency, determined from $t\bar{t}$ MC events, is 80%, with a misidentification (mis-tag) rate for light-quark/gluon jets of less than 1%. Correction factors are applied as functions of the p_T and η of the jets to all MC samples to correct for small differences in the b -tagging performance observed between data and simulation. Jets in the central region, satisfying $p_T > 20$ GeV, $|\eta| < 2.4$, and the b -tagging algorithm, are defined as b -jets, or B20. Central light jets are required to have $|\eta| < 2.4$, and not be identified as b -jets. To remove jets that originated from pile-up collisions, a central light jet with $p_T < 50$ GeV must have at least one track with $p_T > 400$ MeV associated with it and with the primary vertex of the event. Depending on their transverse momentum, central light jets are referred to as L30 (L50) if they have $p_T > 30$ (50) GeV. Forward jets, or F30, must satisfy $p_T > 30$ GeV and $2.4 < |\eta| < 4.5$.

For the background estimation and validation described in section 8, events containing isolated electrons or muons are selected. Isolated electrons and muons are defined as follows. The summed scalar p_T of tracks above 400 MeV within a cone of size $\Delta R = 0.3$ around each electron or muon candidate (excluding the candidate itself) and associated with the primary vertex is required to be less than 16% of the electron or muon p_T . The

distance of closest approach in the transverse plane of an electron or muon candidate to the event primary vertex must be within five (for electron candidates) or three (for muon candidates) standard deviations from its measurement in the transverse plane. For isolated electrons, the sum of transverse energies of the surrounding calorimeter energy clusters within $\Delta R = 0.3$ of each electron candidate, corrected for the deposition of energy from pile-up interactions, is required to be less than 18% of the electron p_T . The longitudinal impact parameter of an electron, z_0 , must satisfy $|z_0 \sin \theta| < 0.4$ mm. Muon candidates are required to satisfy $|z_0 \sin \theta| < 0.1$ mm. Furthermore, isolated electrons must satisfy the “tight” criteria [86, 92] placed on the ratio of calorimetric energy to track momentum, and the number of high-threshold hits in the TRT.

The simulation is corrected for differences in the efficiency of the tau identification and trigger algorithms between data and MC simulation. For hadronically decaying taus coming from prompt boson decays, the corrections are calculated with a “tag-and-probe” method in a sample of $Z \rightarrow \tau\tau$ events where one tau decays hadronically and the other leptonically into a muon and two neutrinos [89]. For misidentified taus from electrons a sample of $Z \rightarrow ee$ events is used, while the mis-identification rate of taus from light jets is measured in a sample of $Z \rightarrow \mu\mu$ events with associated jets. The efficiencies for electrons and muons to satisfy the reconstruction, identification and isolation criteria are measured in samples of Z and J/ψ leptonic decays, and corrections are applied to the simulated samples to reproduce the efficiencies in data.

7 Event selection

Events are required to have at least two candidate taus, and at least one must satisfy the tight jet BDT quality requirement. At least one of the selected tau pairs must contain taus with opposite electrical charge. Two of the reconstructed taus must have fired the di-tau trigger, and satisfy the p_T requirements to be in the region where the trigger efficiency is constant, i.e. the more (less) energetic tau must have $p_T > 40$ (25) GeV. The di-tau invariant mass of any opposite-sign (OS) pair must be larger than 12 GeV to remove taus from low-mass resonances. This requirement has negligible effect on the signal efficiency. Events with additional light leptons (defined as candidate electrons or muons after resolving the overlap between the various reconstructed objects as described in section 6) are vetoed to allow for a statistical combination with other ATLAS analyses [36, 37].

To enhance the sensitivity to the SUSY signal and suppress SM backgrounds, additional requirements are applied that define the so-called signal regions (SR). At tree level, no jet is present in the SUSY processes of interest; however, jets can be generated from initial-state radiation (ISR). Vetoing events containing jets suppresses background contributions involving top quarks but may also reduce the signal efficiency due to ISR. To maximise the signal-to-background ratio, three event-based jet vetoes are used depending on the SR: a “ b -jet veto”, where only events with no b -jets, i.e. $N(\text{B20}) = 0$, are accepted; a “jet veto”, where only events with $N(\text{B20}) + N(\text{L30}) + N(\text{F30}) = 0$ are selected; and a “looser jet-veto”, where $N(\text{B20}) + N(\text{L50}) + N(\text{F30}) = 0$ is required. The rejection factors of the

b -jet veto, jet veto, and looser jet-veto measured on MC samples of top quark backgrounds ($t\bar{t}$, single top and $t\bar{t}+V$) are about 6, 50, and 20, respectively.

To reject backgrounds with a Z boson, events where at least one of the oppositely charged tau pairs has a reconstructed invariant mass within 10 GeV of the visible Z boson mass (81 GeV) are vetoed. The visible Z boson mass is obtained from the mean value of a gaussian fit of the reconstructed invariant mass distribution of OS tau pairs in a MC sample of $Z(\rightarrow \tau\tau)$ +jets events. This requirement is referred to as the “ Z -veto”. The Z -veto reduces the contribution from background processes containing Z decays by a factor of three. An additional requirement on the angular separation between the leading and next-to-leading tau, $\Delta R(\tau, \tau) < 3$, is effective in discriminating against back-to-back events such as multi-jet production or Z decays.

To further improve the signal to background ratio, additional requirements on a selection of sensitive kinematic variables are applied depending on the SR. The “stransverse” mass m_{T2} [93, 94] is defined as:

$$m_{T2} = \min_{\mathbf{q}_T} [\max (m_T(\mathbf{p}_T^{\tau 1}, \mathbf{q}_T), m_T(\mathbf{p}_T^{\tau 2}, \mathbf{p}_T^{\text{miss}} - \mathbf{q}_T))],$$

where $\mathbf{p}_T^{\tau 1}$ and $\mathbf{p}_T^{\tau 2}$ are the transverse momenta of the two taus, and \mathbf{q}_T is a transverse vector that minimises the larger of the two transverse masses m_T . The latter is defined by

$$m_T(\mathbf{p}_T, \mathbf{q}_T) = \sqrt{2(p_T q_T - \mathbf{p}_T \cdot \mathbf{q}_T)}.$$

In events where more than two taus are selected, m_{T2} is computed among all possible tau pairs and the combination leading to the largest value is chosen. For $t\bar{t}$ and WW events, in which two on-shell W bosons decay leptonically and $\mathbf{p}_T^{\text{miss}}$ is the sum of the transverse momenta of the two neutrinos, the m_{T2} distribution has an upper end-point at the W mass. For large mass differences between the next-to-lightest neutralinos, the charginos, or the staus and the lightest neutralino, the m_{T2} distribution for signal events extends significantly beyond the distributions of the $t\bar{t}$ and WW events.

Two additional kinematic variables, sensitive to the additional missing transverse momentum due to the LSPs, are used to discriminate SUSY from SM events. These are the effective mass $m_{\text{eff}} = E_T^{\text{miss}} + p_T^{\tau 1} + p_T^{\tau 2}$, defined as the scalar sum of the missing transverse energy and the transverse momenta of the two leading taus, and $m_{T\tau 1} + m_{T\tau 2}$, where $m_{T\tau 1}$ ($m_{T\tau 2}$) is the transverse mass computed from the transverse momentum of the leading (next-to-leading) tau and $\mathbf{p}_T^{\text{miss}}$. The correlation among the above defined kinematical variables varies between 20% and 90% according to the signal model.

Four SRs are defined in this analysis, targeting various SUSY production processes.³ The requirements for each SR are summarised in table 1. At least two OS taus are required in all SRs except for SR-C1C1, where exactly two OS taus are required. The first two SRs, SR-C1N2 and SR-C1C1, target $\tilde{\chi}_1^\pm \tilde{\chi}_2^0$ and $\tilde{\chi}_1^\pm \tilde{\chi}_1^\mp$ production, respectively. SR-C1N2 is based on moderate E_T^{miss} and large m_{T2} requirements. In SR-C1C1, events with moderate

³In the SR definitions, the following mnemonic naming conventions are used: “C1” stands for $\tilde{\chi}_1^\pm$, “N2” for $\tilde{\chi}_2^0$, and “DS” for direct stau production.

m_{T2} and large $m_{T\tau 1} + m_{T\tau 2}$ are selected. The last two SRs, SR-DS-highMass and SR-DS-lowMass, are designed to cover direct stau production and are optimised for different ranges of the stau mass. The four SRs are not mutually exclusive.

The signal acceptance for events passing all analysis requirements is of order a few percent for SUSY models to which this analysis is sensitive in all SRs. The trigger efficiency varies between 55% and 70% according to the signal region and the SUSY model considered, while the total reconstruction efficiency is about 15%.

Table 1. Signal region definitions.

SR-C1N2	SR-C1C1	SR-DS-highMass	SR-DS-lowMass
≥ 2 OS taus	2 OS taus	≥ 2 OS taus	≥ 2 OS taus
b -jet veto	jet veto	looser jet-veto	looser jet-veto
Z -veto	Z -veto	Z -veto	Z -veto
		$\Delta R(\tau, \tau) < 3$	$\Delta R(\tau, \tau) < 3$
$E_T^{\text{miss}} > 40$ GeV	$m_{T2} > 30$ GeV	$m_{T2} > 60$ GeV	$m_{T2} > 30$ GeV
$m_{T2} > 100$ GeV	$m_{T\tau 1} + m_{T\tau 2} > 250$ GeV	$m_{\text{eff}} > 230$ GeV	$m_{\text{eff}} > 260$ GeV

8 Standard Model background estimation

The main SM processes contributing to the selected final states are multi-jet, W +jets and diboson production. Decays of the SM Higgs boson, assuming a mass of 125 GeV, into a $\tau\tau$ final state have negligible contribution in all SRs (less than 0.1%). Background events may contain a combination of ‘real’ taus, defined as correctly identified tau leptons, or ‘fake’ taus, which can originate from a misidentified light-flavour quark or gluon jet, an electron or a muon.

In multi-jet events all tau candidates are misidentified jets. Due to the large cross section and the poor MC modelling of the tau mis-identification rate from jets, the multi-jet contribution in the SRs is estimated from data, as described in section 8.1. The contribution arising from heavy-flavour multi-jet events containing a real tau lepton from the heavy-flavour quark decay is included in the multi-jet estimate. The contribution of W +jets events, which contain one real tau from the W decay and one or more misidentified jets, is estimated from MC simulation, and normalised to data in a dedicated control region, as described in section 8.2.

Diboson production contributes mainly with events containing real tau leptons coming from WW and ZZ decaying into a $\tau\tau\nu\nu$ final state. Additional SM backgrounds arise from Z +jets production, or events which contain a top quark or top quark pair in association with jets or additional W or Z bosons (collectively referred to as ‘top’ background in the following). The contribution from real taus exceeds 90% in Z +jets and diboson production, and ranges from 45% to 75% in backgrounds containing top quarks. The contribution of fake taus from heavy-flavour decays in jets is negligible. To estimate the irreducible

background, which includes diboson, Z +jets and top quark events, only MC simulated samples are used, as described in section 8.3. The available MC sample sizes in the SRs are limited for Z +jets and top backgrounds. To improve the statistical precision, the prediction in the SRs for these processes is extrapolated from regions with large MC statistics.

Finally, for each signal region, a simultaneous fit based on the profile likelihood method [95] is performed to normalise the multi-jet and W +jets background estimates, as described in section 8.4. Details of the sources of systematic uncertainty on the background estimates described in this section are given in section 9.

8.1 Multi-jet background estimation

One of the dominant backgrounds in the SRs originates from jets misidentified as taus in multi-jet production (from 13% to 30% of the total background, depending on the SR). This contribution is estimated from data using the “ABCD” method. Four exclusive regions, labelled as A, B, C (the “control regions”) and D (the SR), are defined in a two-dimensional plane as a function of two uncorrelated discriminating variables. In this case, the ratio of the numbers of events in the control regions (CR) A and B equals that of SR D to control region C: the number of events in the SR D, N_D , can therefore be calculated from that in control region A, N_A , multiplied by the transfer factor $T = N_C/N_B$.

The tau identification criterion (tau-id) based on the jet BDT quality requirement and a kinematic variable chosen depending on the SR are used as the two discriminating variables to define the regions A, B, C and D. The following kinematic variables are used: m_{T2} for SR-C1N2, $m_{T\tau1} + m_{T\tau2}$ for SR-C1C1, and m_{eff} for SR-DS-highMass and SR-DS-lowMass.

The control region A and the signal region D are defined in the same way except that in the control region A all candidate taus must satisfy the “loose” but fail the “tight” jet BDT requirement (tight tau event veto). The same requirement on the tau-id as in control region A (signal region D) is applied in control region B (control region C). In control regions B and C, less stringent requirements on the kinematic variables defined above are applied. The definitions of the control regions are summarised in table 2.

Furthermore, two validation regions E and F are defined. The validation region E (F) has the same definition as the control region A (signal region D) except for intermediate requirements on the kinematic variable, as listed in table 3. The validation regions are used to verify the extrapolation of the ABCD estimation to the SR, and to estimate the systematic uncertainty from the residual correlation between the tau-id and the kinematic variable. The regions A–F are drawn schematically in figure 2.

The number of multi-jet events in the control and validation regions is estimated from data after subtraction of other SM contributions estimated from MC simulation. Over 80% of the events contributing to the control regions B and C come from multi-jet production. In control region A the multi-jet purity ranges from 60% to 70%, except for SR-DS-highMass for which the purity is 35%. The prediction in this region is affected by a large statistical uncertainty.

The distributions of the kinematic variables in the control regions A, B and in validation region E are shown in figure 3. The results of the ABCD method are summarised in table

Table 2. The multi-jet control region definitions. Only those requirements that are different in the CRs with respect to the SRs are listed.

Regions	A	B	C
CR-C1N2	$m_{T2} > 100$ GeV at least 2 loose taus tight tau veto	$m_{T2} < 40$ GeV at least 2 loose taus tight tau veto	$m_{T2} < 40$ GeV at least 1 medium tau at least 1 tight tau
CR-C1C1	$m_{T\tau1} + m_{T\tau2} > 250$ GeV at least 2 loose taus tight tau veto	$80 < m_{T\tau1} + m_{T\tau2} < 150$ GeV at least 2 loose taus tight tau veto	$80 < m_{T\tau1} + m_{T\tau2} < 150$ GeV at least 1 medium tau at least 1 tight tau
CR-DS-highMass	$m_{\text{eff}} > 230$ GeV at least 2 loose taus tight tau veto	$130 \text{ GeV} < m_{\text{eff}} < 150 \text{ GeV}$ at least 2 loose taus tight tau veto	$130 \text{ GeV} < m_{\text{eff}} < 150 \text{ GeV}$ at least 1 medium tau at least 1 tight tau
CR-DS-lowMass	$m_{\text{eff}} > 260$ GeV at least 2 loose taus tight tau veto	$100 \text{ GeV} < m_{\text{eff}} < 150 \text{ GeV}$ at least 2 loose taus tight tau veto	$100 \text{ GeV} < m_{\text{eff}} < 150 \text{ GeV}$ at least 1 medium tau at least 1 tight tau

Table 3. The requirement on the kinematic variables used to define the validation regions E and F. Only those requirements that are different with respect to the A, B, and C CRs and the SRs are listed.

Regions	E/F
VR-C1N2	$40 \text{ GeV} < m_{T2} < 100 \text{ GeV}$
VR-C1C1	$150 \text{ GeV} < m_{T\tau1} + m_{T\tau2} < 250 \text{ GeV}$
VR-DS-highMass	$150 \text{ GeV} < m_{\text{eff}} < 230 \text{ GeV}$
VR-DS-lowMass	$150 \text{ GeV} < m_{\text{eff}} < 260 \text{ GeV}$

4. The SM predictions are in agreement with the observed data counts in the multi-jet validation regions, as shown in table 5.

8.2 W +jets background estimation

The production of W +jets events with at least one misidentified tau is an important background in the SRs, ranging from 25% to 50%. A dedicated control region (W CR) is used to normalise the W +jets MC estimation to data. The W CR is designed to be kinematically as close as possible to the signal regions, and is enriched in events where the W decays leptonically into a muon and a neutrino to suppress multi-jet contamination. Events containing exactly one isolated muon and one tau passing the tight jet BDT requirement are selected. The selected leptons must have opposite electrical charge. To reduce the contribution from Z +jets production, $m_{T,\tau} + m_{T,\mu} > 80$ GeV is required, and the reconstructed invariant mass of the two leptons, $m_{\tau,\mu}$, must be outside the Z mass window ($12 \text{ GeV} < m_{\tau,\mu} < 40 \text{ GeV}$ or $m_{\tau,\mu} > 100 \text{ GeV}$). To further suppress multi-jet and Z +jets events, $E_{\text{T}}^{\text{miss}} > 40$ GeV is required, and the leptons must not be back-to-back, i.e. $|\Delta\phi(\tau, \mu)| < 2.7$ and $|\Delta\eta(\tau, \mu)| < 2.0$. The contribution from events with top quarks is suppressed by rejecting events containing b -tagged jets, i.e. $N(\text{B20}) = 0$. The definition of the W CR is given in table 6.

The multi-jet contribution in the W CR is estimated by counting the number of events

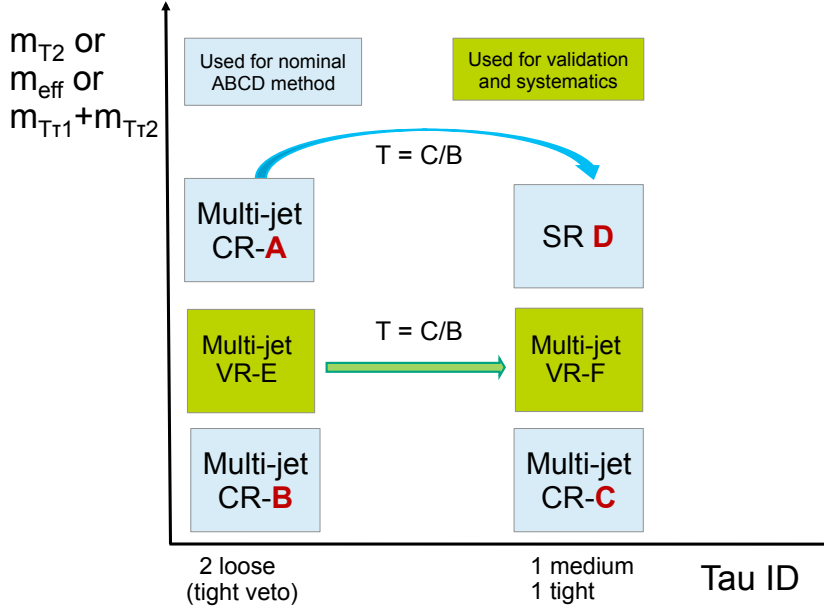


Figure 2. Illustration of the ABCD method for the multi-jet background determination. The control regions A, B, C, and signal region D for the ABCD method described in the text (labelled as Multi-jet CR-A/B/C and SR D) are drawn as light blue boxes. Shown in green and labelled as Multi-jet-VR are the regions E and F, which are used to validate the ABCD method and to estimate the systematic uncertainties.

in data satisfying the same requirements as the W CR but with same-sign (SS) charge of the two leptons. Events from SM processes other than multi-jet production are subtracted from the data counts in the SS region, using their MC prediction. The method relies on the fact that in the multi-jet background the ratio of SS to OS events is close to unity, whilst a significant difference from unity is expected for W +jets production. The latter is dominated by gu/gd -initiated processes that often give rise to a jet originating from a quark, the charge of which is anti-correlated with the W boson charge.

The W +jets estimate is tested in a validation region (W VR) where the W is required to decay leptonically into an electron and a neutrino. The W VR is defined in the same way as the W CR except that events with one tight tau and one isolated electron are selected. The multi-jet contribution in the W VR is estimated using the same technique as in the W CR. The event yields in the W +jets control and validation regions are given in table 7. The purity of the selection in W +jets events is around 80% (75%) in the W CR (VR). Good agreement between data and SM predictions is observed. The large uncertainties stem from the corrections applied for the trigger and identification efficiency for misidentified taus from light jets. Distributions of the kinematic variables defining the SRs are shown in figure 4. The distribution of the effective mass m_{eff} in the W VR is shown in figure 5 (a).

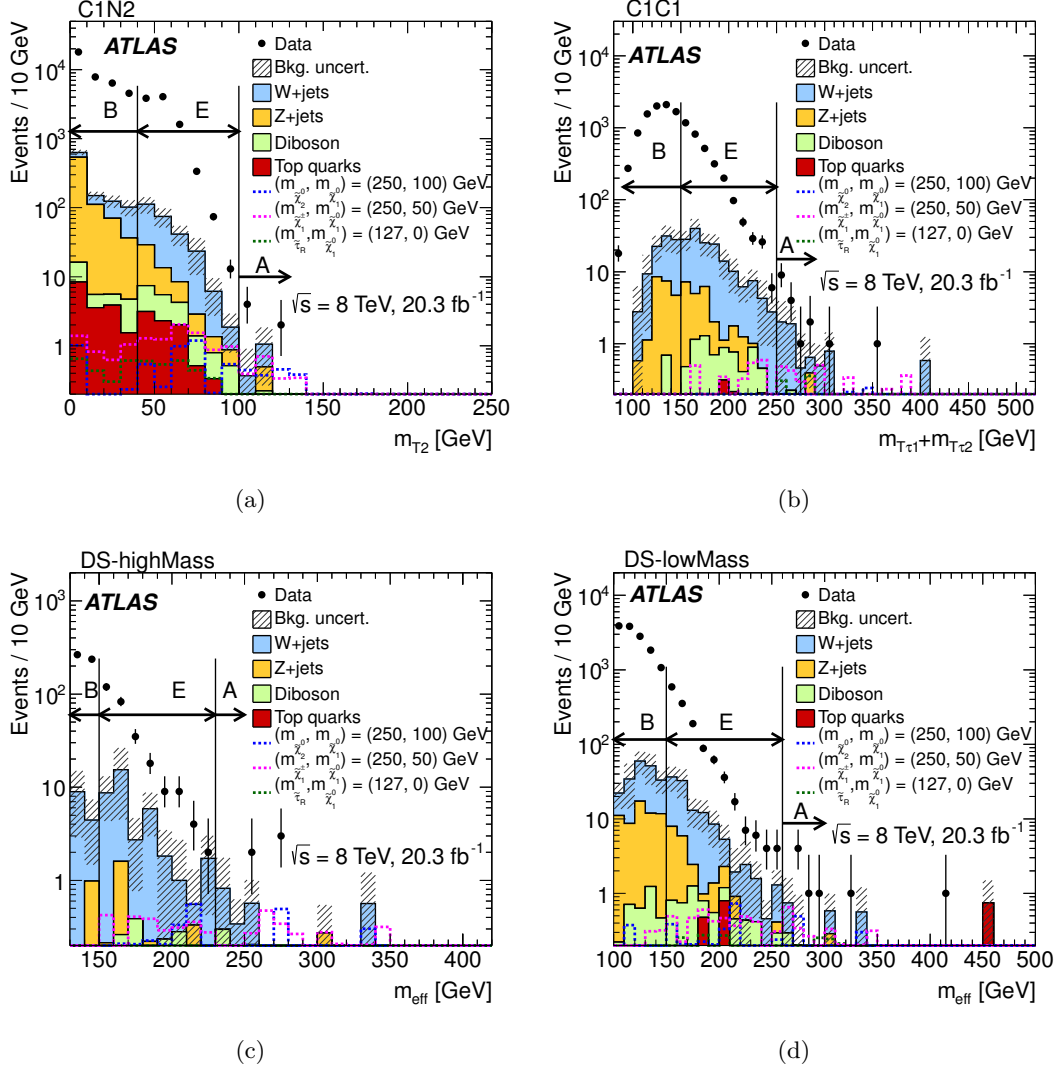


Figure 3. (a) m_{T2} , (b) $m_{T\tau1} + m_{T\tau2}$ and (c,d) m_{eff} distributions in the multi-jet background CRs A and B and in the validation region E defined in tables 2 and 3. The stacked histograms show the contribution of the non-multi-jet SM backgrounds from MC simulation, normalised to 20.3 fb^{-1} . The hatched bands represent the combined statistical and systematic uncertainties on the sum of the SM backgrounds shown. For illustration, the distributions of the SUSY reference points (see section 5.2) are also shown as dashed lines.

8.3 Estimation of irreducible backgrounds

Irreducible SM backgrounds arise mainly from $t\bar{t}$, single top, $t\bar{t}+V$, $Z/\gamma^*+\text{jets}$ and diboson (WW , WZ and ZZ) processes and are estimated with MC simulation and validated in data. Other SM backgrounds are negligible.

The diboson background accounts for 15–35% of the total SM contribution in the signal regions, and mainly arises from $WW \rightarrow \tau\nu\tau\nu$ and $ZZ \rightarrow \tau\nu\nu\nu$ events. To validate the MC modelling and normalisation of the WW process, validation regions with enriched

Table 4. The MC predicted backgrounds in the multi-jet control regions, including both the statistical and systematic uncertainties, and the expected multi-jet contribution (in italics), obtained by subtracting the MC contributions from observed data (in bold). Predicted event yields for the SUSY reference points in the control regions are also shown. The estimated multi-jet contribution in the SRs is given in the last column. The details of the systematic uncertainties reported here are discussed in section 9.

	Sample	Region A	Region B	Region C	T = C/B	Multi-jet in SR (D)
C1N2	Data	6	36907	24601	0.55 ± 0.03	2.3 ± 1.4
	Z+jets	0.28 ± 0.16	730 ± 260	3980 ± 1060		
	W+jets	1.0 ± 0.4	250 ± 82	590 ± 180		
	diboson	0.51 ± 0.26	14.6 ± 4.8	72 ± 20		
	top	0.10 ± 0.06	17.3 ± 6.1	68 ± 22		
	<i>multi-jet</i>	<i>4.1 ± 2.5</i>	<i>35900 ± 330</i>	<i>19890 ± 1090</i>		
	Ref. point 1	1.9 ± 0.9	1.4 ± 0.7	17.8 ± 6.2		
C1C1	Data	18	8479	4551	0.51 ± 0.01	5.8 ± 2.3
	Z+jets	0.06 ± 0.06	21 ± 10	80 ± 25		
	W+jets	5.6 ± 1.2	71 ± 32	160 ± 46		
	diboson	0.9 ± 0.4	1.2 ± 0.6	5.4 ± 2.2		
	top	0.11 ± 0.06	0.0 ± 1.0	0.6 ± 0.5		
	<i>multi-jet</i>	<i>11.3 ± 4.4</i>	<i>8390 ± 98</i>	<i>4300 ± 85</i>		
	Ref. point 2	3.9 ± 1.0	0.13 ± 0.09	1.4 ± 0.4		
DS-highMass	Data	5	500	268	0.50 ± 0.05	0.9 ± 1.2
	Z+jets	0.24 ± 0.18	1.0 ± 0.7	1.7 ± 1.0		
	W+jets	2.2 ± 0.7	12.3 ± 6.6	20.6 ± 9.6		
	diboson	0.7 ± 0.4	0.2 ± 0.1	0.6 ± 0.3		
	top	0.06 ± 0.03	0.0 ± 1.0	0.8 ± 0.6		
	<i>multi-jet</i>	<i>1.8 ± 2.4</i>	<i>487 ± 23</i>	<i>244 ± 19</i>		
	Ref. point 3	0.9 ± 0.4	0.0 ± 1.0	0.20 ± 0.13		
DS-lowMass	Data	8	13419	7632	0.54 ± 0.01	2.8 ± 1.7
	Z+jets	0.14 ± 0.09	57 ± 26	180 ± 49		
	W+jets	2.3 ± 0.7	140 ± 51	290 ± 75		
	diboson	0.40 ± 0.24	3.1 ± 1.4	10.7 ± 3.6		
	top	0.09 ± 0.05	0.1 ± 0.1	3.8 ± 1.9		
	<i>multi-jet</i>	<i>5.1 ± 2.9</i>	<i>13220 ± 130</i>	<i>7150 ± 130</i>		
	Ref. point 3	1.4 ± 0.5	0.11 ± 0.11	1.3 ± 0.4		

$WW \rightarrow e\nu\mu\nu$ contribution are defined for each SR. Events with exactly one OS electron–muon pair are selected. To keep the same phase space as the SRs, the WW VRs are defined in the same way except for intermediate requirements on the relevant kinematic variable to reduce possible signal contamination, i.e. $50 \text{ GeV} < m_{T2} < 100 \text{ GeV}$ for SR-C1N2, $150 \text{ GeV} < m_{T,\mu} + m_{T,e} < 250 \text{ GeV}$ for SR-C1C1, $150 \text{ GeV} < m_{\text{eff}} < 230 \text{ GeV}$ for SR-DS-highMass and $150 \text{ GeV} < m_{\text{eff}} < 260 \text{ GeV}$ for SR-DS-lowMass. The purity of the selection in WW events ranges from 70% to 80% in all validation regions. The agreement between data and SM predictions is found to be good, and the data yields match the SM predictions within uncertainties (of the order of 10%), as shown in figure 5 (c).

The inclusive contribution from $t\bar{t}$, single top, $t\bar{t}+V$ and $Z/\gamma^*+\text{jets}$ amounts to about 5–20% of the total background in the signal regions. The MC estimates are validated in

Table 5. Number of events in the multi-jet validation regions F for data and SM backgrounds, including both statistical and systematic uncertainties. The SM MC backgrounds are normalised to 20.3 fb^{-1} . The multi-jet contribution is estimated from data with the ABCD method, by multiplying the number of events in region E and the transfer factor T.

Sample	VR-C1N2	VR-C1C1	VR-DS-highMass	VR-DS-lowMass
Data	5585	1846	163	764
SM total	5840 ± 340	1870 ± 87	170 ± 24	860 ± 110
Multi-jet	5370 ± 320	1570 ± 61	120 ± 19	670 ± 100
W +jets	320 ± 93	240 ± 60	37 ± 15	130 ± 42
Z +jets	97 ± 39	34 ± 12	5.6 ± 2.9	36 ± 14
Diboson	27 ± 8	15.1 ± 5.4	5.1 ± 1.5	12.9 ± 3.6
Top	24 ± 10	5.0 ± 2.1	3.6 ± 1.7	9.5 ± 3.3

Table 6. Definition of the W +jets control region.

1 tight tau and 1 isolated muon with opposite charge
b -jet veto
$\Delta\phi(\tau, \mu) < 2.7$
$ \Delta\eta(\tau, \mu) < 2.0$
$E_T^{\text{miss}} > 40 \text{ GeV}$
$m_{T,\tau} + m_{T,\mu} > 80 \text{ GeV}$
$12 \text{ GeV} < m_{\tau,\mu} < 40 \text{ GeV}$ or $m_{\tau,\mu} > 100 \text{ GeV}$

Table 7. Event yields in the W +jets control and validation regions. The SM backgrounds other than multi-jet production are estimated from MC simulation and normalised to 20.3 fb^{-1} . The multi-jet contribution is estimated from data in the same-sign region, by subtracting all other SM backgrounds from the data counts. The quoted uncertainty is the sum in quadrature of statistical and systematic uncertainties.

Sample	W CR	W VR
Data	4120	3420
SM total	4100 ± 900	3500 ± 600
W +jets	3300 ± 800	2600 ± 500
Top	250 ± 80	240 ± 70
Diboson	180 ± 50	170 ± 40
Z +jets	140 ± 40	99 ± 31
Multi-jet	250 ± 250	400 ± 200

regions enriched in Z +jets and $t\bar{t}$ events.

In the Z +jets validation region events containing one isolated electron or muon and one tau with opposite electrical charge are selected. The invariant mass of the dilepton pair must satisfy $40 \text{ GeV} < m_{\ell\tau} < 75 \text{ GeV}$. To suppress contributions from other SM processes, $m_{T,\ell} + m_{T,\tau} < 80 \text{ GeV}$, $|\Delta\phi(\ell, \tau)| > 2.4$ and $N(\text{B20}) = 0$ veto are required. The multi-jet

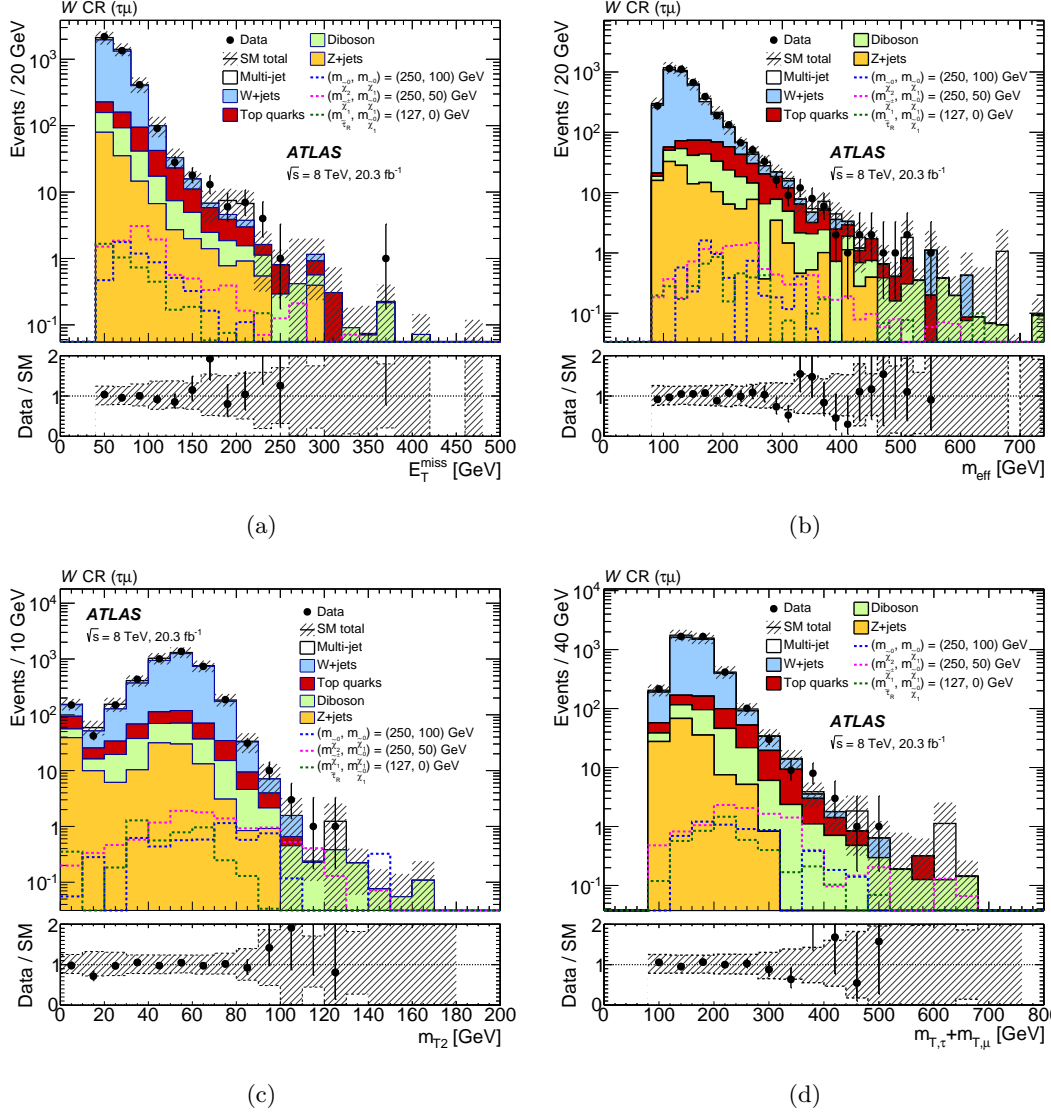


Figure 4. Distributions in the W +jets control region of the kinematic variables which are used in the signal region definition. The SM backgrounds other than multi-jet production are estimated from MC simulation and normalised to 20.3 fb^{-1} . The multi-jet contribution is estimated from data in the same-sign region, by subtracting all other SM backgrounds from the data counts. The hatched bands represent the combined statistical and systematic uncertainties on the total SM background. For illustration, the distributions of the SUSY reference points are also shown as dashed lines. The lower panels show the ratio of data to the SM background estimate.

contribution in the Z VR is estimated with the same method as in the W CR and VR.

The top quark validation region is defined by requiring at least two candidate taus, and at least one must satisfy the tight jet BDT quality requirement. At least one of the selected tau pairs must contain taus with opposite electrical charge. To increase the contribution from top events, two b -tagged jets with $p_T > 20$ GeV are required, and the events should be kinematically compatible with $t\bar{t}$ production (top-tagged) through the

use of the variable m_{CT} [96]. The scalar sum of the p_T of the two taus and of at least one combination of two jets in an event must exceed 100 GeV. Furthermore, top-tagged events are required to possess m_{CT} values calculated from combinations of jets and taus consistent with the expected bounds from $t\bar{t}$ events as described in Ref. [97]. Requirements of $50 \text{ GeV} < E_T^{\text{miss}} < 100 \text{ GeV}$ and $m_{T\tau 1} + m_{T\tau 2} > 80 \text{ GeV}$ are applied to suppress contributions from SM backgrounds not containing top quarks.

The purity of the selection in Z +jets and $t\bar{t}$ events is above 80% in the respective validation regions and good agreement between the data and SM expectation is observed. Distributions of relevant kinematic variables in the Z and top VRs are shown in figure 5 (b) and (d).

8.4 Fitting procedure

For each signal region, a simultaneous fit is performed based on the profile likelihood method [95]. The inputs to the fit are: the number of observed events in the multi-jet CR A and W CR, the expected non-multi-jet and non- W contributions to the multi-jet CR A and W CR, the expected contributions of multi-jet and W to the multi-jet CR A and W CR, as described in sections 8.1 – 8.2, and the transfer factors, which relate the number of multi-jet or W +jets events in their associated control region to that predicted in the signal region. The number of events in a given CR is described using a Poisson distribution, the mean of which is the sum of the expected contributions from all background sources. The free parameters in the fit are the normalisations of the W +jets and multi-jet contributions. The systematic uncertainties on the expected background yields are included as nuisance parameters, assumed to be Gaussian distributed with a width determined from the size of the uncertainty. Correlations between control and signal regions, and background processes are taken into account with common nuisance parameters. The fit parameters are determined by maximising the product of the Poisson probability functions and the constraints for the nuisance parameters.

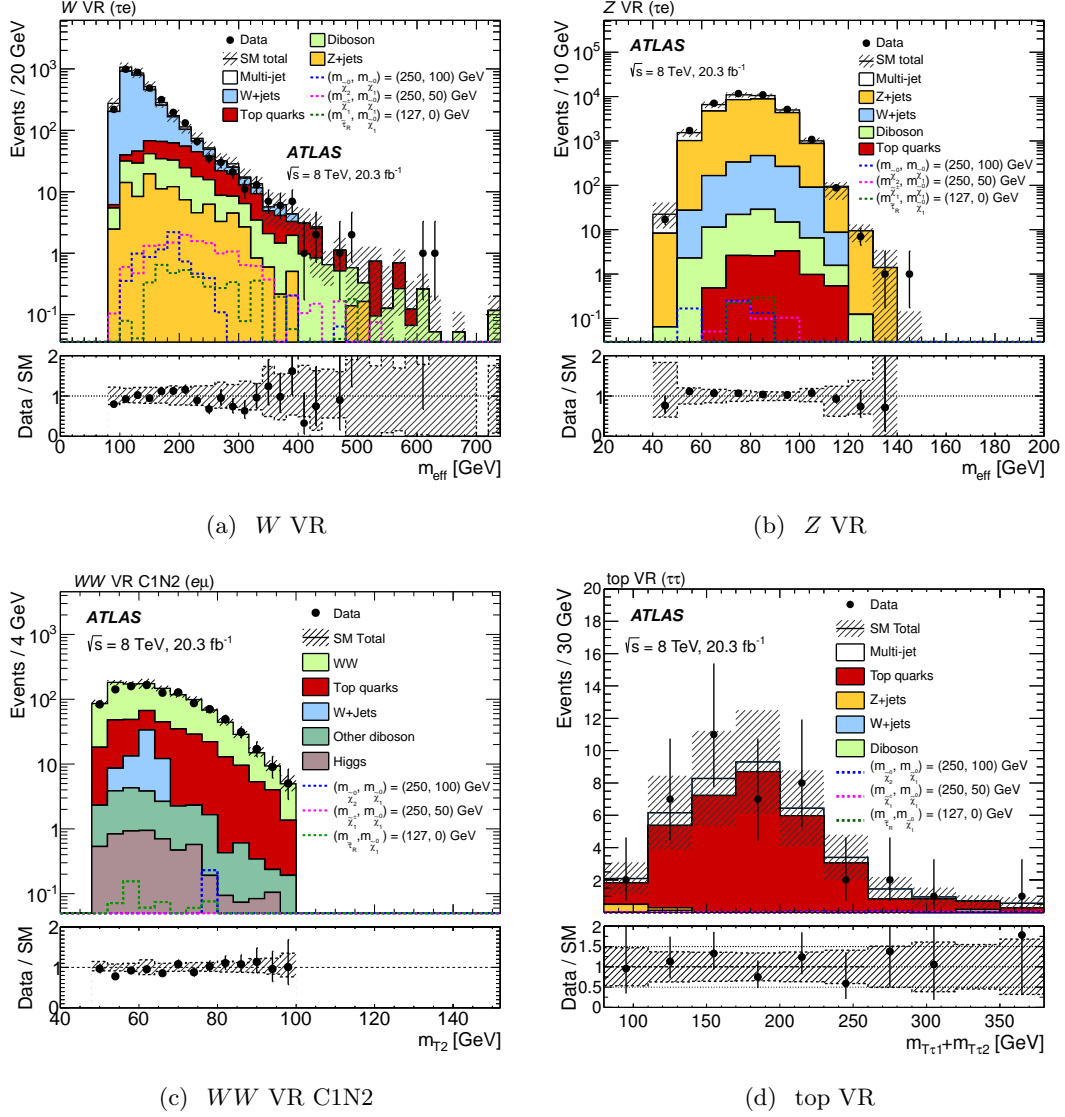


Figure 5. Distributions of relevant kinematic variables in the validation regions: m_{eff} in the (a) W and (b) Z VRs, (c) m_{T2} in the WW VR C1N2, and (d) $m_{T\tau1} + m_{T\tau2}$ in the top VR. In the Z VR, events containing one electron and one tau are shown. The SM backgrounds other than multi-jet production are estimated from MC simulation and normalised to 20.3 fb $^{-1}$. The hatched bands represent the combined statistical and systematic uncertainties on the total SM background. For illustration, the distributions of the SUSY reference points are also shown as dashed lines. The lower panels show the ratio of data to the SM background estimate.

9 Systematic uncertainties

Systematic uncertainties have an impact on the estimates of the background and signal event yields in the control and signal regions. Several sources of systematic uncertainty are considered for the ABCD method used to determine the multi-jet background: the correlation between the kinematic variable (m_{T2} , $m_{T\tau1} + m_{T\tau2}$, or m_{eff}) and the tau iden-

tification variable, the limited number of events in the CRs, and the subtraction of other SM backgrounds. The systematic uncertainty on the correlation is estimated by comparing the transfer factor from the region B to region C to that of the region E to F (see figure 2). The systematic uncertainty due to the limited number of events in the control regions is estimated by considering the statistical uncertainty on the number of data events and the other SM background components. The systematic uncertainty on the non-multi-jet background subtraction in the control regions A, B, and C is estimated by considering the systematic uncertainty in the MC estimations of the non-multi-jet background in the CRs. A summary of the systematic uncertainties on the multi-jet background estimation in the SRs is shown in table 8. The dominant source is given by the limited number of events in the multi-jet control regions.

The dominating uncertainty in the multi-jet estimation from SS events in the W control region and in the W and Z validation regions stems from the different fractions of quark and gluon jets in the OS and SS regions. The relative difference in the tau mis-identification rates measured in events with OS and SS lepton pairs varies between 20% and 70% in most of the phase space of interest for this analysis; however, it goes up to 100% in regions with few events.

Table 8. Summary of the systematic uncertainties for the multi-jet background estimation. The total uncertainty is the sum in quadrature of each source.

Systematic Source	SR-C1N2	SR-C1C1	SR-DS-highMass	SR-DS-lowMass
Correlation	4.9%	1.6%	8.0%	14%
Non-multi-jet subtraction in Region A	8.0%	12%	21%	13%
Non-multi-jet subtraction in Region B	1.0%	0.4%	1.2%	0.5%
Non-multi-jet subtraction in Region C	2.7%	1.4%	3.6%	2.0%
Number of events in Region A	61%	38%	133%	57%
Number of events in Regions C and B	1.0%	2.0%	8.4%	1.5%
Total	62%	40%	135%	60%

The experimental systematic uncertainties on the SM backgrounds estimated with MC simulation are due to those on the jet energy scale and resolution [84], E_T^{miss} energy scale and resolution [90], b -tagging and mis-identification efficiency [98], and tau identification, trigger efficiency and energy scale [88]. The main contribution comes from the uncertainty on the corrections applied to the tau identification and trigger efficiency in the simulated samples, and from the tau energy scale uncertainty. The uncertainty on the correction for the tau identification efficiency is of the order of 2–3% for taus with p_T between 20 and 200 GeV. Uncertainties on the trigger efficiency are around 2–4% for taus with p_T between 30 and 50 GeV, and increase to 8–10% for taus with $p_T > 50$ GeV. The uncertainty on the tau energy scale is of the order of a few percent, with no significant dependence on pile-up or on the tau pseudorapidity.

A systematic uncertainty of the order of 10% associated with the simulation of pile-up is also taken into account. The luminosity uncertainty is 2.8% [50].

Theoretical uncertainties affecting the generator predictions arise from the finite num-

ber of partons (FNP) from the hard primary interaction for diboson and top processes, the effect of the renormalisation (μ_R) and factorisation (μ_F) scales for diboson, W +jets and Z +jets production, and the impact of the merging scale of the matrix element with the parton shower (ME-PS) for diboson and top processes. The FNP-induced uncertainty is calculated by comparing the baseline samples which contain up to three additional partons from the hard interaction to samples with up to two additional partons. The uncertainty due to the μ_R and μ_F scales is determined by the comparison with samples with these scales varied up and down by a factor of two, while the ME-PS merging scale uncertainty is determined by a comparison with samples with varied merging scale. For W +jets events, the uncertainty due to the jet p_T threshold used for parton–jet matching is calculated by comparing the baseline samples with jet p_T threshold set to 15 GeV to samples with a threshold of 25 GeV. The theoretical uncertainties associated with the top sample vary from 10% to 20% while the W/Z +jets and diboson theoretical uncertainties vary from 17% to 30%, depending on the process and the signal region. The uncertainty due to the PDF choice is 1–2% for W/Z +jets and diboson production, and around 6% for $t\bar{t}$, single top and $t\bar{t}+V$ processes. The theoretical uncertainties on the cross sections are 5% for Z +jets [99], 10% for $t\bar{t}$, 3%, 4% and 7% for single top in the t -, s - and Wt - channels, respectively, 22% for $t\bar{t}+W/Z$, and 5%, 5% and 7% for WW , ZZ and WZ , respectively [73].

The various sources of uncertainty for the non-multi-jet background estimates in the SRs are summarised in table 9. In the W CR, the total uncertainty on the W +jets estimation is around 20%, and it is dominated by theory uncertainties and corrections due to trigger and tau identification efficiency.

Table 9. Summary of the various sources of uncertainty for the non-multi-jet background estimates in the signal regions. The first row shows the uncertainty due to the limited statistics in the MC samples. The second row shows the total systematic uncertainty from theory. The main experimental systematic uncertainties are given in the rows labelled with “Tau ID and trigger” and “Tau Energy scale”, while the row “Others” shows the contribution from the remaining sources of experimental systematic uncertainty as described in the text. The “Total” uncertainty is the sum in quadrature of each source.

Source	W +jets	Diboson	Z +jets	Top
MC statistics	16–36%	15–28%	44–80%	23–50%
Theoretical uncertainty	17–30%	17–27%	25–30%	10–20%
Tau ID and trigger	10–18%	20–21%	10–20%	22–28%
Tau Energy Scale	12–20%	3–13%	4–12%	2–7%
Others	1–10%	3–9%	5–10%	10–20%
Total	34–48%	35–44%	58–85%	43–62%

Signal cross sections are calculated to NLO. Their uncertainties are taken from an envelope of cross-section predictions using different PDF sets and factorisation and renormalisation scales [100]. Uncertainties associated with modelling of ISR in SUSY signal samples were evaluated for a few benchmark samples and found to be negligible. Sys-

tematic uncertainties associated with the signal selection efficiency include those due to the tau trigger efficiency, tau identification and energy scale, jet reconstruction and E_T^{miss} calculation. The uncertainty on the integrated luminosity also affects the predicted signal yield. The total uncertainty varies between 20% and 30% for SUSY scenarios to which this measurement is sensitive. The dominant experimental uncertainty is due to the tau trigger efficiency, and is around 20%.

10 Results

The observed number of events in each signal region and the expected contributions from SM processes are given in table 10. The contributions of multi-jet and W +jets events were scaled with the normalisation factors obtained from the fit described in section 8.4. The normalisation factors do not deviate from unity by more than 1%. Due to the limited number of events in the multi-jet CRs, the uncertainty on the multi-jet normalisation varies between 54% and 131% depending on the CR, while the uncertainty on the W +jets normalisation is around 10%. All statistical uncertainties arising from the limited number of MC events are included. The effect of limited data events in the CRs is included in the systematic uncertainty. All systematic uncertainties except for the jet energy scale and jet energy resolution are obtained taking into account the correlations among control regions and background processes. The total uncertainties are the sum in quadrature of systematic and statistical uncertainties. Due to the simultaneous fit, the uncertainty on the W +jets estimation decreases by 10% with respect to the numbers in table 9, while the uncertainties on the remaining non-multi-jet backgrounds vary by less than 2% depending on the SR. Due to the large uncertainty on the multi-jet normalisation, the uncertainty on the multi-jet estimate increases by up to 25% depending on the SR with respect to the numbers quoted in table 4. Agreement is found between observations and background expectations within 1σ in all signal regions except for SR-C1C1. In SR-C1C1, the observed number of events fluctuates below the number of expected SM events by 2.2σ , mainly in the region $250 \text{ GeV} < m_{T\tau 1} + m_{T\tau 2} < 270 \text{ GeV}$.

For each SR, the significance of a possible excess of observed events over the SM prediction is quantified by the one-sided probability, p_0 , of the background alone to fluctuate to the observed number of events or higher using the asymptotic formula described in [95]. A fit similar to the one described in section 8.4 is used, except that the number of events observed in the SR is added as an input to the fit, and an additional parameter for the non-SM signal strength, constrained to be non-negative, is fit. Upper limits at 95% confidence level (CL) on the number of non-SM events in the SRs are derived using the CLs prescription [101] and neglecting any possible signal contamination in the control regions. Normalising these by the integrated luminosity of the data sample, they can be interpreted as upper limits on the visible non-SM cross section, σ_{vis}^{95} , which is defined as the product of acceptance, reconstruction efficiency and production cross section. All systematic uncertainties and their correlations are taken into account via nuisance parameters. The accuracy of the limits obtained by the asymptotic formula was tested for all SRs by randomly generating

Table 10. Observed and expected numbers of events in the signal regions for 20.3 fb^{-1} . The contributions of multi-jet and W +jets events were scaled with the normalisation factors obtained from the fit described in section 8.4. The shown uncertainties are the sum in quadrature of statistical and systematic uncertainties. The correlation of systematic uncertainties among control regions and background processes is fully taken into account and, as a result, the numbers given here may be different from those in tables 4 and 9. Expected event yields for the SUSY reference points (see section 5.2) are also shown. The one-sided p_0 -values and the observed and expected 95% CL upper limits on the visible non-SM cross section (σ_{vis}^{95}), obtained from the fit described in section 10, are given. Values of $p_0 > 0.5$ are truncated to $p_0 = 0.5$.

SM process	SR-C1N2	SR-C1C1	SR-DS-highMass	SR-DS-lowMass
Top	0.30 ± 0.19	0.7 ± 0.4	0.9 ± 0.4	1.3 ± 0.6
Z +jets	0.9 ± 0.5	0.20 ± 0.17	0.6 ± 0.4	0.40 ± 0.27
W +jets	2.2 ± 0.8	11.2 ± 2.8	2.7 ± 0.9	4.1 ± 1.2
Diboson	2.2 ± 0.9	3.8 ± 1.4	2.5 ± 1.0	2.9 ± 1.0
Multi-jet	2.3 ± 2.0	5.8 ± 3.3	0.9 ± 1.2	2.8 ± 2.3
SM total	7.9 ± 2.4	22 ± 5	7.5 ± 1.9	11.5 ± 2.9
Observed	11	12	7	15
Ref. point 1	11.3 ± 2.8	8.5 ± 2.2	10.2 ± 2.6	7.5 ± 2.0
Ref. point 2	9.2 ± 2.1	20 ± 4	12.4 ± 2.8	12.8 ± 2.7
Ref. point 3	0.8 ± 0.5	7.6 ± 1.9	3.8 ± 1.0	5.2 ± 1.3
p_0	0.20	0.50	0.50	0.21
Expected σ_{vis}^{95} (fb)	$< 0.42^{+0.19}_{-0.11}$	$< 0.56^{+0.25}_{-0.14}$	$< 0.37^{+0.17}_{-0.10}$	$< 0.51^{+0.18}_{-0.15}$
Observed σ_{vis}^{95} (fb)	< 0.59	< 0.37	< 0.37	< 0.66

a large number of pseudo-datasets and repeating the fit, and good agreement was found. The results are given in table 10.

In figure 6 the distributions of the relevant kinematic variables are shown for data, SM expectations and illustrative SUSY benchmark models. The SM background distributions are taken from MC simulation, except for the multi-jet contribution, which is estimated using the ABCD method described in section 8.1. The normalisation factors obtained from the fit detailed in section 8.4 are used to correct the expected distributions of the W +jets and multi-jet processes.

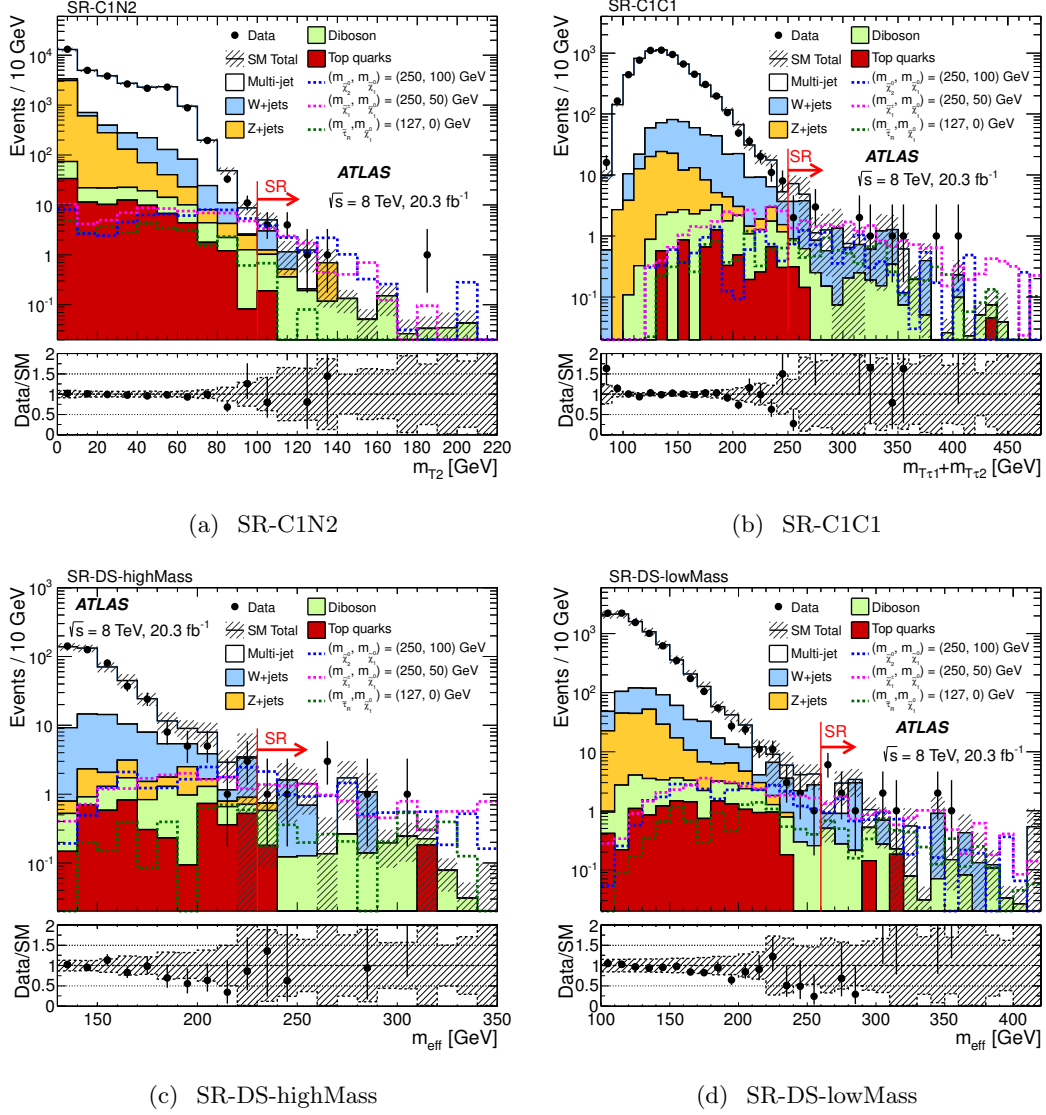


Figure 6. Distributions of relevant kinematic variables before the requirement on the given variable is applied: (a) m_{T2} for SR-C1N2, (b) $m_{T\tau 1} + m_{T\tau 2}$ for SR-C1C1, (c) m_{eff} for SR-DS-highMass, and (d) m_{eff} for SR-DS-lowMass. The stacked histograms show the expected SM backgrounds normalised to 20.3 fb^{-1} . The multi-jet contribution is estimated from data using the ABCD method. The hatched bands represent the sum in quadrature of systematic and statistical uncertainties on the total SM background. The lower panels show the ratio of data to the total SM background estimate.

11 Interpretation

In the absence of a significant excess over the SM background expectations, the observed numbers of events in the signal regions are used to place model-dependent exclusion limits at 95% CL for the pMSSM and the simplified models described in section 5.2. The same CLs limit-setting procedure as described in section 10 is used, except that the SUSY signal

is allowed to populate both the signal and the control regions. All SRs defined in section 7 are considered in order to derive limits for all the SUSY models considered in this paper, regardless of the specific production mode for which they were optimised. Since the SRs are not mutually exclusive, for each point in the parameter space the SR which gives the best expected limit is used.

The results are shown in figures 7–9. The solid (dashed) lines show the observed (expected) exclusion contours. The band around the expected limit shows the $\pm 1\sigma$ variations, including all uncertainties except theoretical uncertainties on the signal cross section. The dotted lines around the observed limit indicate the sensitivity to $\pm 1\sigma$ variations of the theoretical uncertainties. All mass limits hereafter quoted correspond to the observed limits reduced by 1σ of the signal cross sections.

11.1 Simplified models: chargino–neutralino and chargino–chargino production

The exclusion limits for the simplified models characterised by $\tilde{\chi}_1^\pm \tilde{\chi}_2^0$ and $\tilde{\chi}_1^\pm \tilde{\chi}_1^\mp$ production with intermediate staus are shown in figure 7. In figure 7(a), both production processes are considered simultaneously, whereas in figure 7(b) only chargino–chargino production is assumed.

Chargino masses up to 345 GeV are excluded for a massless lightest neutralino in the scenario of direct production of chargino pairs. In the case of associated production of mass-degenerate charginos and next-to-lightest neutralinos, chargino masses up to 410 GeV are excluded for a massless lightest neutralino. These limits improve the results from the ATLAS three-lepton analysis [37], where only production of $\tilde{\chi}_1^\pm \tilde{\chi}_2^0$ was considered due to the low sensitivity to the decays of $\tilde{\chi}_1^\pm \tilde{\chi}_1^\mp$. For the scenario of direct production of chargino pairs, SR-C1C1 (SR-DS-highMass) provides the best exclusion limit for low (high) chargino masses, while for the associated production of mass-degenerate charginos and next-to-lightest neutralinos, SR-C1N2 and SR-DS-highMass have the highest sensitivity over the whole parameter space.

11.2 Direct stau production

Due to the low cross section, the sensitivity of this analysis to the direct production of stau pairs is degraded relative to the sensitivity obtained for models of electroweak production of charginos and neutralinos. Upper limits on the cross section were derived for the direct stau production model described in section 5.2, and are shown separately for the production of $\tilde{\tau}_R \tilde{\tau}_R$ and $\tilde{\tau}_L \tilde{\tau}_L$ in figure 8. For large stau masses, SR-DS-highMass provides the best upper limits, while SR-C1C1 has the best performance for low stau masses. The results in SR-C1C1 lead to a stronger observed exclusion limit than expected due to the number of observed events being fewer than the SM prediction.

The signal strength is defined as the scaling factor that should be applied to the theoretical cross section to exclude the considered model at 95% CL. The upper limit on the signal strength for the associated production of $\tilde{\tau}_R \tilde{\tau}_R$ and $\tilde{\tau}_L \tilde{\tau}_L$, for different lightest neutralino masses and as a function of the $\tilde{\tau}_R$ mass is shown in figure 9.

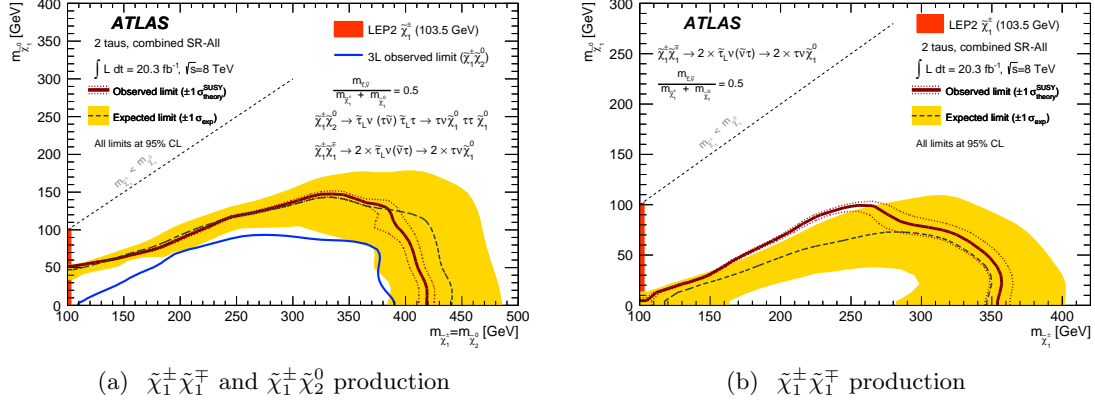


Figure 7. 95% CL exclusion limits for simplified models with (a) a combination of chargino–neutralino and chargino–chargino production and (b) chargino–chargino production only. See text for details of exclusion curves and uncertainty bands. Also shown is the LEP limit [39] on the mass of the chargino. The blue contour in (a) corresponds to the observed limit from the ATLAS three-lepton analysis [37], where only $\tilde{\chi}_1^\pm \tilde{\chi}_2^0$ production was considered.

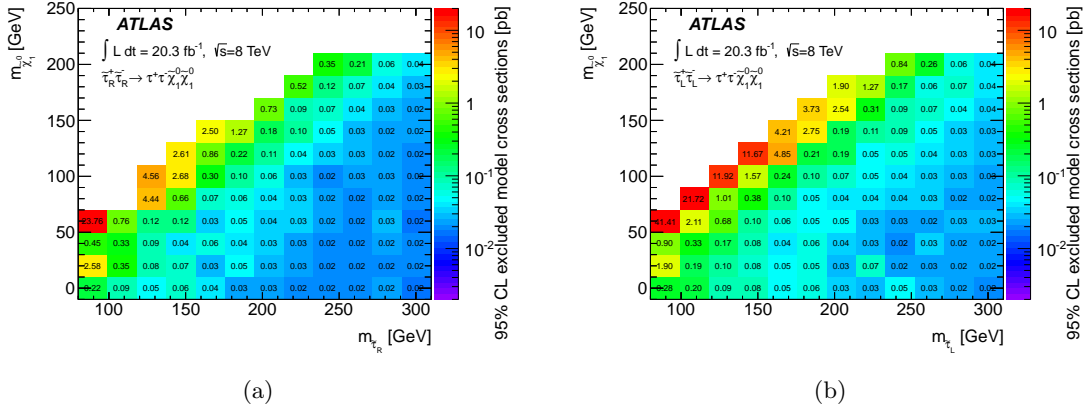


Figure 8. Upper limits on the cross section for production of only (a) $\tilde{\tau}_R \tilde{\tau}_R$ or (b) $\tilde{\tau}_L \tilde{\tau}_L$ pairs.

The best observed upper limit on the signal strength is found for a mass of the $\tilde{\tau}_R$ ($\tilde{\tau}_L$) of 90.6 (93.1) GeV and a massless $\tilde{\chi}_1^0$. For this combination of stau and LSP masses, the theoretical cross section at NLO is 0.07 (0.17) pb for $\tilde{\tau}_R \tilde{\tau}_R$ ($\tilde{\tau}_L \tilde{\tau}_L$) production, while the excluded cross section is 0.22 (0.28) pb and the upper limit on the signal strength for the combined production of $\tilde{\tau}_R \tilde{\tau}_R$ and $\tilde{\tau}_L \tilde{\tau}_L$ is 0.95.

11.3 The pMSSM model

Limits on the mass parameters M_2 and μ are set within the pMSSM framework with parameters described in section 5.2. In figure 10(a), the exclusion limits for the pMSSM model with fixed stau mass are shown in the μ - M_2 plane. The region at low M_2 cannot be excluded since it corresponds to points in the parameter space where the chargino and neutralino are lighter than the stau. Since in this model the cross section for direct stau

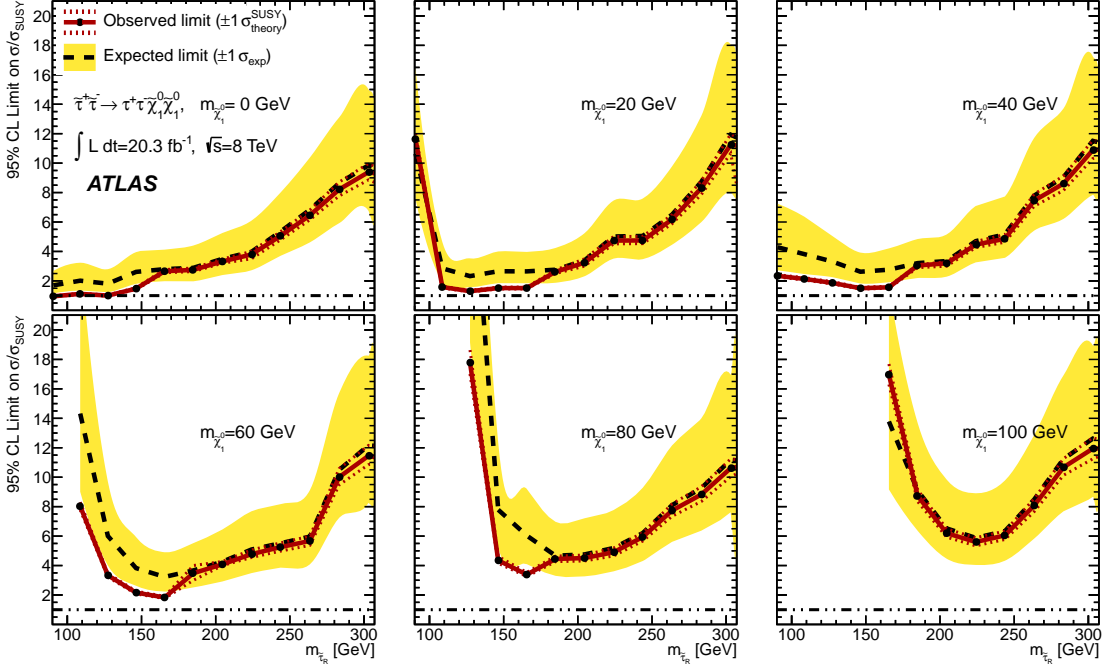


Figure 9. Upper limit on the signal strength for the associated production of $\tilde{\tau}_R \tilde{\tau}_R$ and $\tilde{\tau}_L \tilde{\tau}_L$, for different lightest neutralino masses and as a function of the $\tilde{\tau}_R$ mass. See text for details of exclusion curves and uncertainty bands.

production is constant, this process dominates in the remaining allowed region at large M_2 and μ . Direct stau production accounts for 60% of the events for $M_2 = \mu = 400$ GeV, and 85% of the events for $M_2 = \mu = 500$ GeV.

Figure 10(b) shows the exclusion limits in the μ - M_2 plane for the pMSSM model with variable stau mass. For both pMSSM models, the excluded $\tilde{\chi}_1^\pm$ ($\tilde{\chi}_2^0$) mass range is 100–350 GeV as can be seen from the light grey iso-mass lines of $\tilde{\chi}_1^\pm$ ($\tilde{\chi}_2^0$). For values of μ larger than those simulated for this analysis, the pMSSM phenomenology is similar to that studied here. For larger values of M_2 , the production cross section of heavier neutralinos and charginos increases. In general, the shown limits on the lightest chargino mass can be expected to be similar also at large μ (M_2) for values of M_2 (μ) in the range 150–350 (100–300) GeV.

In the pMSSM model with fixed stau mass, SR-DS-highMass provides better exclusion at high μ , M_2 . For $M_2, \mu < 200$ GeV, SR-C1N2 and SR-C1C1 provide the most stringent limits. In the pMSSM model with variable stau mass, SR-C1N2 and SR-DS-highMass give the best sensitivity in the whole parameter space.

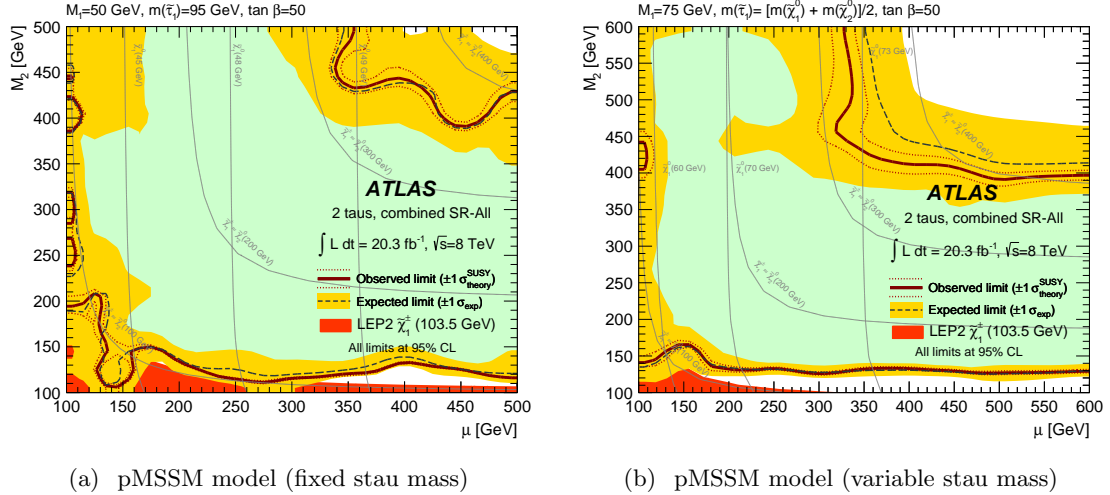


Figure 10. 95% CL exclusion limits in the μ – M_2 mass plane for the pMSSM models with (a) fixed and (b) variable stau mass. See text for details of exclusion curves and uncertainty bands. The areas excluded by the -1σ expected limit are shown in green. The LEP limit [39] on the mass of the chargino is also shown in red.

12 Conclusion

Searches for the electroweak production of supersymmetric particles in events with at least two hadronically decaying taus, missing transverse momentum and low jet activity in the final state are performed using 20.3 fb^{-1} of proton–proton collision data at $\sqrt{s} = 8 \text{ TeV}$ recorded with the ATLAS experiment at the Large Hadron Collider. Agreement between data and SM expectations is observed in all signal regions. These results are used to set limits on the visible cross section for non-SM events in each signal region. Exclusion limits are placed on parameters of the pMSSM and simplified models.

For simplified models, chargino masses up to 345 GeV are excluded for a massless lightest neutralino in the scenario of direct production of wino-like chargino pairs, with each chargino decaying into the lightest neutralino via an intermediate on-shell stau. In the case of associated production of mass-degenerate charginos and next-to-lightest neutralinos, masses up to 410 GeV are excluded for a massless lightest neutralino. In pMSSM models the excluded $\tilde{\chi}_1^\pm$ ($\tilde{\chi}_2^0$) mass range is between 100 and 350 GeV. For direct stau production, the best upper limit on the signal strength is found for a mass of the $\tilde{\tau}_R$ ($\tilde{\tau}_L$) of 90.6 (93.1) GeV and a massless $\tilde{\chi}_1^0$. The excluded cross section for $\tilde{\tau}_R \tilde{\tau}_R$ ($\tilde{\tau}_L \tilde{\tau}_L$) is 0.22 (0.28) pb for this combination of stau and lightest supersymmetric particle masses, while the theoretical cross section at NLO is 0.07 (0.17) pb.

13 Acknowledgements

We thank CERN for the very successful operation of the LHC, as well as the support staff from our institutions without whom ATLAS could not be operated efficiently.

We acknowledge the support of ANPCyT, Argentina; YerPhI, Armenia; ARC, Australia; BMWFW and FWF, Austria; ANAS, Azerbaijan; SSTC, Belarus; CNPq and FAPESP, Brazil; NSERC, NRC and CFI, Canada; CERN; CONICYT, Chile; CAS, MOST and NSFC, China; COLCIENCIAS, Colombia; MSMT CR, MPO CR and VSC CR, Czech Republic; D NRF, DNSRC and Lundbeck Foundation, Denmark; EPLANET, ERC and NSRF, European Union; IN2P3-CNRS, CEA-DSM/IRFU, France; GNSF, Georgia; BMBF, DFG, HGF, MPG and AvH Foundation, Germany; GSRT and NSRF, Greece; ISF, MINERVA, GIF, I-CORE and Benoziyo Center, Israel; INFN, Italy; MEXT and JSPS, Japan; CNRST, Morocco; FOM and NWO, Netherlands; BRF and RCN, Norway; MNiSW and NCN, Poland; GRICES and FCT, Portugal; MNE/IFA, Romania; MES of Russia and ROSATOM, Russian Federation; JINR; MSTD, Serbia; MSSR, Slovakia; ARRS and MIZŠ, Slovenia; DST/NRF, South Africa; MINECO, Spain; SRC and Wallenberg Foundation, Sweden; SER, SNSF and Cantons of Bern and Geneva, Switzerland; NSC, Taiwan; TAEK, Turkey; STFC, the Royal Society and Leverhulme Trust, United Kingdom; DOE and NSF, United States of America.

The crucial computing support from all WLCG partners is acknowledged gratefully, in particular from CERN and the ATLAS Tier-1 facilities at TRIUMF (Canada), NDGF (Denmark, Norway, Sweden), CC-IN2P3 (France), KIT/GridKA (Germany), INFN-CNAF (Italy), NL-T1 (Netherlands), PIC (Spain), ASGC (Taiwan), RAL (UK) and BNL (USA) and in the Tier-2 facilities worldwide.

References

- [1] H. Miyazawa, *Baryon Number Changing Currents*, *Prog. Theor. Phys.* **36** (6) (1966) 1266.
- [2] P. Ramond, *Dual Theory for Free Fermions*, *Phys. Rev.* **D 3** (1971) 2415.
- [3] Y. A. Gol’fand and E. P. Likhtman, *Extension of the Algebra of Poincare Group Generators and Violation of p Invariance*, *JETP Lett.* **13** (1971) 323. [*Pisma Zh. Eksp. Teor. Fiz.* **13** (1971) 452].
- [4] A. Neveu and J. H. Schwarz, *Factorizable dual model of pions*, *Nucl. Phys.* **B 31** (1971) 86.
- [5] A. Neveu and J. H. Schwarz, *Quark Model of Dual Pions*, *Phys. Rev.* **D 4** (1971) 1109.
- [6] J. Gervais and B. Sakita, *Field theory interpretation of supergauges in dual models*, *Nucl. Phys.* **B 34** (1971) 632.
- [7] D. V. Volkov and V. P. Akulov, *Is the Neutrino a Goldstone Particle?*, *Phys. Lett.* **B 46** (1973) 109.
- [8] J. Wess and B. Zumino, *A Lagrangian Model Invariant Under Supergauge Transformations*, *Phys. Lett.* **B 49** (1974) 52.
- [9] J. Wess and B. Zumino, *Supergauge Transformations in Four-Dimensions*, *Nucl. Phys.* **B 70** (1974) 39.
- [10] S. Weinberg, *Implications of Dynamical Symmetry Breaking*, *Phys. Rev.* **D 13** (1976) 974.
- [11] E. Gildener, *Gauge Symmetry Hierarchies*, *Phys. Rev.* **D 14** (1976) 1667.
- [12] S. Weinberg, *Implications of Dynamical Symmetry Breaking: An Addendum*, *Phys. Rev.* **D 19** (1979) 1277.

- [13] L. Susskind, *Dynamics of Spontaneous Symmetry Breaking in the Weinberg- Salam Theory*, *Phys. Rev. D* **20** (1979) 2619.
- [14] P. Fayet, *Supersymmetry and Weak, Electromagnetic and Strong Interactions*, *Phys. Lett. B* **64** (1976) 159.
- [15] P. Fayet, *Spontaneously Broken Supersymmetric Theories of Weak, Electromagnetic and Strong Interactions*, *Phys. Lett. B* **69** (1977) 489.
- [16] G. R. Farrar and P. Fayet, *Phenomenology of the Production, Decay, and Detection of New Hadronic States Associated with Supersymmetry*, *Phys. Lett. B* **76** (1978) 575.
- [17] P. Fayet, *Relations Between the Masses of the Superpartners of Leptons and Quarks, the Goldstino Couplings and the Neutral Currents*, *Phys. Lett. B* **84** (1979) 416.
- [18] S. Dimopoulos and H. Georgi, *Softly Broken Supersymmetry and $SU(5)$* , *Nucl. Phys. B* **193** (1981) 150.
- [19] G. Jungman, M. Kamionkowski, and K. Griest, *Supersymmetric dark matter*, *Physics Reports* **267** (1996) 195.
- [20] H. Goldberg, *Constraint on the photino mass from cosmology*, *Phys. Rev. Lett.* **50** (1983) 1419.
- [21] J. Ellis, J. Hagelin, D. Nanopoulos, K. Olive, and M. Srednicki, *Supersymmetric relics from the Big Bang*, *Nucl. Phys. B* **238** (1984) 453.
- [22] L. Evans and P. Bryant, *LHC Machine*, *JINST* **3** (2008) S08001.
- [23] R. Barbieri and G. F. Giudice, *Upper Bounds on Supersymmetric Particle Masses*, *Nucl. Phys. B* **306** (1988) 63.
- [24] B. de Carlos and J. A. Casas, *One loop analysis of the electroweak breaking in supersymmetric models and the fine tuning problem*, *Phys. Lett. B* **309** (1993) 320, [[hep-ph/9303291](#)].
- [25] G. Belanger, F. Boudjema, A. Cottrant, A. Pukhov, and A. Semenov, *WMAP constraints on SUGRA models with non-universal gaugino masses and prospects for direct detection*, *Nucl. Phys. B* **706** (2005) 411, [[hep-ph/0407218](#)].
- [26] S. King, J. Roberts, and D. Roy, *Natural dark matter in SUSY GUTs with non-universal gaugino masses*, *JHEP* **0710** (2007) 106, [[arXiv:0705.4219](#)].
- [27] M. Dine and W. Fischler, *A Phenomenological Model of Particle Physics Based on Supersymmetry*, *Phys. Lett. B* **110** (1982) 227.
- [28] L. Alvarez-Gaume, M. Claudson, and M. B. Wise, *Low-Energy Supersymmetry*, *Nucl. Phys. B* **207** (1982) 96.
- [29] C. R. Nappi and B. A. Ovrut, *Supersymmetric Extension of the $SU(3) \times SU(2) \times U(1)$ Model*, *Phys. Lett. B* **113** (1982) 175.
- [30] M. Dine and A. E. Nelson, *Dynamical supersymmetry breaking at low-energies*, *Phys. Rev. D* **48** (1993) 1277, [[hep-ph/9303230](#)].
- [31] M. Dine, A. E. Nelson, and Y. Shirman, *Low-energy dynamical supersymmetry breaking simplified*, *Phys. Rev. D* **51** (1995) 1362, [[hep-ph/9408384](#)].
- [32] M. Dine, A. E. Nelson, Y. Nir, and Y. Shirman, *New tools for low-energy dynamical supersymmetry breaking*, *Phys. Rev. D* **53** (1996) 2658, [[hep-ph/9507378](#)].

- [33] L. Randall and R. Sundrum, *Out of this world supersymmetry breaking*, *Nucl. Phys. B* **557** (1999) 79, [[hep-th/9810155](#)].
- [34] G. F. Giudice, M. A. Luty, H. Murayama, and R. Rattazzi, *Gaugino mass without singlets*, *JHEP* **9812** (1998) 027, [[hep-ph/9810442](#)].
- [35] D. Albornoz Vásquez, G. Bélanger, and C. Boehm, *Revisiting light neutralino scenarios in the MSSM*, *Phys. Rev. D* **84** (2011) 095015, [[arXiv:1108.1338](#)].
- [36] **ATLAS** Collaboration, *Search for direct production of charginos, neutralinos and sleptons in final states with two leptons and missing transverse momentum in pp collisions at $\sqrt{s} = 8$ TeV with the ATLAS detector*, *JHEP* **1405** (2014) 071, [[arXiv:1403.5294](#)].
- [37] **ATLAS** Collaboration, *Search for direct production of charginos and neutralinos in events with three leptons and missing transverse momentum in pp collisions at $\sqrt{s} = 8$ TeV with the ATLAS detector*, *JHEP* **1404** (2014) 169, [[arXiv:1402.7029](#)].
- [38] **CMS** Collaboration, *Searches for electroweak production of charginos, neutralinos, and sleptons decaying to leptons and W, Z, and Higgs bosons in pp collisions at 8 TeV*, [arXiv:1405.7570](#).
- [39] LEP SUSY Working Group (ALEPH, DELPHI, L3, OPAL). Notes LEPSUSYWG/01-03.1, 04-01.1, <http://lepsusy.web.cern.ch/lepsusy/Welcome.html>.
- [40] **DELPHI** Collaboration, J. Abdallah et al., *Searches for supersymmetric particles in e^+e^- collisions up to 208 GeV and interpretation of the results within the MSSM*, *Eur. Phys. J. C* **31** (2003) 421, [[hep-ex/0311019](#)].
- [41] **L3** Collaboration, M. Acciarri et al., *Search for charginos and neutralinos in e^+e^- collisions at $\sqrt{s} = 189$ GeV*, *Phys. Lett. B* **472** (2000) 420, [[hep-ex/9910007](#)].
- [42] **OPAL** Collaboration, G. Abbiendi et al., *Search for chargino and neutralino production at $\sqrt{s} = 192$ GeV to 209 GeV at LEP*, *Eur. Phys. J. C* **35** (2004) 1, [[hep-ex/0401026](#)].
- [43] A. Djouadi, J.-L. Kneur, and G. Moultaka, *SuSpect: A Fortran code for the supersymmetric and Higgs particle spectrum in MSSM*, *Comput. Phys. Commun.* **176** (2007) 426, [[hep-ph/0211331](#)].
- [44] C. F. Berger, J. S. Gainer, J. L. Hewett, and T. G. Rizzo, *Supersymmetry Without Prejudice*, *JHEP* **0902** (2009) 023, [[arXiv:0812.0980](#)].
- [45] S. S. AbdusSalam, B. Allanach, F. Quevedo, F. Feroz, and M. Hobson, *Fitting the Phenomenological MSSM*, *Phys. Rev. D* **81** (2010) 095012, [[arXiv:0904.2548](#)].
- [46] J. Alwall, P. Schuster, and N. Toro, *Simplified Models for a First Characterization of New Physics at the LHC*, *Phys. Rev. D* **79** (2009) 075020, [[arXiv:0810.3921](#)].
- [47] D. Alves et al., *Simplified Models for LHC New Physics Searches*, *J. Phys. G* **39** (2012) 105005, [[arXiv:1105.2838](#)].
- [48] H. Baer, C. Chen, F. Paige, and X. Tata, *Detecting Sleptons at Hadron Colliders and Supercolliders*, *Phys. Rev. D* **49** (1994) 3283, [[hep-ph/9311248](#)].
- [49] **ATLAS** Collaboration, *The ATLAS Experiment at the CERN Large Hadron Collider*, *JINST* **3** (2008) S08003.
- [50] **ATLAS** Collaboration, *Improved luminosity determination in pp collisions at $\sqrt{s} = 7$ TeV using the ATLAS detector at the LHC*, *Eur. Phys. J. C* **73** (2013) 2518, [[arXiv:1302.4393](#)].

- [51] **ATLAS** Collaboration, *Performance of the ATLAS Tau Trigger in 2011*, *ATLAS-CONF-2013-006*, [<http://cdsweb.cern.ch/record/1510157>].
- [52] **ATLAS** Collaboration, *The ATLAS Simulation Infrastructure*, *Eur. Phys. J. C* **70** (2010) 823, [[arXiv:1005.4568](https://arxiv.org/abs/1005.4568)].
- [53] **GEANT4** Collaboration, S. Agostinelli et al., *GEANT4: A simulation toolkit*, *Nucl. Instrum. Meth. A* **506** (2003) 250.
- [54] T. Gleisberg et al., *Event generation with sherpa 1.1*, *JHEP* **0902** (2009) 007, [[arXiv:0811.4622](https://arxiv.org/abs/0811.4622)].
- [55] T. Binoth, M. Ciccolini, N. Kauer, and M. Kramer, *Gluon-induced W-boson pair production at the LHC*, *JHEP* **0612** (2006) 046, [[hep-ph/0611170](https://arxiv.org/abs/hep-ph/0611170)].
- [56] J. Alwall, M. Herquet, F. Maltoni, O. Mattelaer, and T. Stelzer, *MadGraph 5 : Going Beyond*, *JHEP* **1106** (2011) 128, [[arXiv:1106.0522](https://arxiv.org/abs/1106.0522)].
- [57] T. Sjostrand, S. Mrenna, and P. Z. Skands, *PYTHIA 6.4 Physics and Manual*, *JHEP* **0605** (2006) 026, [[hep-ph/0603175](https://arxiv.org/abs/hep-ph/0603175)].
- [58] T. Sjostrand, S. Mrenna, and P. Skands, *Brief Introduction to PYTHIA 8.1*, *Comput. Phys. Comm.* **178** (2008) 852, [[arXiv:0710.3820](https://arxiv.org/abs/0710.3820)].
- [59] S. Frixione and B. R. Webber, *Matching NLO QCD computations and parton shower simulations*, *JHEP* **0206** (2002) 029, [[hep-ph/0204244](https://arxiv.org/abs/hep-ph/0204244)].
- [60] S. Frixione, P. Nason, and B. R. Webber, *Matching NLO QCD and parton showers in heavy flavour production*, *JHEP* **0308** (2003) 007, [[hep-ph/0305252](https://arxiv.org/abs/hep-ph/0305252)].
- [61] S. Frixione, E. Laenen, P. Motylinski, and B. R. Webber, *Single-top production in MC@NLO*, *JHEP* **0603** (2006) 092, [[hep-ph/0512250](https://arxiv.org/abs/hep-ph/0512250)].
- [62] B. P. Kersevan and E. Richter-Was, *The Monte Carlo event generator AcerMC versions 2.0 to 3.8 with interfaces to PYTHIA 6.4, HERWIG 6.5 and ARIADNE 4.1*, *Comp. Phys. Commun.* **184** (2013) 919, [[hep-ph/0201302](https://arxiv.org/abs/hep-ph/0201302)].
- [63] M. L. Mangano, M. Moretti, F. Piccinini, R. Pittau, and A. D. Polosa, *Alpgen, a generator for hard multiparton processes in hadronic collisions*, *JHEP* **0307** (2003) 001, [[hep-ph/0206293](https://arxiv.org/abs/hep-ph/0206293)].
- [64] S. Frixione, P. Nason, and C. Oleari, *Matching NLO QCD computations with Parton Shower simulations: the POWHEG method*, *JHEP* **0711** (2007) 070, [[arXiv:0709.2092](https://arxiv.org/abs/0709.2092)].
- [65] **ATLAS** Collaboration, *ATLAS tunes of PYTHIA 6 and Pythia 8 for MC11*, ATLAS-PHYS-PUB-2011-009, [<http://cds.cern.ch/record/1363300>].
- [66] P. Z. Skands, *Tuning Monte Carlo Generators: The Perugia Tunes*, *Phys. Rev. D* **82** (2010) 074018, [[arXiv:1005.3457](https://arxiv.org/abs/1005.3457)].
- [67] H.-L. Lai et al., *New parton distributions for collider physics*, *Phys. Rev. D* **82** (2010) 074024, [[arXiv:1007.2241](https://arxiv.org/abs/1007.2241)].
- [68] J. Pumplin et al., *New generation of parton distributions with uncertainties from global QCD analysis*, *JHEP* **0207** (2002) 012, [[hep-ph/0201195](https://arxiv.org/abs/hep-ph/0201195)].
- [69] S. Catani, L. Cieri, G. Ferrera, D. de Florian, and M. Grazzini, *Vector boson production at hadron colliders: A Fully exclusive QCD calculation at NNLO*, *Phys. Rev. Lett.* **103** (2009) 082001, [[arXiv:0903.2120](https://arxiv.org/abs/0903.2120)].

- [70] A. Martin, W. Stirling, R. Thorne and G. Watt, *Update of parton distributions at NNLO*, *Phys. Lett. B* **652** (2007) 292, [[arXiv:0706.0459](#)].
- [71] M. Czakon and A. Mitov, *Top++: A Program for the Calculation of the Top-Pair Cross-Section at Hadron Colliders*, [arXiv:1112.5675](#).
- [72] J. M. Campbell and R. K. Ellis, *An Update on vector boson pair production at hadron colliders*, *Phys. Rev. D* **60** (1999) 113006, [[hep-ph/9905386](#)].
- [73] J. M. Campbell, R. K. Ellis, and C. Williams, *Vector boson pair production at the LHC*, *JHEP* **1107** (2011) 018, [[arXiv:1105.0020](#)].
- [74] J. M. Campbell and R. K. Ellis, *$t\bar{t}W^\pm$ production and decay at NLO*, *JHEP* **1207** (2012) 052, [[arXiv:1204.5678](#)].
- [75] M. Garzelli, A. Kardos, C. Papadopoulos, and Z. Trocsanyi, *$t\bar{t}W^\pm$ and $t\bar{t}Z$ hadroproduction at NLO accuracy in QCD with parton shower and hadronization effects*, *JHEP* **1211** (2012) 056, [[arXiv:1208.2665](#)].
- [76] M. Bahr et al., *Herwig++ Physics and Manual*, *Eur. Phys. J. C* **58** (2008) 639, [[arXiv:0803.0883](#)].
- [77] W. Beenakker, M. Klasen, M. Kramer, T. Plehn, M. Spira, et al., *The Production of charginos/neutralinos and sleptons at hadron colliders*, *Phys. Rev. Lett.* **83** (1999) 3780–3783, [[hep-ph/9906298](#)].
- [78] B. Fuks, M. Klasen, D. R. Lamprea, and M. Rothering, *Gaugino production in proton-proton collisions at a center-of-mass energy of 8 TeV*, *JHEP* **1210** (2012) 081, [[arXiv:1207.2159](#)].
- [79] B. Fuks, M. Klasen, D. R. Lamprea, and M. Rothering, *Precision predictions for electroweak superpartner production at hadron colliders with Resummino*, *Eur. Phys. J. C* **73** (2013) 2480, [[arXiv:1304.0790](#)].
- [80] B. Fuks, M. Klasen, D. R. Lamprea, and M. Rothering, *Revisiting slepton pair production at the Large Hadron Collider*, *JHEP* **1401** (2014) 168, [[arXiv:1310.2621](#)].
- [81] S. S. AbdusSalam et al., *Benchmark Models, Planes, Lines and Points for Future SUSY Searches at the LHC*, *Eur. Phys. J. C* **71** (2011) 1835, [[arXiv:1109.3859](#)].
- [82] M. Cacciari, G. P. Salam, and G. Soyez, *The anti- k_T jet clustering algorithm*, *JHEP* **0804** (2008) 063, [[arXiv:0802.1189](#)].
- [83] M. Cacciari and G. P. Salam, *Dispelling the N^3 myth for the k_t jet-finder*, *Phys. Lett. B* **641** (2006) 57, [[hep-ph/0512210](#)].
- [84] **ATLAS** Collaboration, *Jet energy measurement with the ATLAS detector in proton-proton collisions at $\sqrt{s} = 7$ TeV*, *Eur. Phys. J. C* **73** (2013) 2304, [[arXiv:1112.6426](#)].
- [85] M. Cacciari and G. P. Salam, *Pileup subtraction using jet areas*, *Phys. Lett. B* **659** (2008) 119, [[arXiv:0707.1378](#)].
- [86] **ATLAS** Collaboration, *Electron performance measurements with the ATLAS detector using the 2010 LHC proton-proton collision data*, *Eur. Phys. J. C* **72** (2012) 1909, [[arXiv:1110.3174](#)].
- [87] **ATLAS** Collaboration, *Preliminary results on the muon reconstruction efficiency, momentum resolution, and momentum scale in ATLAS 2012 pp collision data*, ATLAS-CONF-2013-088, <http://cdsweb.cern.ch/record/1580207>.

- [88] **ATLAS** Collaboration, *Determination of the tau energy scale and the associated systematic uncertainty in proton-proton collisions at $\sqrt{s} = 8$ TeV with the ATLAS detector at the LHC in 2012*, ATLAS-CONF-2013-044 [<http://cdsweb.cern.ch/record/1544036>].
- [89] **ATLAS** Collaboration, *Identification of Hadronic Decays of Tau Leptons in 2012 Data with the ATLAS Detector*, ATLAS-CONF-2013-064 [<http://cdsweb.cern.ch/record/1562839>].
- [90] **ATLAS** Collaboration, *Performance of Missing Transverse Momentum Reconstruction in Proton-Proton Collisions at 7 TeV with ATLAS*, *Eur. Phys. J. C* **72** (2012) 1844, [[arXiv:1108.5602](https://arxiv.org/abs/1108.5602)].
- [91] **ATLAS** Collaboration, *Commissioning of the ATLAS high-performance b-tagging algorithms in the 7 TeV collision data*, ATLAS-CONF-2011-102 [<http://cdsweb.cern.ch/record/1369219>].
- [92] **ATLAS** Collaboration, *Electron reconstruction and identification efficiency measurements with the ATLAS detector using the 2011 LHC proton-proton collision data*, [arXiv:1404.2240](https://arxiv.org/abs/1404.2240).
- [93] C. G. Lester and D. J. Summers, *Measuring masses of semiinvisibly decaying particles pair produced at hadron colliders*, *Phys. Lett. B* **463** (1999) 99, [[hep-ph/9906349](https://arxiv.org/abs/hep-ph/9906349)].
- [94] A. Barr, C. Lester, and P. Stephens, *m_{T2} : The Truth behind the glamour*, *J. Phys. G* **29** (2003) 2343, [[hep-ph/0304226](https://arxiv.org/abs/hep-ph/0304226)].
- [95] G. Cowan, K. Cranmer, E. Gross, and O. Vitells, *Asymptotic formulae for likelihood-based tests of new physics*, *Eur. Phys. J. C* **71** (2011) 1554, [[arXiv:1007.1727](https://arxiv.org/abs/1007.1727)].
- [96] D. Tovey, *On measuring the masses of pair-produced semi-invisibly decaying particles at hadron colliders*, *JHEP* **0804** (2008) 034, [[arXiv:0802.2879](https://arxiv.org/abs/0802.2879)].
- [97] G. Polesello and D. Tovey, *Supersymmetric particle mass measurement with the boost-corrected contranverse mass*, *JHEP* **1003** (2010) 030, [[arXiv:0910.0174](https://arxiv.org/abs/0910.0174)].
- [98] **ATLAS** Collaboration, *Measuring the b-tag efficiency in a $t\bar{t}$ sample with 4.7 fb^{-1} of data from the ATLAS detector*, ATLAS-CONF-2012-097 [<http://cds.cern.ch/record/1460443>].
- [99] J. Alwall et al., *Comparative study of various algorithms for the merging of parton showers and matrix elements in hadronic collisions*, *Eur. Phys. J. C* **53** (2008) 473, [[arXiv:0706.2569](https://arxiv.org/abs/0706.2569)].
- [100] M. Kramer, A. Kulesza, R. van der Leeuw, M. Mangano, S. Padhi, et al., *Supersymmetry production cross sections in pp collisions at $\sqrt{s} = 7$ TeV*, [arXiv:1206.2892](https://arxiv.org/abs/1206.2892).
- [101] A. L. Read, *Presentation of search results: the CLs technique*, *J. Phys. G* **28** (2002) 2693.

The ATLAS Collaboration

G. Aad⁸⁴, B. Abbott¹¹², J. Abdallah¹⁵², S. Abdel Khalek¹¹⁶, O. Abdinov¹¹, R. Aben¹⁰⁶, B. Abi¹¹³, M. Abolins⁸⁹, O.S. AbouZeid¹⁵⁹, H. Abramowicz¹⁵⁴, H. Abreu¹⁵³, R. Abreu³⁰, Y. Abulaiti^{147a,147b}, B.S. Acharya^{165a,165b,a}, L. Adamczyk^{38a}, D.L. Adams²⁵, J. Adelman¹⁷⁷, S. Adomeit⁹⁹, T. Adye¹³⁰, T. Agatonovic-Jovin^{13a}, J.A. Aguilar-Saavedra^{125a,125f}, M. Agustoni¹⁷, S.P. Ahlen²², F. Ahmadov^{64,b}, G. Aielli^{134a,134b}, H. Akerstedt^{147a,147b}, T.P.A. Åkesson⁸⁰, G. Akimoto¹⁵⁶, A.V. Akimov⁹⁵, G.L. Alberghi^{20a,20b}, J. Albert¹⁷⁰, S. Albrand⁵⁵, M.J. Alconada Verzini⁷⁰, M. Aleksa³⁰, I.N. Aleksandrov⁶⁴, C. Alexa^{26a}, G. Alexander¹⁵⁴, G. Alexandre⁴⁹, T. Alexopoulos¹⁰, M. Alhroob^{165a,165c}, G. Alimonti^{90a}, L. Alio⁸⁴, J. Alison³¹, B.M.M. Allbrooke¹⁸, L.J. Allison⁷¹, P.P. Allport⁷³, J. Almond⁸³, A. Aloisio^{103a,103b}, A. Alonso³⁶, F. Alonso⁷⁰, C. Alpigiani⁷⁵, A. Altheimer³⁵, B. Alvarez Gonzalez⁸⁹, M.G. Alviggi^{103a,103b}, K. Amako⁶⁵, Y. Amaral Coutinho^{24a}, C. Amelung²³, D. Amidei⁸⁸, S.P. Amor Dos Santos^{125a,125c}, A. Amorim^{125a,125b}, S. Amoroso⁴⁸, N. Amram¹⁵⁴, G. Amundsen²³, C. Anastopoulos¹⁴⁰, L.S. Ancu⁴⁹, N. Andari³⁰, T. Andeen³⁵, C.F. Anders^{58b}, G. Anders³⁰, K.J. Anderson³¹, A. Andreazza^{90a,90b}, V. Andrei^{58a}, X.S. Anduaga⁷⁰, S. Angelidakis⁹, I. Angelozzi¹⁰⁶, P. Anger⁴⁴, A. Angerami³⁵, F. Anghinolfi³⁰, A.V. Anisenkov¹⁰⁸, N. Anjos^{125a}, A. Annovi⁴⁷, A. Antonaki⁹, M. Antonelli⁴⁷, A. Antonov⁹⁷, J. Antos^{145b}, F. Anulli^{133a}, M. Aoki⁶⁵, L. Aperio Bella¹⁸, R. Apolle^{119,c}, G. Arabidze⁸⁹, I. Aracena¹⁴⁴, Y. Arai⁶⁵, J.P. Araque^{125a}, A.T.H. Arce⁴⁵, J-F. Arguin⁹⁴, S. Argyropoulos⁴², M. Arik^{19a}, A.J. Armbruster³⁰, O. Arnaez³⁰, V. Arnal⁸¹, H. Arnold⁴⁸, M. Arratia²⁸, O. Arslan²¹, A. Artamonov⁹⁶, G. Artoni²³, S. Asai¹⁵⁶, N. Asbah⁴², A. Ashkenazi¹⁵⁴, B. Åsman^{147a,147b}, L. Asquith⁶, K. Assamagan²⁵, R. Astalos^{145a}, M. Atkinson¹⁶⁶, N.B. Atlay¹⁴², B. Auerbach⁶, K. Augsten¹²⁷, M. Aurousseau^{146b}, G. Avolio³⁰, G. Azuelos^{94,d}, Y. Azuma¹⁵⁶, M.A. Baak³⁰, A. Baas^{58a}, C. Bacci^{135a,135b}, H. Bachacou¹³⁷, K. Bachas¹⁵⁵, M. Backes³⁰, M. Backhaus³⁰, J. Backus Mayes¹⁴⁴, E. Badescu^{26a}, P. Bagiacchi^{133a,133b}, P. Bagnaia^{133a,133b}, Y. Bai^{33a}, T. Bain³⁵, J.T. Baines¹³⁰, O.K. Baker¹⁷⁷, P. Balek¹²⁸, F. Balli¹³⁷, E. Banas³⁹, Sw. Banerjee¹⁷⁴, A.A.E. Bannoura¹⁷⁶, V. Bansal¹⁷⁰, H.S. Bansil¹⁸, L. Barak¹⁷³, S.P. Baranov⁹⁵, E.L. Barberio⁸⁷, D. Barberis^{50a,50b}, M. Barbero⁸⁴, T. Barillari¹⁰⁰, M. Barisonzi¹⁷⁶, T. Barklow¹⁴⁴, N. Barlow²⁸, B.M. Barnett¹³⁰, R.M. Barnett¹⁵, Z. Barnovska⁵, A. Baroncelli^{135a}, G. Barone⁴⁹, A.J. Barr¹¹⁹, F. Barreiro⁸¹, J. Barreiro Guimarães da Costa⁵⁷, R. Bartoldus¹⁴⁴, A.E. Barton⁷¹, P. Bartos^{145a}, V. Bartsch¹⁵⁰, A. Bassalat¹¹⁶, A. Basye¹⁶⁶, R.L. Bates⁵³, J.R. Batley²⁸, M. Battaglia¹³⁸, M. Battistin³⁰, F. Bauer¹³⁷, H.S. Bawa^{144,e}, M.D. Beattie⁷¹, T. Beau⁷⁹, P.H. Beauchemin¹⁶², R. Beccherle^{123a,123b}, P. Bechtel²¹, H.P. Beck¹⁷, K. Becker¹⁷⁶, S. Becker⁹⁹, M. Beckingham¹⁷¹, C. Becot¹¹⁶, A.J. Beddall^{19c}, A. Beddall^{19c}, S. Bedikian¹⁷⁷, V.A. Bednyakov⁶⁴, C.P. Bee¹⁴⁹, L.J. Beemster¹⁰⁶, T.A. Beermann¹⁷⁶, M. Begel²⁵, K. Behr¹¹⁹, C. Belanger-Champagne⁸⁶, P.J. Bell⁴⁹, W.H. Bell⁴⁹, G. Bella¹⁵⁴, L. Bellagamba^{20a}, A. Bellerive²⁹, M. Bellomo⁸⁵, K. Belotskiy⁹⁷, O. Beltramello³⁰, O. Benary¹⁵⁴, D. Bencheikroun^{136a}, K. Bendtz^{147a,147b}, N. Benekos¹⁶⁶, Y. Benhammou¹⁵⁴, E. Benhar Noccioli⁴⁹, J.A. Benitez Garcia^{160b}, D.P. Benjamin⁴⁵, J.R. Bensinger²³, K. Benslama¹³¹, S. Bentvelsen¹⁰⁶, D. Berge¹⁰⁶, E. Bergeaas Kuutmann¹⁶, N. Berger⁵,

F. Berghaus¹⁷⁰, J. Beringer¹⁵, C. Bernard²², P. Bernat⁷⁷, C. Bernius⁷⁸,
 F.U. Bernlochner¹⁷⁰, T. Berry⁷⁶, P. Berta¹²⁸, C. Bertella⁸⁴, G. Bertoli^{147a,147b},
 F. Bertolucci^{123a,123b}, C. Bertsche¹¹², D. Bertsche¹¹², M.I. Besana^{90a}, G.J. Besjes¹⁰⁵,
 O. Bessidskaia^{147a,147b}, M.F. Bessner⁴², N. Besson¹³⁷, C. Betancourt⁴⁸, S. Bethke¹⁰⁰,
 W. Bhimji⁴⁶, R.M. Bianchi¹²⁴, L. Bianchini²³, M. Bianco³⁰, O. Biebel⁹⁹, S.P. Bieniek⁷⁷,
 K. Bierwagen⁵⁴, J. Biesiada¹⁵, M. Biglietti^{135a}, J. Bilbao De Mendizabal⁴⁹, H. Bilokon⁴⁷,
 M. Bindi⁵⁴, S. Binet¹¹⁶, A. Bingul^{19c}, C. Bini^{133a,133b}, C.W. Black¹⁵¹, J.E. Black¹⁴⁴,
 K.M. Black²², D. Blackburn¹³⁹, R.E. Blair⁶, J.-B. Blanchard¹³⁷, T. Blazek^{145a}, I. Bloch⁴²,
 C. Blocker²³, W. Blum^{82,*}, U. Blumenschein⁵⁴, G.J. Bobbink¹⁰⁶, V.S. Bobrovnikov¹⁰⁸,
 S.S. Bocchetta⁸⁰, A. Bocci⁴⁵, C. Bock⁹⁹, C.R. Boddy¹¹⁹, M. Boehler⁴⁸, T.T. Boek¹⁷⁶,
 J.A. Bogaerts³⁰, A.G. Bogdanchikov¹⁰⁸, A. Bogouch^{91,*}, C. Bohm^{147a}, J. Bohm¹²⁶,
 V. Boisvert⁷⁶, T. Bold^{38a}, V. Boldea^{26a}, A.S. Boldyrev⁹⁸, M. Bomben⁷⁹, M. Bona⁷⁵,
 M. Boonekamp¹³⁷, A. Borisov¹²⁹, G. Borissov⁷¹, M. Borri⁸³, S. Borroni⁴², J. Bortfeldt⁹⁹,
 V. Bortolotto^{135a,135b}, K. Bos¹⁰⁶, D. Boscherini^{20a}, M. Bosman¹², H. Boterenbrood¹⁰⁶,
 J. Boudreau¹²⁴, J. Bouffard², E.V. Bouhova-Thacker⁷¹, D. Boumediene³⁴,
 C. Bourdarios¹¹⁶, N. Bousson¹¹³, S. Boutouil^{136d}, A. Boveia³¹, J. Boyd³⁰, I.R. Boyko⁶⁴,
 J. Bracinik¹⁸, A. Brandt⁸, G. Brandt¹⁵, O. Brandt^{58a}, U. Bratzler¹⁵⁷, B. Brau⁸⁵,
 J.E. Brau¹¹⁵, H.M. Braun^{176,*}, S.F. Brazzale^{165a,165c}, B. Brelier¹⁵⁹, K. Brendlinger¹²¹,
 A.J. Brennan⁸⁷, R. Brenner¹⁶⁷, S. Bressler¹⁷³, K. Bristow^{146c}, T.M. Bristow⁴⁶,
 D. Britton⁵³, F.M. Brochu²⁸, I. Brock²¹, R. Brock⁸⁹, C. Bromberg⁸⁹, J. Bronner¹⁰⁰,
 G. Brooijmans³⁵, T. Brooks⁷⁶, W.K. Brooks^{32b}, J. Brosamer¹⁵, E. Brost¹¹⁵, J. Brown⁵⁵,
 P.A. Bruckman de Renstrom³⁹, D. Bruncko^{145b}, R. Bruneliere⁴⁸, S. Brunet⁶⁰, A. Bruni^{20a},
 G. Bruni^{20a}, M. Bruschi^{20a}, L. Bryngemark⁸⁰, T. Buanes¹⁴, Q. Buat¹⁴³, F. Bucci⁴⁹,
 P. Buchholz¹⁴², R.M. Buckingham¹¹⁹, A.G. Buckley⁵³, S.I. Buda^{26a}, I.A. Budagov⁶⁴,
 F. Buehrer⁴⁸, L. Bugge¹¹⁸, M.K. Bugge¹¹⁸, O. Bulekov⁹⁷, A.C. Bundock⁷³,
 H. Burckhart³⁰, S. Burdin⁷³, B. Burghgrave¹⁰⁷, S. Burke¹³⁰, I. Burmeister⁴³, E. Busato³⁴,
 D. Büscher⁴⁸, V. Büscher⁸², P. Bussey⁵³, C.P. Buszello¹⁶⁷, B. Butler⁵⁷, J.M. Butler²²,
 A.I. Butt³, C.M. Buttar⁵³, J.M. Butterworth⁷⁷, P. Butti¹⁰⁶, W. Buttinger²⁸, A. Buzatu⁵³,
 M. Byszewski¹⁰, S. Cabrera Urbán¹⁶⁸, D. Caforio^{20a,20b}, O. Cakir^{4a}, P. Calafiura¹⁵,
 A. Calandri¹³⁷, G. Calderini⁷⁹, P. Calfayan⁹⁹, R. Calkins¹⁰⁷, L.P. Caloba^{24a}, D. Calvet³⁴,
 S. Calvet³⁴, R. Camacho Toro⁴⁹, S. Camarda⁴², D. Cameron¹¹⁸, L.M. Caminada¹⁵,
 R. Caminal Armadans¹², S. Campana³⁰, M. Campanelli⁷⁷, A. Campoverde¹⁴⁹,
 V. Canale^{103a,103b}, A. Canepa^{160a}, M. Cano Bret⁷⁵, J. Cantero⁸¹, R. Cantrill^{125a},
 T. Cao⁴⁰, M.D.M. Capeans Garrido³⁰, I. Caprini^{26a}, M. Caprini^{26a}, M. Capua^{37a,37b},
 R. Caputo⁸², R. Cardarelli^{134a}, T. Carli³⁰, G. Carlino^{103a}, L. Carminati^{90a,90b},
 S. Caron¹⁰⁵, E. Carquin^{32a}, G.D. Carrillo-Montoya^{146c}, J.R. Carter²⁸, J. Carvalho^{125a,125c},
 D. Casadei⁷⁷, M.P. Casado¹², M. Casolino¹², E. Castaneda-Miranda^{146b}, A. Castelli¹⁰⁶,
 V. Castillo Gimenez¹⁶⁸, N.F. Castro^{125a}, P. Catastini⁵⁷, A. Catinaccio³⁰,
 J.R. Catmore¹¹⁸, A. Cattai³⁰, G. Cattani^{134a,134b}, S. Caughron⁸⁹, V. Cavaliere¹⁶⁶,
 D. Cavalli^{90a}, M. Cavalli-Sforza¹², V. Cavasinni^{123a,123b}, F. Ceradini^{135a,135b}, B. Cerio⁴⁵,
 K. Cerny¹²⁸, A.S. Cerqueira^{24b}, A. Cerri¹⁵⁰, L. Cerrito⁷⁵, F. Cerutti¹⁵, M. Cerv³⁰,
 A. Cervelli¹⁷, S.A. Cetin^{19b}, A. Chafaq^{136a}, D. Chakraborty¹⁰⁷, I. Chalupkova¹²⁸,
 P. Chang¹⁶⁶, B. Chapleau⁸⁶, J.D. Chapman²⁸, D. Charfeddine¹¹⁶, D.G. Charlton¹⁸,

C.C. Chau¹⁵⁹, C.A. Chavez Barajas¹⁵⁰, S. Cheatham⁸⁶, A. Chegwidan⁸⁹, S. Chekanov⁶,
 S.V. Chekulaev^{160a}, G.A. Chelkov^{64,f}, M.A. Chelstowska⁸⁸, C. Chen⁶³, H. Chen²⁵,
 K. Chen¹⁴⁹, L. Chen^{33d,g}, S. Chen^{33c}, X. Chen^{146c}, Y. Chen⁶⁶, Y. Chen³⁵, H.C. Cheng⁸⁸,
 Y. Cheng³¹, A. Cheplakov⁶⁴, R. Cherkaoui El Moursli^{136e}, V. Chernyatin^{25,*}, E. Cheu⁷,
 L. Chevalier¹³⁷, V. Chiarella⁴⁷, G. Chiefari^{103a,103b}, J.T. Childers⁶, A. Chilingarov⁷¹,
 G. Chiodini^{72a}, A.S. Chisholm¹⁸, R.T. Chislett⁷⁷, A. Chitan^{26a}, M.V. Chizhov⁶⁴,
 S. Chouridou⁹, B.K.B. Chow⁹⁹, D. Chromek-Burckhart³⁰, M.L. Chu¹⁵², J. Chudoba¹²⁶,
 J.J. Chwastowski³⁹, L. Chytka¹¹⁴, G. Ciapetti^{133a,133b}, A.K. Ciftci^{4a}, R. Ciftci^{4a},
 D. Cinca⁵³, V. Cindro⁷⁴, A. Ciocio¹⁵, P. Cirkovic^{13b}, Z.H. Citron¹⁷³, M. Citterio^{90a},
 M. Ciubancan^{26a}, A. Clark⁴⁹, P.J. Clark⁴⁶, R.N. Clarke¹⁵, W. Cleland¹²⁴, J.C. Clemens⁸⁴,
 C. Clement^{147a,147b}, Y. Coadou⁸⁴, M. Cobal^{165a,165c}, A. Coccaro¹³⁹, J. Cochran⁶³,
 L. Coffey²³, J.G. Cogan¹⁴⁴, J. Coggeshall¹⁶⁶, B. Cole³⁵, S. Cole¹⁰⁷, A.P. Colijn¹⁰⁶,
 J. Collot⁵⁵, T. Colombo^{58c}, G. Colon⁸⁵, G. Compostella¹⁰⁰, P. Conde Muiño^{125a,125b},
 E. Coniavitis⁴⁸, M.C. Conidi¹², S.H. Connell^{146b}, I.A. Connelly⁷⁶, S.M. Consonni^{90a,90b},
 V. Consorti⁴⁸, S. Constantinescu^{26a}, C. Conta^{120a,120b}, G. Conti⁵⁷, F. Conventi^{103a,h},
 M. Cooke¹⁵, B.D. Cooper⁷⁷, A.M. Cooper-Sarkar¹¹⁹, N.J. Cooper-Smith⁷⁶, K. Copic¹⁵,
 T. Cornelissen¹⁷⁶, M. Corradi^{20a}, F. Corriveau^{86,i}, A. Corso-Radu¹⁶⁴,
 A. Cortes-Gonzalez¹², G. Cortiana¹⁰⁰, G. Costa^{90a}, M.J. Costa¹⁶⁸, D. Costanzo¹⁴⁰,
 D. Côté⁸, G. Cottin²⁸, G. Cowan⁷⁶, B.E. Cox⁸³, K. Cranmer¹⁰⁹, G. Cree²⁹,
 S. Crépe-Renaudin⁵⁵, F. Crescioli⁷⁹, W.A. Cribbs^{147a,147b}, M. Crispin Ortuzar¹¹⁹,
 M. Cristinziani²¹, V. Croft¹⁰⁵, G. Crosetti^{37a,37b}, C.-M. Cuciuc^{26a},
 T. Cuhadar Donszelmann¹⁴⁰, J. Cummings¹⁷⁷, M. Curatolo⁴⁷, C. Cuthbert¹⁵¹,
 H. Cziri¹⁴², P. Czodrowski³, Z. Czyczula¹⁷⁷, S. D'Auria⁵³, M. D'Onofrio⁷³,
 M.J. Da Cunha Sargedas De Sousa^{125a,125b}, C. Da Via⁸³, W. Dabrowski^{38a}, A. Dafinca¹¹⁹,
 T. Dai⁸⁸, O. Dale¹⁴, F. Dallaire⁹⁴, C. Dallapiccola⁸⁵, M. Dam³⁶, A.C. Daniells¹⁸,
 M. Dano Hoffmann¹³⁷, V. Dao⁴⁸, G. Darbo^{50a}, S. Darmora⁸, J.A. Dassoulas⁴²,
 A. Dattagupta⁶⁰, W. Davey²¹, C. David¹⁷⁰, T. Davidek¹²⁸, E. Davies^{119,c}, M. Davies¹⁵⁴,
 O. Davignon⁷⁹, A.R. Davison⁷⁷, P. Davison⁷⁷, Y. Davygora^{58a}, E. Dawe¹⁴³, I. Dawson¹⁴⁰,
 R.K. Daya-Ishmukhametova⁸⁵, K. De⁸, R. de Asmundis^{103a}, S. De Castro^{20a,20b},
 S. De Cecco⁷⁹, N. De Groot¹⁰⁵, P. de Jong¹⁰⁶, H. De la Torre⁸¹, F. De Lorenzi⁶³,
 L. De Nooij¹⁰⁶, D. De Pedis^{133a}, A. De Salvo^{133a}, U. De Sanctis^{165a,165b}, A. De Santo¹⁵⁰,
 J.B. De Vivie De Regie¹¹⁶, W.J. Dearnaley⁷¹, R. Debbé²⁵, C. Debenedetti¹³⁸,
 B. Dechenaux⁵⁵, D.V. Dedovich⁶⁴, I. Deigaard¹⁰⁶, J. Del Peso⁸¹, T. Del Prete^{123a,123b},
 F. Deliot¹³⁷, C.M. Delitzsch⁴⁹, M. Deliyergiyev⁷⁴, A. Dell'Acqua³⁰, L. Dell'Asta²²,
 M. Dell'Orso^{123a,123b}, M. Della Pietra^{103a,h}, D. della Volpe⁴⁹, M. Delmastro⁵,
 P.A. Delsart⁵⁵, C. Deluca¹⁰⁶, S. Demers¹⁷⁷, M. Demichev⁶⁴, A. Demilly⁷⁹, S.P. Denisov¹²⁹,
 D. Derendarz³⁹, J.E. Derkaoui^{136d}, F. Derue⁷⁹, P. Dervan⁷³, K. Desch²¹, C. Deterre⁴²,
 P.O. Deviveiros¹⁰⁶, A. Dewhurst¹³⁰, S. Dhaliwal¹⁰⁶, A. Di Ciaccio^{134a,134b}, L. Di Ciaccio⁵,
 A. Di Domenico^{133a,133b}, C. Di Donato^{103a,103b}, A. Di Girolamo³⁰, B. Di Girolamo³⁰,
 A. Di Mattia¹⁵³, B. Di Micco^{135a,135b}, R. Di Nardo⁴⁷, A. Di Simone⁴⁸, R. Di Sipio^{20a,20b},
 D. Di Valentino²⁹, F.A. Dias⁴⁶, M.A. Diaz^{32a}, E.B. Diehl⁸⁸, J. Dietrich⁴²,
 T.A. Dietzsch^{58a}, S. Diglio⁸⁴, A. Dimitrievska^{13a}, J. Dingfelder²¹, C. Dionisi^{133a,133b},
 P. Dita^{26a}, S. Dita^{26a}, F. Dittus³⁰, F. Djama⁸⁴, T. Djobava^{51b}, M.A.B. do Vale^{24c},

A. Do Valle Wemans^{125a,125g}, T.K.O. Doan⁵, D. Dobos³⁰, C. Doglioni⁴⁹, T. Doherty⁵³,
 T. Dohmae¹⁵⁶, J. Dolejsi¹²⁸, Z. Dolezal¹²⁸, B.A. Dolgoshein^{97,*}, M. Donadelli^{24d},
 S. Donati^{123a,123b}, P. Dondero^{120a,120b}, J. Donini³⁴, J. Dopke¹³⁰, A. Doria^{103a},
 M.T. Dova⁷⁰, A.T. Doyle⁵³, M. Dris¹⁰, J. Dubbert⁸⁸, S. Dube¹⁵, E. Dubreuil³⁴,
 E. Duchovni¹⁷³, G. Duckeck⁹⁹, O.A. Ducu^{26a}, D. Duda¹⁷⁶, A. Dudarev³⁰, F. Dudziak⁶³,
 L. Duflot¹¹⁶, L. Duguid⁷⁶, M. Dührssen³⁰, M. Dunford^{58a}, H. Duran Yildiz^{4a}, M. Düren⁵²,
 A. Durglishvili^{51b}, M. Dwuznik^{38a}, M. Dyndal^{38a}, J. Ebke⁹⁹, W. Edson², N.C. Edwards⁴⁶,
 W. Ehrenfeld²¹, T. Eifert¹⁴⁴, G. Eigen¹⁴, K. Einsweiler¹⁵, T. Ekelof¹⁶⁷, M. El Kacimi^{136c},
 M. Ellert¹⁶⁷, S. Elles⁵, F. Ellinghaus⁸², N. Ellis³⁰, J. Elmsheuser⁹⁹, M. Elsing³⁰,
 D. Emelianov¹³⁰, Y. Enari¹⁵⁶, O.C. Endner⁸², M. Endo¹¹⁷, R. Engelmann¹⁴⁹,
 J. Erdmann¹⁷⁷, A. Ereditato¹⁷, D. Eriksson^{147a}, G. Ernis¹⁷⁶, J. Ernst², M. Ernst²⁵,
 J. Ernwein¹³⁷, D. Errede¹⁶⁶, S. Errede¹⁶⁶, E. Ertel⁸², M. Escalier¹¹⁶, H. Esch⁴³,
 C. Escobar¹²⁴, B. Esposito⁴⁷, A.I. Etienvre¹³⁷, E. Etzion¹⁵⁴, H. Evans⁶⁰, A. Ezhilov¹²²,
 L. Fabbri^{20a,20b}, G. Facini³¹, R.M. Fakhruddinov¹²⁹, S. Falciano^{133a}, R.J. Falla⁷⁷,
 J. Faltova¹²⁸, Y. Fang^{33a}, M. Fanti^{90a,90b}, A. Farbin⁸, A. Farilla^{135a}, T. Farooque¹²,
 S. Farrell¹⁵, S.M. Farrington¹⁷¹, P. Farthouat³⁰, F. Fassi^{136e}, P. Fassnacht³⁰,
 D. Fassouliotis⁹, A. Favareto^{50a,50b}, L. Fayard¹¹⁶, P. Federic^{145a}, O.L. Fedin^{122,j},
 W. Fedorko¹⁶⁹, M. Fehling-Kaschek⁴⁸, S. Feigl³⁰, L. Feligioni⁸⁴, C. Feng^{33d}, E.J. Feng⁶,
 H. Feng⁸⁸, A.B. Fenyuk¹²⁹, S. Fernandez Perez³⁰, S. Ferrag⁵³, J. Ferrando⁵³,
 A. Ferrari¹⁶⁷, P. Ferrari¹⁰⁶, R. Ferrari^{120a}, D.E. Ferreira de Lima⁵³, A. Ferrer¹⁶⁸,
 D. Ferrere⁴⁹, C. Ferretti⁸⁸, A. Ferretto Parodi^{50a,50b}, M. Fiascaris³¹, F. Fiedler⁸²,
 A. Filipčić⁷⁴, M. Filipuzzi⁴², F. Filthaut¹⁰⁵, M. Fincke-Keeler¹⁷⁰, K.D. Finelli¹⁵¹,
 M.C.N. Fiolhais^{125a,125c}, L. Fiorini¹⁶⁸, A. Firan⁴⁰, A. Fischer², J. Fischer¹⁷⁶,
 W.C. Fisher⁸⁹, E.A. Fitzgerald²³, M. Flechl⁴⁸, I. Fleck¹⁴², P. Fleischmann⁸⁸,
 S. Fleischmann¹⁷⁶, G.T. Fletcher¹⁴⁰, G. Fletcher⁷⁵, T. Flick¹⁷⁶, A. Floderus⁸⁰,
 L.R. Flores Castillo^{174,k}, A.C. Florez Bustos^{160b}, M.J. Flowerdew¹⁰⁰, A. Formica¹³⁷,
 A. Forti⁸³, D. Fortin^{160a}, D. Fournier¹¹⁶, H. Fox⁷¹, S. Fracchia¹², P. Francavilla⁷⁹,
 M. Franchini^{20a,20b}, S. Franchino³⁰, D. Francis³⁰, L. Franconi¹¹⁸, M. Franklin⁵⁷,
 S. Franz⁶¹, M. Fraternali^{120a,120b}, S.T. French²⁸, C. Friedrich⁴², F. Friedrich⁴⁴,
 D. Froidevaux³⁰, J.A. Frost²⁸, C. Fukunaga¹⁵⁷, E. Fullana Torregrosa⁸², B.G. Fulson¹⁴⁴,
 J. Fuster¹⁶⁸, C. Gabaldon⁵⁵, O. Gabizon¹⁷³, A. Gabrielli^{20a,20b}, A. Gabrielli^{133a,133b},
 S. Gadatsch¹⁰⁶, S. Gadomski⁴⁹, G. Gagliardi^{50a,50b}, P. Gagnon⁶⁰, C. Galea¹⁰⁵,
 B. Galhardo^{125a,125c}, E.J. Gallas¹¹⁹, V. Gallo¹⁷, B.J. Gallop¹³⁰, P. Gallus¹²⁷, G. Galster³⁶,
 K.K. Gan¹¹⁰, R.P. Gandrajula⁶², J. Gao^{33b,g}, Y.S. Gao^{144,e}, F.M. Garay Walls⁴⁶,
 F. Garbersson¹⁷⁷, C. García¹⁶⁸, J.E. García Navarro¹⁶⁸, M. Garcia-Sciveres¹⁵,
 R.W. Gardner³¹, N. Garelli¹⁴⁴, V. Garonne³⁰, C. Gatti⁴⁷, G. Gaudio^{120a}, B. Gaur¹⁴²,
 L. Gauthier⁹⁴, P. Gauzzi^{133a,133b}, I.L. Gavrilenko⁹⁵, C. Gay¹⁶⁹, G. Gaycken²¹,
 E.N. Gazis¹⁰, P. Ge^{33d}, Z. Gecse¹⁶⁹, C.N.P. Gee¹³⁰, D.A.A. Geerts¹⁰⁶,
 Ch. Geich-Gimbel²¹, K. Gellerstedt^{147a,147b}, C. Gemme^{50a}, A. Gemmell⁵³, M.H. Genest⁵⁵,
 S. Gentile^{133a,133b}, M. George⁵⁴, S. George⁷⁶, D. Gerbaudo¹⁶⁴, A. Gershon¹⁵⁴,
 H. Ghazlane^{136b}, N. Ghodbane³⁴, B. Giacobbe^{20a}, S. Giagu^{133a,133b}, V. Giangiobbe¹²,
 P. Giannetti^{123a,123b}, F. Gianotti³⁰, B. Gibbard²⁵, S.M. Gibson⁷⁶, M. Gilchriese¹⁵,
 T.P.S. Gillam²⁸, D. Gillberg³⁰, G. Gilles³⁴, D.M. Gingrich^{3,d}, N. Giokaris⁹,

M.P. Giordani^{165a,165c}, R. Giordano^{103a,103b}, F.M. Giorgi^{20a}, F.M. Giorgi¹⁶,
P.F. Giraud¹³⁷, D. Giugni^{90a}, C. Giuliani⁴⁸, M. Giulini^{58b}, B.K. Gjelsten¹¹⁸,
S. Gkaitatzis¹⁵⁵, I. Gkialas^{155,l}, L.K. Gladilin⁹⁸, C. Glasman⁸¹, J. Glatzer³⁰,
P.C.F. Glaysher⁴⁶, A. Glazov⁴², G.L. Glonti⁶⁴, M. Goblirsch-Kolb¹⁰⁰, J.R. Goddard⁷⁵,
J. Godfrey¹⁴³, J. Godlewski³⁰, C. Goeringer⁸², S. Goldfarb⁸⁸, T. Golling¹⁷⁷,
D. Golubkov¹²⁹, A. Gomes^{125a,125b,125d}, L.S. Gomez Fajardo⁴², R. Gonalo^{125a},
J. Goncalves Pinto Firmino Da Costa¹³⁷, L. Gonella²¹, S. Gonzalez de la Hoz¹⁶⁸,
G. Gonzalez Parra¹², S. Gonzalez-Sevilla⁴⁹, L. Goossens³⁰, P.A. Gorbounov⁹⁶,
H.A. Gordon²⁵, I. Gorelov¹⁰⁴, B. Gorini³⁰, E. Gorini^{72a,72b}, A. Gorišek⁷⁴, E. Gornicki³⁹,
A.T. Goshaw⁶, C. Gossling⁴³, M.I. Gostkin⁶⁴, M. Gouighri^{136a}, D. Goujdami^{136c},
M.P. Goulette⁴⁹, A.G. Goussiou¹³⁹, C. Goy⁵, S. Gozpinar²³, H.M.X. Grabas¹³⁷,
L. Graber⁵⁴, I. Grabowska-Bold^{38a}, P. Grafstrom^{20a,20b}, K-J. Grahn⁴², J. Gramling⁴⁹,
E. Gramstad¹¹⁸, S. Grancagnolo¹⁶, V. Grassi¹⁴⁹, V. Gratchev¹²², H.M. Gray³⁰,
E. Graziani^{135a}, O.G. Grebenyuk¹²², Z.D. Greenwood^{78,m}, K. Gregersen⁷⁷, I.M. Gregor⁴²,
P. Grenier¹⁴⁴, J. Griffiths⁸, A.A. Grillo¹³⁸, K. Grimm⁷¹, S. Grinstein^{12,n}, Ph. Gris³⁴,
Y.V. Grishkevich⁹⁸, J.-F. Grivaz¹¹⁶, J.P. Grohs⁴⁴, A. Grohsjean⁴², E. Gross¹⁷³,
J. Grosse-Knetter⁵⁴, G.C. Grossi^{134a,134b}, J. Groth-Jensen¹⁷³, Z.J. Grout¹⁵⁰, L. Guan^{33b},
F. Guescini⁴⁹, D. Guest¹⁷⁷, O. Gueta¹⁵⁴, C. Guicheney³⁴, E. Guido^{50a,50b},
T. Guillemin¹¹⁶, S. Guindon², U. Gul⁵³, C. Gumpert⁴⁴, J. Gunther¹²⁷, J. Guo³⁵,
S. Gupta¹¹⁹, P. Gutierrez¹¹², N.G. Gutierrez Ortiz⁵³, C. Gutschew⁷⁷, N. Guttman¹⁵⁴,
C. Guyot¹³⁷, C. Gwenlan¹¹⁹, C.B. Gwilliam⁷³, A. Haas¹⁰⁹, C. Haber¹⁵, H.K. Hadavand⁸,
N. Haddad^{136e}, P. Haefner²¹, S. Hagebock²¹, Z. Hajduk³⁹, H. Hakobyan¹⁷⁸, M. Haleem⁴²,
D. Hall¹¹⁹, G. Halladjian⁸⁹, K. Hamacher¹⁷⁶, P. Hamal¹¹⁴, K. Hamano¹⁷⁰, M. Hamer⁵⁴,
A. Hamilton^{146a}, S. Hamilton¹⁶², G.N. Hamity^{146c}, P.G. Hamnett⁴², L. Han^{33b},
K. Hanagaki¹¹⁷, K. Hanawa¹⁵⁶, M. Hance¹⁵, P. Hanke^{58a}, R. Hanna¹³⁷, J.B. Hansen³⁶,
J.D. Hansen³⁶, P.H. Hansen³⁶, K. Hara¹⁶¹, A.S. Hard¹⁷⁴, T. Harenberg¹⁷⁶, F. Hariri¹¹⁶,
S. Harkusha⁹¹, D. Harper⁸⁸, R.D. Harrington⁴⁶, O.M. Harris¹³⁹, P.F. Harrison¹⁷¹,
F. Hartjes¹⁰⁶, M. Hasegawa⁶⁶, S. Hasegawa¹⁰², Y. Hasegawa¹⁴¹, A. Hasib¹¹²,
S. Hassani¹³⁷, S. Haug¹⁷, M. Hauschild³⁰, R. Hauser⁸⁹, M. Havranek¹²⁶, C.M. Hawkes¹⁸,
R.J. Hawkings³⁰, A.D. Hawkins⁸⁰, T. Hayashi¹⁶¹, D. Hayden⁸⁹, C.P. Hays¹¹⁹,
H.S. Hayward⁷³, S.J. Haywood¹³⁰, S.J. Head¹⁸, T. Heck⁸², V. Hedberg⁸⁰, L. Heelan⁸,
S. Heim¹²¹, T. Heim¹⁷⁶, B. Heinemann¹⁵, L. Heinrich¹⁰⁹, J. Hejbal¹²⁶, L. Helary²²,
C. Heller⁹⁹, M. Heller³⁰, S. Hellman^{147a,147b}, D. Hellmich²¹, C. Helsen³⁰,
J. Henderson¹¹⁹, R.C.W. Henderson⁷¹, Y. Heng¹⁷⁴, C. Hengler⁴², A. Henrichs¹⁷⁷,
A.M. Henriques Correia³⁰, S. Henrot-Versille¹¹⁶, C. Hensel⁵⁴, G.H. Herbert¹⁶,
Y. Hernandez Jimenez¹⁶⁸, R. Herrberg-Schubert¹⁶, G. Herten⁴⁸, R. Hertenberger⁹⁹,
L. Hervas³⁰, G.G. Hesketh⁷⁷, N.P. Hessey¹⁰⁶, R. Hickling⁷⁵, E. Higon-Rodriguez¹⁶⁸,
E. Hill¹⁷⁰, J.C. Hill²⁸, K.H. Hiller⁴², S. Hillert²¹, S.J. Hillier¹⁸, I. Hinchliffe¹⁵, E. Hines¹²¹,
M. Hirose¹⁵⁸, D. Hirschbuehl¹⁷⁶, J. Hobbs¹⁴⁹, N. Hod¹⁰⁶, M.C. Hodgkinson¹⁴⁰,
P. Hodgson¹⁴⁰, A. Hoecker³⁰, M.R. Hoferkamp¹⁰⁴, F. Hoenig⁹⁹, J. Hoffman⁴⁰,
D. Hoffmann⁸⁴, J.I. Hofmann^{58a}, M. Hohlfeld⁸², T.R. Holmes¹⁵, T.M. Hong¹²¹,
L. Hooft van Huysduynen¹⁰⁹, J-Y. Hostachy⁵⁵, S. Hou¹⁵², A. Hoummada^{136a},
J. Howard¹¹⁹, J. Howarth⁴², M. Hrabovsky¹¹⁴, I. Hristova¹⁶, J. Hrivnac¹¹⁶, T. Hryn'ova⁵,

C. Hsu^{146c}, P.J. Hsu⁸², S.-C. Hsu¹³⁹, D. Hu³⁵, X. Hu²⁵, Y. Huang⁴², Z. Hubacek³⁰,
 F. Hubaut⁸⁴, F. Huegging²¹, T.B. Huffman¹¹⁹, E.W. Hughes³⁵, G. Hughes⁷¹,
 M. Huhtinen³⁰, T.A. Hülsing⁸², M. Hurwitz¹⁵, N. Huseynov^{64,b}, J. Huston⁸⁹, J. Huth⁵⁷,
 G. Iacobucci⁴⁹, G. Iakovidis¹⁰, I. Ibragimov¹⁴², L. Iconomidou-Fayard¹¹⁶, E. Ideal¹⁷⁷,
 P. Iengo^{103a}, O. Igonkina¹⁰⁶, T. Iizawa¹⁷², Y. Ikegami⁶⁵, K. Ikematsu¹⁴², M. Ikeno⁶⁵,
 Y. Ilchenko^{31,o}, D. Iliadis¹⁵⁵, N. Ilic¹⁵⁹, Y. Inamaru⁶⁶, T. Ince¹⁰⁰, P. Ioannou⁹,
 M. Iodice^{135a}, K. Iordanidou⁹, V. Ippolito⁵⁷, A. Irlles Quiles¹⁶⁸, C. Isaksson¹⁶⁷,
 M. Ishino⁶⁷, M. Ishitsuka¹⁵⁸, R. Ishmukhametov¹¹⁰, C. Issever¹¹⁹, S. Istin^{19a},
 J.M. Iturbe Ponce⁸³, R. Iuppa^{134a,134b}, J. Ivarsson⁸⁰, W. Iwanski³⁹, H. Iwasaki⁶⁵,
 J.M. Izen⁴¹, V. Izzo^{103a}, B. Jackson¹²¹, M. Jackson⁷³, P. Jackson¹, M.R. Jaekel³⁰,
 V. Jain², K. Jakobs⁴⁸, S. Jakobsen³⁰, T. Jakoubek¹²⁶, J. Jakubek¹²⁷, D.O. Jamin¹⁵²,
 D.K. Jana⁷⁸, E. Jansen⁷⁷, H. Jansen³⁰, J. Janssen²¹, M. Janus¹⁷¹, G. Jarlskog⁸⁰,
 N. Javadov^{64,b}, T. Javůrek⁴⁸, L. Jeanty¹⁵, J. Jejelava^{51a,p}, G.-Y. Jeng¹⁵¹, D. Jennens⁸⁷,
 P. Jenni^{48,q}, J. Jentzsch⁴³, C. Jeske¹⁷¹, S. Jézéquel⁵, H. Ji¹⁷⁴, J. Jia¹⁴⁹, Y. Jiang^{33b},
 M. Jimenez Belenguer⁴², S. Jin^{33a}, A. Jinaru^{26a}, O. Jinnouchi¹⁵⁸, M.D. Joergensen³⁶,
 K.E. Johansson^{147a,147b}, P. Johansson¹⁴⁰, K.A. Johns⁷, K. Jon-And^{147a,147b}, G. Jones¹⁷¹,
 R.W.L. Jones⁷¹, T.J. Jones⁷³, J. Jongmanns^{58a}, P.M. Jorge^{125a,125b}, K.D. Joshi⁸³,
 J. Jovicevic¹⁴⁸, X. Ju¹⁷⁴, C.A. Jung⁴³, R.M. Jungst³⁰, P. Jussel⁶¹, A. Juste Rozas^{12,n},
 M. Kaci¹⁶⁸, A. Kaczmarek³⁹, M. Kado¹¹⁶, H. Kagan¹¹⁰, M. Kagan¹⁴⁴, E. Kajomovitz⁴⁵,
 C.W. Kalderon¹¹⁹, S. Kama⁴⁰, A. Kamenshchikov¹²⁹, N. Kanaya¹⁵⁶, M. Kaneda³⁰,
 S. Kaneti²⁸, V.A. Kantserov⁹⁷, J. Kanzaki⁶⁵, B. Kaplan¹⁰⁹, A. Kapliy³¹, D. Kar⁵³,
 K. Karakostas¹⁰, N. Karastathis¹⁰, M. Karnevskiy⁸², S.N. Karpov⁶⁴, Z.M. Karpova⁶⁴,
 K. Karthik¹⁰⁹, V. Kartvelishvili⁷¹, A.N. Karyukhin¹²⁹, L. Kashif¹⁷⁴, G. Kasieczka^{58b},
 R.D. Kass¹¹⁰, A. Kastanas¹⁴, Y. Kataoka¹⁵⁶, A. Katre⁴⁹, J. Katzy⁴², V. Kaushik⁷,
 K. Kawagoe⁶⁹, T. Kawamoto¹⁵⁶, G. Kawamura⁵⁴, S. Kazama¹⁵⁶, V.F. Kazanin¹⁰⁸,
 M.Y. Kazarinov⁶⁴, R. Keeler¹⁷⁰, R. Kehoe⁴⁰, M. Keil⁵⁴, J.S. Keller⁴², J.J. Kempster⁷⁶,
 H. Keoshkerian⁵, O. Kepka¹²⁶, B.P. Kerševan⁷⁴, S. Kersten¹⁷⁶, K. Kessoku¹⁵⁶,
 J. Keung¹⁵⁹, F. Khalil-zada¹¹, H. Khandanyan^{147a,147b}, A. Khanov¹¹³, A. Khodinov⁹⁷,
 A. Khomich^{58a}, T.J. Khoo²⁸, G. Khoriali²¹, A. Khoroshilov¹⁷⁶, V. Khovanskiy⁹⁶,
 E. Khramov⁶⁴, J. Khubua^{51b}, H.Y. Kim⁸, H. Kim^{147a,147b}, S.H. Kim¹⁶¹, N. Kimura¹⁷²,
 O. Kind¹⁶, B.T. King⁷³, M. King¹⁶⁸, R.S.B. King¹¹⁹, S.B. King¹⁶⁹, J. Kirk¹³⁰,
 A.E. Kiryunin¹⁰⁰, T. Kishimoto⁶⁶, D. Kisielewska^{38a}, F. Kiss⁴⁸, T. Kittelmann¹²⁴,
 K. Kiuchi¹⁶¹, E. Kladiva^{145b}, M. Klein⁷³, U. Klein⁷³, K. Kleinknecht⁸², P. Klimek^{147a,147b},
 A. Klimentov²⁵, R. Klingenberg⁴³, J.A. Klinger⁸³, T. Klioutchnikova³⁰, P.F. Klok¹⁰⁵,
 E.-E. Kluge^{58a}, P. Kluit¹⁰⁶, S. Kluth¹⁰⁰, E. Kneringer⁶¹, E.B.F.G. Knoops⁸⁴, A. Knue⁵³,
 D. Kobayashi¹⁵⁸, T. Kobayashi¹⁵⁶, M. Kobel⁴⁴, M. Kocian¹⁴⁴, P. Kodys¹²⁸,
 P. Koevesarki²¹, T. Koffas²⁹, E. Koffeman¹⁰⁶, L.A. Kogan¹¹⁹, S. Kohlmann¹⁷⁶,
 Z. Kohout¹²⁷, T. Kohriki⁶⁵, T. Koi¹⁴⁴, H. Kolanoski¹⁶, I. Koletsou⁵, J. Koll⁸⁹,
 A.A. Komar^{95,*}, Y. Komori¹⁵⁶, T. Kondo⁶⁵, N. Kondrashova⁴², K. Köneke⁴⁸,
 A.C. König¹⁰⁵, S. König⁸², T. Kono^{65,r}, R. Konoplich^{109,s}, N. Konstantinidis⁷⁷,
 R. Kopeliansky¹⁵³, S. Koperny^{38a}, L. Köpke⁸², A.K. Kopp⁴⁸, K. Korcyl³⁹, K. Kordas¹⁵⁵,
 A. Korn⁷⁷, A.A. Korol^{108,t}, I. Korolkov¹², E.V. Korolkova¹⁴⁰, V.A. Korotkov¹²⁹,
 O. Kortner¹⁰⁰, S. Kortner¹⁰⁰, V.V. Kostyukhin²¹, V.M. Kotov⁶⁴, A. Kotwal⁴⁵,

C. Kourkoumelis⁹, V. Kouskoura¹⁵⁵, A. Koutsman^{160a}, R. Kowalewski¹⁷⁰,
 T.Z. Kowalski^{38a}, W. Kozanecki¹³⁷, A.S. Kozhin¹²⁹, V. Kral¹²⁷, V.A. Kramarenko⁹⁸,
 G. Kramberger⁷⁴, D. Krasnopevtsev⁹⁷, M.W. Krasny⁷⁹, A. Krasznahorkay³⁰,
 J.K. Kraus²¹, A. Kravchenko²⁵, S. Kreiss¹⁰⁹, M. Kretz^{58c}, J. Kretzschmar⁷³,
 K. Kreutzfeldt⁵², P. Krieger¹⁵⁹, K. Kroeninger⁵⁴, H. Kroha¹⁰⁰, J. Kroll¹²¹, J. Kroseberg²¹,
 J. Krstic^{13a}, U. Kruchonak⁶⁴, H. Krüger²¹, T. Kruker¹⁷, N. Krumnack⁶³,
 Z.V. Krumshteyn⁶⁴, A. Kruse¹⁷⁴, M.C. Kruse⁴⁵, M. Kruskal²², T. Kubota⁸⁷, S. Kuday^{4a},
 S. Kuehn⁴⁸, A. Kugel^{58c}, A. Kuhl¹³⁸, T. Kuhl⁴², V. Kukhtin⁶⁴, Y. Kulchitsky⁹¹,
 S. Kuleshov^{32b}, M. Kuna^{133a,133b}, J. Kunkle¹²¹, A. Kupco¹²⁶, H. Kurashige⁶⁶,
 Y.A. Kurochkin⁹¹, R. Kurumida⁶⁶, V. Kus¹²⁶, E.S. Kuwertz¹⁴⁸, M. Kuze¹⁵⁸, J. Kvita¹¹⁴,
 A. La Rosa⁴⁹, L. La Rotonda^{37a,37b}, C. Lacasta¹⁶⁸, F. Lacava^{133a,133b}, J. Lacey²⁹,
 H. Lacker¹⁶, D. Lacour⁷⁹, V.R. Lacuesta¹⁶⁸, E. Ladygin⁶⁴, R. Lafaye⁵, B. Laforge⁷⁹,
 T. Lagouri¹⁷⁷, S. Lai⁴⁸, H. Laier^{58a}, L. Lambourne⁷⁷, S. Lammers⁶⁰, C.L. Lampen⁷,
 W. Lampl⁷, E. Lançon¹³⁷, U. Landgraf⁴⁸, M.P.J. Landon⁷⁵, V.S. Lang^{58a},
 A.J. Lankford¹⁶⁴, F. Lanni²⁵, K. Lantzschi³⁰, S. Laplace⁷⁹, C. Lapoire²¹, J.F. Laporte¹³⁷,
 T. Lari^{90a}, M. Lassnig³⁰, P. Laurelli⁴⁷, W. Lavrijsen¹⁵, A.T. Law¹³⁸, P. Laycock⁷³,
 O. Le Dortz⁷⁹, E. Le Guirriec⁸⁴, E. Le Menedeu¹², T. LeCompte⁶, F. Ledroit-Guillon⁵⁵,
 C.A. Lee¹⁵², H. Lee¹⁰⁶, J.S.H. Lee¹¹⁷, S.C. Lee¹⁵², L. Lee¹⁷⁷, G. Lefebvre⁷⁹,
 M. Lefebvre¹⁷⁰, F. Legger⁹⁹, C. Leggett¹⁵, A. Lehan⁷³, M. Lehmacher²¹,
 G. Lehmann Miotto³⁰, X. Lei⁷, W.A. Leight²⁹, A. Leisos¹⁵⁵, A.G. Leister¹⁷⁷,
 M.A.L. Leite^{24d}, R. Leitner¹²⁸, D. Lellouch¹⁷³, B. Lemmer⁵⁴, K.J.C. Leney⁷⁷, T. Lenz²¹,
 G. Lenzen¹⁷⁶, B. Lenzi³⁰, R. Leone⁷, S. Leone^{123a,123b}, K. Leonhardt⁴⁴,
 C. Leonidopoulos⁴⁶, S. Leontsinis¹⁰, C. Leroy⁹⁴, C.G. Lester²⁸, C.M. Lester¹²¹,
 M. Levchenko¹²², J. Levêque⁵, D. Levin⁸⁸, L.J. Levinson¹⁷³, M. Levy¹⁸, A. Lewis¹¹⁹,
 G.H. Lewis¹⁰⁹, A.M. Leyko²¹, M. Leyton⁴¹, B. Li^{33b,u}, B. Li⁸⁴, H. Li¹⁴⁹, H.L. Li³¹,
 L. Li⁴⁵, L. Li^{33e}, S. Li⁴⁵, Y. Li^{33c,v}, Z. Liang¹³⁸, H. Liao³⁴, B. Liberti^{134a}, P. Lichard³⁰,
 K. Lie¹⁶⁶, J. Liebal²¹, W. Liebig¹⁴, C. Limbach²¹, A. Limosani⁸⁷, S.C. Lin^{152,w},
 T.H. Lin⁸², F. Linde¹⁰⁶, B.E. Lindquist¹⁴⁹, J.T. Linnemann⁸⁹, E. Lipeles¹²¹,
 A. Lipniacka¹⁴, M. Lisovyi⁴², T.M. Liss¹⁶⁶, D. Lissauer²⁵, A. Lister¹⁶⁹, A.M. Litke¹³⁸,
 B. Liu¹⁵², D. Liu¹⁵², J.B. Liu^{33b}, K. Liu^{33b,x}, L. Liu⁸⁸, M. Liu⁴⁵, M. Liu^{33b}, Y. Liu^{33b},
 M. Livan^{120a,120b}, S.S.A. Livermore¹¹⁹, A. Lleres⁵⁵, J. Llorente Merino⁸¹, S.L. Lloyd⁷⁵,
 F. Lo Sterzo¹⁵², E. Lobodzinska⁴², P. Loch⁷, W.S. Lockman¹³⁸, T. Loddenkoetter²¹,
 F.K. Loebinger⁸³, A.E. Loevschall-Jensen³⁶, A. Loginov¹⁷⁷, T. Lohse¹⁶, K. Lohwasser⁴²,
 M. Lokajicek¹²⁶, V.P. Lombardo⁵, B.A. Long²², J.D. Long⁸⁸, R.E. Long⁷¹, L. Lopes^{125a},
 D. Lopez Mateos⁵⁷, B. Lopez Paredes¹⁴⁰, I. Lopez Paz¹², J. Lorenz⁹⁹,
 N. Lorenzo Martinez⁶⁰, M. Losada¹⁶³, P. Loscutoff¹⁵, X. Lou⁴¹, A. Lounis¹¹⁶, J. Love⁶,
 P.A. Love⁷¹, A.J. Lowe^{144,e}, F. Lu^{33a}, N. Lu⁸⁸, H.J. Lubatti¹³⁹, C. Luci^{133a,133b},
 A. Lucotte⁵⁵, F. Luehring⁶⁰, W. Lukas⁶¹, L. Luminari^{133a}, O. Lundberg^{147a,147b},
 B. Lund-Jensen¹⁴⁸, M. Lungwitz⁸², D. Lynn²⁵, R. Lysak¹²⁶, E. Lytken⁸⁰, H. Ma²⁵,
 L.L. Ma^{33d}, G. Maccarrone⁴⁷, A. Macchiolo¹⁰⁰, J. Machado Miguens^{125a,125b}, D. Macina³⁰,
 D. Madaffari⁸⁴, R. Madar⁴⁸, H.J. Maddocks⁷¹, W.F. Mader⁴⁴, A. Madsen¹⁶⁷, M. Maeno⁸,
 T. Maeno²⁵, E. Magradze⁵⁴, K. Mahboubi⁴⁸, J. Mahlstedt¹⁰⁶, S. Mahmoud⁷³,
 C. Maiani¹³⁷, C. Maidantchik^{24a}, A.A. Maier¹⁰⁰, A. Maio^{125a,125b,125d}, S. Majewski¹¹⁵,

Y. Makida⁶⁵, N. Makovec¹¹⁶, P. Mal^{137,y}, B. Malaescu⁷⁹, Pa. Malecki³⁹, V.P. Maleev¹²²,
 F. Malek⁵⁵, U. Mallik⁶², D. Malon⁶, C. Malone¹⁴⁴, S. Maltezos¹⁰, V.M. Malyshev¹⁰⁸,
 S. Malyukov³⁰, J. Mamuzic^{13b}, B. Mandelli³⁰, L. Mandelli^{90a}, I. Mandić⁷⁴,
 R. Mandrysch⁶², J. Maneira^{125a,125b}, A. Manfredini¹⁰⁰, L. Manhaes de Andrade Filho^{24b},
 J.A. Manjarres Ramos^{160b}, A. Mann⁹⁹, P.M. Manning¹³⁸, A. Manousakis-Katsikakis⁹,
 B. Mansoulie¹³⁷, R. Mantifel⁸⁶, L. Mapelli³⁰, L. March¹⁶⁸, J.F. Marchand²⁹,
 G. Marchiori⁷⁹, M. Marcisovsky¹²⁶, C.P. Marino¹⁷⁰, M. Marjanovic^{13a}, C.N. Marques^{125a},
 F. Marroquim^{24a}, S.P. Marsden⁸³, Z. Marshall¹⁵, L.F. Marti¹⁷, S. Marti-Garcia¹⁶⁸,
 B. Martin³⁰, B. Martin⁸⁹, T.A. Martin¹⁷¹, V.J. Martin⁴⁶, B. Martin dit Latour¹⁴,
 H. Martinez¹³⁷, M. Martinez^{12,n}, S. Martin-Haugh¹³⁰, A.C. Martyniuk⁷⁷, M. Marx¹³⁹,
 F. Marzano^{133a}, A. Marzin³⁰, L. Masetti⁸², T. Mashimo¹⁵⁶, R. Mashinistov⁹⁵, J. Masik⁸³,
 A.L. Maslennikov¹⁰⁸, I. Massa^{20a,20b}, L. Massa^{20a,20b}, N. Massol⁵, P. Mastrandrea¹⁴⁹,
 A. Mastroberardino^{37a,37b}, T. Masubuchi¹⁵⁶, P. Mättig¹⁷⁶, J. Mattmann⁸², J. Maurer^{26a},
 S.J. Maxfield⁷³, D.A. Maximov^{108,t}, R. Mazini¹⁵², L. Mazzaferro^{134a,134b},
 G. Mc Goldrick¹⁵⁹, S.P. Mc Kee⁸⁸, A. McCarn⁸⁸, R.L. McCarthy¹⁴⁹, T.G. McCarthy²⁹,
 N.A. McCubbin¹³⁰, K.W. McFarlane^{56,*}, J.A. Mcfayden⁷⁷, G. Mchedlidze⁵⁴,
 S.J. McMahon¹³⁰, R.A. McPherson^{170,i}, A. Meade⁸⁵, J. Mechnich¹⁰⁶, M. Medinnis⁴²,
 S. Meehan³¹, S. Mehlhase⁹⁹, A. Mehta⁷³, K. Meier^{58a}, C. Meineck⁹⁹, B. Meirose⁸⁰,
 C. Melachrinou³¹, B.R. Mellado Garcia^{146c}, F. Meloni¹⁷, A. Mengarelli^{20a,20b},
 S. Menke¹⁰⁰, E. Meoni¹⁶², K.M. Mercurio⁵⁷, S. Mergelmeyer²¹, N. Meric¹³⁷, P. Mermod⁴⁹,
 L. Merola^{103a,103b}, C. Meroni^{90a}, F.S. Merritt³¹, H. Merritt¹¹⁰, A. Messina^{30,z},
 J. Metcalfe²⁵, A.S. Mete¹⁶⁴, C. Meyer⁸², C. Meyer¹²¹, J-P. Meyer¹³⁷, J. Meyer³⁰,
 R.P. Middleton¹³⁰, S. Migas⁷³, L. Mijović²¹, G. Mikenberg¹⁷³, M. Mikestikova¹²⁶,
 M. Mikuž⁷⁴, A. Milic³⁰, D.W. Miller³¹, C. Mills⁴⁶, A. Milov¹⁷³, D.A. Milstead^{147a,147b},
 D. Milstein¹⁷³, A.A. Minaenko¹²⁹, I.A. Minashvili⁶⁴, A.I. Mincer¹⁰⁹, B. Mindur^{38a},
 M. Mineev⁶⁴, Y. Ming¹⁷⁴, L.M. Mir¹², G. Mirabelli^{133a}, T. Mitani¹⁷², J. Mitrevski⁹⁹,
 V.A. Mitsou¹⁶⁸, S. Mitsui⁶⁵, A. Miucci⁴⁹, P.S. Miyagawa¹⁴⁰, J.U. Mjörnmark⁸⁰,
 T. Moa^{147a,147b}, K. Mochizuki⁸⁴, S. Mohapatra³⁵, W. Mohr⁴⁸, S. Molander^{147a,147b},
 R. Moles-Valls¹⁶⁸, K. Mönig⁴², C. Monini⁵⁵, J. Monk³⁶, E. Monnier⁸⁴,
 J. Montejó Berlingen¹², F. Monticelli⁷⁰, S. Monzani^{133a,133b}, R.W. Moore³, A. Moraes⁵³,
 N. Morange⁶², D. Moreno⁸², M. Moreno Llácer⁵⁴, P. Morettini^{50a}, M. Morgenstern⁴⁴,
 M. Morii⁵⁷, S. Moritz⁸², A.K. Morley¹⁴⁸, G. Mornacchi³⁰, J.D. Morris⁷⁵, L. Morvaj¹⁰²,
 H.G. Moser¹⁰⁰, M. Mosidze^{51b}, J. Moss¹¹⁰, K. Motohashi¹⁵⁸, R. Mount¹⁴⁴,
 E. Mountricha²⁵, S.V. Mouraviev^{95,*}, E.J.W. Moyse⁸⁵, S. Muanza⁸⁴, R.D. Mudd¹⁸,
 F. Mueller^{58a}, J. Mueller¹²⁴, K. Mueller²¹, T. Mueller²⁸, T. Mueller⁸²,
 D. Muenstermann⁴⁹, Y. Munwes¹⁵⁴, J.A. Murillo Quijada¹⁸, W.J. Murray^{171,130},
 H. Musheghyan⁵⁴, E. Musto¹⁵³, A.G. Myagkov^{129,aa}, M. Myska¹²⁷, O. Nackenhorst⁵⁴,
 J. Nadal⁵⁴, K. Nagai⁶¹, R. Nagai¹⁵⁸, Y. Nagai⁸⁴, K. Nagano⁶⁵, A. Nagarkar¹¹⁰,
 Y. Nagasaka⁵⁹, M. Nagel¹⁰⁰, A.M. Nairz³⁰, Y. Nakahama³⁰, K. Nakamura⁶⁵,
 T. Nakamura¹⁵⁶, I. Nakano¹¹¹, H. Namasivayam⁴¹, G. Nanava²¹, R. Narayan^{58b},
 T. Nattermann²¹, T. Naumann⁴², G. Navarro¹⁶³, R. Nayyar⁷, H.A. Neal⁸⁸,
 P.Yu. Nechaeva⁹⁵, T.J. Neep⁸³, P.D. Nef¹⁴⁴, A. Negri^{120a,120b}, G. Negri³⁰, M. Negrini^{20a},
 S. Nektarijević⁴⁹, A. Nelson¹⁶⁴, T.K. Nelson¹⁴⁴, S. Nemecek¹²⁶, P. Nemethy¹⁰⁹,

A.A. Nepomuceno^{24a}, M. Nessi^{30,ab}, M.S. Neubauer¹⁶⁶, M. Neumann¹⁷⁶, R.M. Neves¹⁰⁹,
 P. Nevski²⁵, P.R. Newman¹⁸, D.H. Nguyen⁶, R.B. Nickerson¹¹⁹, R. Nicolaidou¹³⁷,
 B. Nicquevert³⁰, J. Nielsen¹³⁸, N. Nikiforou³⁵, A. Nikiforov¹⁶, V. Nikolaenko^{129,aa},
 I. Nikolic-Audit⁷⁹, K. Nikolics⁴⁹, K. Nikolopoulos¹⁸, P. Nilsson⁸, Y. Ninomiya¹⁵⁶,
 A. Nisati^{133a}, R. Nisius¹⁰⁰, T. Nobe¹⁵⁸, L. Nodulman⁶, M. Nomachi¹¹⁷, I. Nomidis²⁹,
 S. Norberg¹¹², M. Nordberg³⁰, O. Novgorodova⁴⁴, S. Nowak¹⁰⁰, M. Nozaki⁶⁵, L. Nozka¹¹⁴,
 K. Ntekas¹⁰, G. Nunes Hanninger⁸⁷, T. Nunnemann⁹⁹, E. Nurse⁷⁷, F. Nuti⁸⁷,
 B.J. O'Brien⁴⁶, F. O'grady⁷, D.C. O'Neil¹⁴³, V. O'Shea⁵³, F.G. Oakham^{29,d},
 H. Oberlack¹⁰⁰, T. Obermann²¹, J. Ocariz⁷⁹, A. Ochi⁶⁶, M.I. Ochoa⁷⁷, S. Oda⁶⁹,
 S. Odaka⁶⁵, H. Ogren⁶⁰, A. Oh⁸³, S.H. Oh⁴⁵, C.C. Ohm¹⁵, H. Ohman¹⁶⁷, W. Okamura¹¹⁷,
 H. Okawa²⁵, Y. Okumura³¹, T. Okuyama¹⁵⁶, A. Olariu^{26a}, A.G. Olchevski⁶⁴,
 S.A. Olivares Pino⁴⁶, D. Oliveira Damazio²⁵, E. Oliver Garcia¹⁶⁸, A. Olszewski³⁹,
 J. Olszowska³⁹, A. Onofre^{125a,125e}, P.U.E. Onyisi^{31,o}, C.J. Oram^{160a}, M.J. Oreglia³¹,
 Y. Oren¹⁵⁴, D. Orestano^{135a,135b}, N. Orlando^{72a,72b}, C. Oropeza Barrera⁵³, R.S. Orr¹⁵⁹,
 B. Osculati^{50a,50b}, R. Ospanov¹²¹, G. Otero y Garzon²⁷, H. Otono⁶⁹, M. Ouchrif^{136d},
 E.A. Ouellette¹⁷⁰, F. Ould-Saada¹¹⁸, A. Ouraou¹³⁷, K.P. Oussoren¹⁰⁶, Q. Ouyang^{33a},
 A. Ovcharova¹⁵, M. Owen⁸³, V.E. Ozcan^{19a}, N. Ozturk⁸, K. Pachal¹¹⁹,
 A. Pacheco Pages¹², C. Padilla Aranda¹², M. Pagáčová⁴⁸, S. Pagan Griso¹⁵,
 E. Paganis¹⁴⁰, C. Pahl¹⁰⁰, F. Paige²⁵, P. Pais⁸⁵, K. Pajchel¹¹⁸, G. Palacino^{160b},
 S. Palestini³⁰, M. Palka^{38b}, D. Pallin³⁴, A. Palma^{125a,125b}, J.D. Palmer¹⁸, Y.B. Pan¹⁷⁴,
 E. Panagiotopoulou¹⁰, J.G. Panduro Vazquez⁷⁶, P. Pani¹⁰⁶, N. Panikashvili⁸⁸,
 S. Panitkin²⁵, D. Pantea^{26a}, L. Paolozzi^{134a,134b}, Th.D. Papadopoulou¹⁰,
 K. Papageorgiou^{155,l}, A. Paramonov⁶, D. Paredes Hernandez³⁴, M.A. Parker²⁸,
 F. Parodi^{50a,50b}, J.A. Parsons³⁵, U. Parzefall⁴⁸, E. Pasqualucci^{133a}, S. Passaggio^{50a},
 A. Passeri^{135a}, F. Pastore^{135a,135b,*}, Fr. Pastore⁷⁶, G. Pásztor²⁹, S. Patariaia¹⁷⁶,
 N.D. Patel¹⁵¹, J.R. Pater⁸³, S. Patricelli^{103a,103b}, T. Pauly³⁰, J. Pearce¹⁷⁰, M. Pedersen¹¹⁸,
 S. Pedraza Lopez¹⁶⁸, R. Pedro^{125a,125b}, S.V. Peleganchuk¹⁰⁸, D. Pelikan¹⁶⁷, H. Peng^{33b},
 B. Penning³¹, J. Penwell⁶⁰, D.V. Perepelitsa²⁵, E. Perez Codina^{160a},
 M.T. Pérez García-Estañ¹⁶⁸, V. Perez Reale³⁵, L. Perini^{90a,90b}, H. Pernegger³⁰,
 R. Perrino^{72a}, R. Peschke⁴², V.D. Peshekhonov⁶⁴, K. Peters³⁰, R.F.Y. Peters⁸³,
 B.A. Petersen³⁰, T.C. Petersen³⁶, E. Petit⁴², A. Petridis^{147a,147b}, C. Petridou¹⁵⁵,
 E. Petrolo^{133a}, F. Petrucci^{135a,135b}, N.E. Pettersson¹⁵⁸, R. Pezoa^{32b}, P.W. Phillips¹³⁰,
 G. Piacquadio¹⁴⁴, E. Pianori¹⁷¹, A. Picazio⁴⁹, E. Piccaro⁷⁵, M. Piccinini^{20a,20b},
 R. Piegai²⁷, D.T. Pignotti¹¹⁰, J.E. Pilcher³¹, A.D. Pilkington⁷⁷, J. Pina^{125a,125b,125d},
 M. Pinamonti^{165a,165c,ac}, A. Pinder¹¹⁹, J.L. Pinfold³, A. Pingel³⁶, B. Pinto^{125a}, S. Pires⁷⁹,
 M. Pitt¹⁷³, C. Pizio^{90a,90b}, L. Plazak^{145a}, M.-A. Pleier²⁵, V. Pleskot¹²⁸, E. Plotnikova⁶⁴,
 P. Plucinski^{147a,147b}, S. Poddar^{58a}, F. Podlyski³⁴, R. Poettgen⁸², L. Poggioli¹¹⁶,
 D. Pohl²¹, M. Pohl⁴⁹, G. Polesello^{120a}, A. Policicchio^{37a,37b}, R. Polifka¹⁵⁹, A. Polini^{20a},
 C.S. Pollard⁴⁵, V. Polychronakos²⁵, K. Pommès³⁰, L. Pontecorvo^{133a}, B.G. Pope⁸⁹,
 G.A. Popeneciu^{26b}, D.S. Popovic^{13a}, A. Poppleton³⁰, X. Portell Bueso¹², S. Pospisil¹²⁷,
 K. Potamianos¹⁵, I.N. Potrap⁶⁴, C.J. Potter¹⁵⁰, C.T. Potter¹¹⁵, G. Poulard³⁰,
 J. Poveda⁶⁰, V. Pozdnyakov⁶⁴, P. Pralavorio⁸⁴, A. Pranko¹⁵, S. Prasad³⁰, R. Pravahan⁸,
 S. Prell⁶³, D. Price⁸³, J. Price⁷³, L.E. Price⁶, D. Prieur¹²⁴, M. Primavera^{72a}, M. Proissl⁴⁶,

K. Prokofiev⁴⁷, F. Prokoshin^{32b}, E. Protopapadaki¹³⁷, S. Protopopescu²⁵, J. Proudfoot⁶,
 M. Przybycien^{38a}, H. Przysieszniak⁵, E. Ptacek¹¹⁵, D. Puddu^{135a,135b}, E. Pueschel⁸⁵,
 D. Puldon¹⁴⁹, M. Purohit^{25,ad}, P. Puzo¹¹⁶, J. Qian⁸⁸, G. Qin⁵³, Y. Qin⁸³, A. Quadt⁵⁴,
 D.R. Quarrie¹⁵, W.B. Quayle^{165a,165b}, M. Queitsch-Maitland⁸³, D. Quilty⁵³,
 A. Qureshi^{160b}, V. Radeka²⁵, V. Radescu⁴², S.K. Radhakrishnan¹⁴⁹, P. Radloff¹¹⁵,
 P. Rados⁸⁷, F. Ragusa^{90a,90b}, G. Rahal¹⁷⁹, S. Rajagopalan²⁵, M. Rammensee³⁰,
 A.S. Randle-Conde⁴⁰, C. Rangel-Smith¹⁶⁷, K. Rao¹⁶⁴, F. Rauscher⁹⁹, T.C. Rave⁴⁸,
 T. Ravenscroft⁵³, M. Raymond³⁰, A.L. Read¹¹⁸, N.P. Readioff⁷³, D.M. Rebuffi^{120a,120b},
 A. Redelbach¹⁷⁵, G. Redlinger²⁵, R. Reece¹³⁸, K. Reeves⁴¹, L. Rehnisch¹⁶, H. Reisin²⁷,
 M. Relich¹⁶⁴, C. Rembser³⁰, H. Ren^{33a}, Z.L. Ren¹⁵², A. Renaud¹¹⁶, M. Rescigno^{133a},
 S. Resconi^{90a}, O.L. Rezanova^{108,t}, P. Reznicek¹²⁸, R. Rezvani⁹⁴, R. Richter¹⁰⁰,
 M. Ridel⁷⁹, P. Rieck¹⁶, J. Rieger⁵⁴, M. Rijssenbeek¹⁴⁹, A. Rimoldi^{120a,120b}, L. Rinaldi^{20a},
 E. Ritsch⁶¹, I. Riu¹², F. Rizatdinova¹¹³, E. Rizvi⁷⁵, S.H. Robertson^{86,i},
 A. Robichaud-Veronneau⁸⁶, D. Robinson²⁸, J.E.M. Robinson⁸³, A. Robson⁵³,
 C. Roda^{123a,123b}, L. Rodrigues³⁰, S. Roe³⁰, O. Røhne¹¹⁸, S. Rolli¹⁶², A. Romaniouk⁹⁷,
 M. Romano^{20a,20b}, E. Romero Adam¹⁶⁸, N. Rompotis¹³⁹, M. Ronzani⁴⁸, L. Roos⁷⁹,
 E. Ros¹⁶⁸, S. Rosati^{133a}, K. Rosbach⁴⁹, M. Rose⁷⁶, P. Rose¹³⁸, P.L. Rosendahl¹⁴,
 O. Rosenthal¹⁴², V. Rossetti^{147a,147b}, E. Rossi^{103a,103b}, L.P. Rossi^{50a}, R. Rosten¹³⁹,
 M. Rotaru^{26a}, I. Roth¹⁷³, J. Rothberg¹³⁹, D. Rousseau¹¹⁶, C.R. Royon¹³⁷, A. Rozanov⁸⁴,
 Y. Rozen¹⁵³, X. Ruan^{146c}, F. Rubbo¹², I. Rubinskiy⁴², V.I. Rud⁹⁸, C. Rudolph⁴⁴,
 M.S. Rudolph¹⁵⁹, F. Rühr⁴⁸, A. Ruiz-Martinez³⁰, Z. Rurikova⁴⁸, N.A. Rusakovich⁶⁴,
 A. Ruschke⁹⁹, J.P. Rutherford⁷, N. Ruthmann⁴⁸, Y.F. Ryabov¹²², M. Rybar¹²⁸,
 G. Rybkin¹¹⁶, N.C. Ryder¹¹⁹, A.F. Saavedra¹⁵¹, S. Sacerdoti²⁷, A. Saddique³, I. Sadeh¹⁵⁴,
 H.F.W. Sadrozinski¹³⁸, R. Sadykov⁶⁴, F. Safai Tehrani^{133a}, H. Sakamoto¹⁵⁶,
 Y. Sakurai¹⁷², G. Salamanna^{135a,135b}, A. Salamon^{134a}, M. Saleem¹¹², D. Salek¹⁰⁶,
 P.H. Sales De Bruin¹³⁹, D. Salihagic¹⁰⁰, A. Salnikov¹⁴⁴, J. Salt¹⁶⁸, D. Salvatore^{37a,37b},
 F. Salvatore¹⁵⁰, A. Salvucci¹⁰⁵, A. Salzburger³⁰, D. Sampsonidis¹⁵⁵, A. Sanchez^{103a,103b},
 J. Sánchez¹⁶⁸, V. Sanchez Martinez¹⁶⁸, H. Sandaker¹⁴, R.L. Sandbach⁷⁵, H.G. Sander⁸²,
 M.P. Sanders⁹⁹, M. Sandhoff¹⁷⁶, T. Sandoval²⁸, C. Sandoval¹⁶³, R. Sandstroem¹⁰⁰,
 D.P.C. Sankey¹³⁰, A. Sansoni⁴⁷, C. Santoni³⁴, R. Santonico^{134a,134b}, H. Santos^{125a},
 I. Santoyo Castillo¹⁵⁰, K. Sapp¹²⁴, A. Saponov⁶⁴, J.G. Saraiva^{125a,125d}, B. Sarrazin²¹,
 G. Sartiso¹⁷⁶, O. Sasaki⁶⁵, Y. Sasaki¹⁵⁶, G. Sauvage^{5,*}, E. Sauvan⁵, P. Savard^{159,d},
 D.O. Savu³⁰, C. Sawyer¹¹⁹, L. Sawyer^{78,m}, D.H. Saxon⁵³, J. Saxon¹²¹, C. Sbarra^{20a},
 A. Sbrizzi³, T. Scanlon⁷⁷, D.A. Scannicchio¹⁶⁴, M. Scarcella¹⁵¹, V. Scarfone^{37a,37b},
 J. Schaarschmidt¹⁷³, P. Schacht¹⁰⁰, D. Schaefer³⁰, R. Schaefer⁴², S. Schaepe²¹,
 S. Schaetzel^{58b}, U. Schäfer⁸², A.C. Schaffer¹¹⁶, D. Schaile⁹⁹, R.D. Schamberger¹⁴⁹,
 V. Scharf^{58a}, V.A. Schegelsky¹²², D. Scheirich¹²⁸, M. Schernau¹⁶⁴, M.I. Scherzer³⁵,
 C. Schiavi^{50a,50b}, J. Schieck⁹⁹, C. Schillo⁴⁸, M. Schioppa^{37a,37b}, S. Schlenker³⁰,
 E. Schmidt⁴⁸, K. Schmieden³⁰, C. Schmitt⁸², C. Schmitt⁹⁹, S. Schmitt^{58b}, B. Schneider¹⁷,
 Y.J. Schnellbach⁷³, U. Schnoor⁴⁴, L. Schoeffel¹³⁷, A. Schoening^{58b}, B.D. Schoenrock⁸⁹,
 A.L.S. Schorlemmer⁵⁴, M. Schott⁸², D. Schouten^{160a}, J. Schovancova²⁵, S. Schramm¹⁵⁹,
 M. Schreyer¹⁷⁵, C. Schroeder⁸², N. Schuh⁸², M.J. Schultens²¹, H.-C. Schultz-Coulon^{58a},
 H. Schulz¹⁶, M. Schumacher⁴⁸, B.A. Schumm¹³⁸, Ph. Schune¹³⁷, C. Schwanenberger⁸³,

A. Schwartzman¹⁴⁴, Ph. Schwegler¹⁰⁰, Ph. Schwemling¹³⁷, R. Schwienhorst⁸⁹,
 J. Schwindling¹³⁷, T. Schwindt²¹, M. Schwoerer⁵, F.G. Sciacca¹⁷, E. Scifo¹¹⁶, G. Sciolla²³,
 W.G. Scott¹³⁰, F. Scuri^{123a,123b}, F. Scutti²¹, J. Searcy⁸⁸, G. Sedov⁴², E. Sedykh¹²²,
 S.C. Seidel¹⁰⁴, A. Seiden¹³⁸, F. Seifert¹²⁷, J.M. Seixas^{24a}, G. Sekhniaidze^{103a},
 S.J. Sekula⁴⁰, K.E. Selbach⁴⁶, D.M. Seliverstov^{122,*}, G. Sellers⁷³,
 N. Semprini-Cesari^{20a,20b}, C. Serfon³⁰, L. Serin¹¹⁶, L. Serkin⁵⁴, T. Serre⁸⁴, R. Seuster^{160a},
 H. Severini¹¹², T. Sfiligoj⁷⁴, F. Sforza¹⁰⁰, A. Sfyrila³⁰, E. Shabalina⁵⁴, M. Shamim¹¹⁵,
 L.Y. Shan^{33a}, R. Shang¹⁶⁶, J.T. Shank²², M. Shapiro¹⁵, P.B. Shatalov⁹⁶, K. Shaw^{165a,165b},
 C.Y. Shehu¹⁵⁰, P. Sherwood⁷⁷, L. Shi^{152,ae}, S. Shimizu⁶⁶, C.O. Shimmin¹⁶⁴,
 M. Shimojima¹⁰¹, M. Shiyakova⁶⁴, A. Shmeleva⁹⁵, M.J. Shochet³¹, D. Short¹¹⁹,
 S. Shrestha⁶³, E. Shulga⁹⁷, M.A. Shupe⁷, S. Shushkevich⁴², P. Sicho¹²⁶,
 O. Sidiropoulou¹⁵⁵, D. Sidorov¹¹³, A. Sidoti^{133a}, F. Siegert⁴⁴, Dj. Sijacki^{13a},
 J. Silva^{125a,125d}, Y. Silver¹⁵⁴, D. Silverstein¹⁴⁴, S.B. Silverstein^{147a}, V. Simak¹²⁷,
 O. Simard⁵, Lj. Simic^{13a}, S. Simion¹¹⁶, E. Simioni⁸², B. Simmons⁷⁷, R. Simoniello^{90a,90b},
 M. Simonyan³⁶, P. Sinervo¹⁵⁹, N.B. Sinev¹¹⁵, V. Sipica¹⁴², G. Siragusa¹⁷⁵, A. Sircar⁷⁸,
 A.N. Sisakyan^{64,*}, S.Yu. Sivoklov⁹⁸, J. Sjölin^{147a,147b}, T.B. Sjursen¹⁴, H.P. Skottowe⁵⁷,
 K.Yu. Skovpen¹⁰⁸, P. Skubic¹¹², M. Slater¹⁸, T. Slavicek¹²⁷, K. Sliwa¹⁶², V. Smakhtin¹⁷³,
 B.H. Smart⁴⁶, L. Smestad¹⁴, S.Yu. Smirnov⁹⁷, Y. Smirnov⁹⁷, L.N. Smirnova^{98,af},
 O. Smirnova⁸⁰, K.M. Smith⁵³, M. Smizanska⁷¹, K. Smolek¹²⁷, A.A. Snesarev⁹⁵,
 G. Snidero⁷⁵, S. Snyder²⁵, R. Sobie^{170,i}, F. Socher⁴⁴, A. Soffer¹⁵⁴, D.A. Soh^{152,ae},
 C.A. Solans³⁰, M. Solar¹²⁷, J. Solc¹²⁷, E.Yu. Soldatov⁹⁷, U. Soldevila¹⁶⁸,
 A.A. Solodkov¹²⁹, A. Soloshenko⁶⁴, O.V. Solovyanov¹²⁹, V. Solovyev¹²², P. Sommer⁴⁸,
 H.Y. Song^{33b}, N. Soni¹, A. Sood¹⁵, A. Sopczak¹²⁷, B. Sopko¹²⁷, V. Sopko¹²⁷, V. Sorin¹²,
 M. Sosebee⁸, R. Soualah^{165a,165c}, P. Soueid⁹⁴, A.M. Soukharev¹⁰⁸, D. South⁴²,
 S. Spagnolo^{72a,72b}, F. Spanò⁷⁶, W.R. Spearman⁵⁷, F. Spettel¹⁰⁰, R. Spighi^{20a}, G. Spigo³⁰,
 M. Spousta¹²⁸, T. Spreitzer¹⁵⁹, B. Spurlock⁸, R.D. St. Denis^{53,*}, S. Staerz⁴⁴,
 J. Stahlman¹²¹, R. Stamen^{58a}, E. Stanecka³⁹, R.W. Stanek⁶, C. Stanescu^{135a},
 M. Stanescu-Bellu⁴², M.M. Stanitzki⁴², S. Stapnes¹¹⁸, E.A. Starchenko¹²⁹, J. Stark⁵⁵,
 P. Staroba¹²⁶, P. Starovoitov⁴², R. Staszewski³⁹, P. Stavina^{145a,*}, P. Steinberg²⁵,
 B. Stelzer¹⁴³, H.J. Stelzer³⁰, O. Stelzer-Chilton^{160a}, H. Stenzel⁵², S. Stern¹⁰⁰,
 G.A. Stewart⁵³, J.A. Stillings²¹, M.C. Stockton⁸⁶, M. Stoebe⁸⁶, G. Stoicea^{26a}, P. Stolte⁵⁴,
 S. Stonjek¹⁰⁰, A.R. Stradling⁸, A. Straessner⁴⁴, M.E. Stramaglia¹⁷, J. Strandberg¹⁴⁸,
 S. Strandberg^{147a,147b}, A. Strandlie¹¹⁸, E. Strauss¹⁴⁴, M. Strauss¹¹², P. Strizeneč^{145b},
 R. Ströhmer¹⁷⁵, D.M. Strom¹¹⁵, R. Stroynowski⁴⁰, S.A. Stucci¹⁷, B. Stugu¹⁴,
 N.A. Styles⁴², D. Su¹⁴⁴, J. Su¹²⁴, R. Subramaniam⁷⁸, A. Succurro¹², Y. Sugaya¹¹⁷,
 C. Suhr¹⁰⁷, M. Suk¹²⁷, V.V. Sulin⁹⁵, S. Sultansoy^{4c}, T. Sumida⁶⁷, S. Sun⁵⁷, X. Sun^{33a},
 J.E. Sundermann⁴⁸, K. Suruliz¹⁴⁰, G. Susinno^{37a,37b}, M.R. Sutton¹⁵⁰, Y. Suzuki⁶⁵,
 M. Svatos¹²⁶, S. Swedish¹⁶⁹, M. Swiatlowski¹⁴⁴, I. Sykora^{145a}, T. Sykora¹²⁸, D. Ta⁸⁹,
 C. Taccini^{135a,135b}, K. Tackmann⁴², J. Taenzer¹⁵⁹, A. Taffard¹⁶⁴, R. Tafirot^{160a},
 N. Taiblum¹⁵⁴, H. Takai²⁵, R. Takashima⁶⁸, H. Takeda⁶⁶, T. Takeshita¹⁴¹, Y. Takubo⁶⁵,
 M. Talby⁸⁴, A.A. Talyshev^{108,t}, J.Y.C. Tam¹⁷⁵, K.G. Tan⁸⁷, J. Tanaka¹⁵⁶, R. Tanaka¹¹⁶,
 S. Tanaka¹³², S. Tanaka⁶⁵, A.J. Tanasijczuk¹⁴³, B.B. Tannenwald¹¹⁰, N. Tannoury²¹,
 S. Tapprogge⁸², S. Tarem¹⁵³, F. Tarrade²⁹, G.F. Tartarelli^{90a}, P. Tas¹²⁸, M. Tasevsky¹²⁶,

T. Tashiro⁶⁷, E. Tassi^{37a,37b}, A. Tavares Delgado^{125a,125b}, Y. Tayalati^{136d}, F.E. Taylor⁹³,
 G.N. Taylor⁸⁷, W. Taylor^{160b}, F.A. Teischinger³⁰, M. Teixeira Dias Castanheira⁷⁵,
 P. Teixeira-Dias⁷⁶, K.K. Temming⁴⁸, H. Ten Kate³⁰, P.K. Teng¹⁵², J.J. Teoh¹¹⁷,
 S. Terada⁶⁵, K. Terashi¹⁵⁶, J. Terron⁸¹, S. Terzo¹⁰⁰, M. Testa⁴⁷, R.J. Teuscher^{159,i},
 J. Therhaag²¹, T. Theveneaux-Pelzer³⁴, J.P. Thomas¹⁸, J. Thomas-Wilsker⁷⁶,
 E.N. Thompson³⁵, P.D. Thompson¹⁸, P.D. Thompson¹⁵⁹, A.S. Thompson⁵³,
 L.A. Thomsen³⁶, E. Thomson¹²¹, M. Thomson²⁸, W.M. Thong⁸⁷, R.P. Thun^{88,*},
 F. Tian³⁵, M.J. Tibbetts¹⁵, V.O. Tikhomirov^{95,ag}, Yu.A. Tikhonov^{108,t}, S. Timoshenko⁹⁷,
 E. Tiouchichine⁸⁴, P. Tipton¹⁷⁷, S. Tisserant⁸⁴, T. Todorov⁵, S. Todorova-Nova¹²⁸,
 B. Toggerson⁷, J. Tojo⁶⁹, S. Tokár^{145a}, K. Tokushuku⁶⁵, K. Tollefson⁸⁹, L. Tomlinson⁸³,
 M. Tomoto¹⁰², L. Tompkins³¹, K. Toms¹⁰⁴, N.D. Topilin⁶⁴, E. Torrence¹¹⁵, H. Torres¹⁴³,
 E. Torró Pastor¹⁶⁸, J. Toth^{84,ah}, F. Touchard⁸⁴, D.R. Tovey¹⁴⁰, H.L. Tran¹¹⁶,
 T. Trefzger¹⁷⁵, L. Tremblet³⁰, A. Tricoli³⁰, I.M. Trigger^{160a}, S. Trincaz-Duvoid⁷⁹,
 M.F. Tripiana¹², W. Trischuk¹⁵⁹, B. Trocme⁵⁵, C. Troncon^{90a}, M. Trottier-McDonald¹⁴³,
 M. Trovatelli^{135a,135b}, P. True⁸⁹, M. Trzebinski³⁹, A. Trzupek³⁹, C. Tsarouchas³⁰,
 J.C-L. Tseng¹¹⁹, P.V. Tsiarashka⁹¹, D. Tsionou¹³⁷, G. Tsipolitis¹⁰, N. Tsirintanis⁹,
 S. Tsiskaridze¹², V. Tsiskaridze⁴⁸, E.G. Tskhadadze^{51a}, I.I. Tsukerman⁹⁶, V. Tsulaia¹⁵,
 S. Tsuno⁶⁵, D. Tsybychev¹⁴⁹, A. Tudorache^{26a}, V. Tudorache^{26a}, A.N. Tuna¹²¹,
 S.A. Tuppuri^{20a,20b}, S. Turchikhin^{98,af}, D. Turecek¹²⁷, I. Turk Cakir^{4d}, R. Turra^{90a,90b},
 P.M. Tuts³⁵, A. Tykhonov⁴⁹, M. Tylmad^{147a,147b}, M. Tyndel¹³⁰, K. Uchida²¹, I. Ueda¹⁵⁶,
 R. Ueno²⁹, M. Ughetto⁸⁴, M. Ugland¹⁴, M. Uhlenbrock²¹, F. Ukegawa¹⁶¹, G. Unal³⁰,
 A. Undrus²⁵, G. Unel¹⁶⁴, F.C. Ungaro⁴⁸, Y. Unno⁶⁵, D. Urbaniec³⁵, P. Urquijo⁸⁷,
 G. Usai⁸, A. Usanova⁶¹, L. Vacavant⁸⁴, V. Vacek¹²⁷, B. Vachon⁸⁶, N. Valencic¹⁰⁶,
 S. Valentinetti^{20a,20b}, A. Valero¹⁶⁸, L. Valery³⁴, S. Valkar¹²⁸, E. Valladolid Gallego¹⁶⁸,
 S. Vallecorsa⁴⁹, J.A. Valls Ferrer¹⁶⁸, W. Van Den Wollenberg¹⁰⁶, P.C. Van Der Deijl¹⁰⁶,
 R. van der Geer¹⁰⁶, H. van der Graaf¹⁰⁶, R. Van Der Leeuw¹⁰⁶, D. van der Ster³⁰,
 N. van Eldik³⁰, P. van Gemmeren⁶, J. Van Nieuwkoop¹⁴³, I. van Vulpen¹⁰⁶,
 M.C. van Woerden³⁰, M. Vanadia^{133a,133b}, W. Vandelli³⁰, R. Vanguri¹²¹, A. Vaniachine⁶,
 P. Vankov⁴², F. Vannucci⁷⁹, G. Vardanyan¹⁷⁸, R. Vari^{133a}, E.W. Varnes⁷, T. Varol⁸⁵,
 D. Varouchas⁷⁹, A. Vartapetian⁸, K.E. Varvell¹⁵¹, F. Vazeille³⁴, T. Vazquez Schroeder⁵⁴,
 J. Veatch⁷, F. Veloso^{125a,125c}, S. Veneziano^{133a}, A. Ventura^{72a,72b}, D. Ventura⁸⁵,
 M. Venturi¹⁷⁰, N. Venturi¹⁵⁹, A. Venturini²³, V. Vercesi^{120a}, M. Verducci^{133a,133b},
 W. Verkerke¹⁰⁶, J.C. Vermeulen¹⁰⁶, A. Vest⁴⁴, M.C. Vetterli^{143,d}, O. Viazlo⁸⁰,
 I. Vichou¹⁶⁶, T. Vickey^{146c,ai}, O.E. Vickey Boeriu^{146c}, G.H.A. Viehhauser¹¹⁹, S. Viel¹⁶⁹,
 R. Vigne³⁰, M. Villa^{20a,20b}, M. Villaplana Perez^{90a,90b}, E. Vilucchi⁴⁷, M.G. Vincter²⁹,
 V.B. Vinogradov⁶⁴, J. Virzi¹⁵, I. Vivarelli¹⁵⁰, F. Vives Vaque³, S. Vlachos¹⁰,
 D. Vladoiu⁹⁹, M. Vlasak¹²⁷, A. Vogel²¹, M. Vogel^{32a}, P. Vokac¹²⁷, G. Volpi^{123a,123b},
 M. Volpi⁸⁷, H. von der Schmitt¹⁰⁰, H. von Radziewski⁴⁸, E. von Toerne²¹, V. Vorobel¹²⁸,
 K. Vorobev⁹⁷, M. Vos¹⁶⁸, R. Voss³⁰, J.H. Vosseveld⁷³, N. Vranjes¹³⁷,
 M. Vranjes Milosavljevic¹⁰⁶, V. Vrba¹²⁶, M. Vreeswijk¹⁰⁶, T. Vu Anh⁴⁸, R. Vuillermet³⁰,
 I. Vukotic³¹, Z. Vykydal¹²⁷, P. Wagner²¹, W. Wagner¹⁷⁶, H. Wahlberg⁷⁰, S. Wahrmund⁴⁴,
 J. Wakabayashi¹⁰², J. Walder⁷¹, R. Walker⁹⁹, W. Walkowiak¹⁴², R. Wall¹⁷⁷, P. Waller⁷³,
 B. Walsh¹⁷⁷, C. Wang^{152,aj}, C. Wang⁴⁵, F. Wang¹⁷⁴, H. Wang¹⁵, H. Wang⁴⁰, J. Wang⁴²,

J. Wang^{33a}, K. Wang⁸⁶, R. Wang¹⁰⁴, S.M. Wang¹⁵², T. Wang²¹, X. Wang¹⁷⁷,
C. Wanotayaroj¹¹⁵, A. Warburton⁸⁶, C.P. Ward²⁸, D.R. Wardrope⁷⁷, M. Warsinsky⁴⁸,
A. Washbrook⁴⁶, C. Wasicki⁴², P.M. Watkins¹⁸, A.T. Watson¹⁸, I.J. Watson¹⁵¹,
M.F. Watson¹⁸, G. Watts¹³⁹, S. Watts⁸³, B.M. Waugh⁷⁷, S. Webb⁸³, M.S. Weber¹⁷,
S.W. Weber¹⁷⁵, J.S. Webster³¹, A.R. Weidberg¹¹⁹, P. Weigell¹⁰⁰, B. Weinert⁶⁰,
J. Weingarten⁵⁴, C. Weiser⁴⁸, H. Weits¹⁰⁶, P.S. Wells³⁰, T. Wenaus²⁵, D. Wendland¹⁶,
Z. Weng^{152,ae}, T. Wengler³⁰, S. Wenig³⁰, N. Wermes²¹, M. Werner⁴⁸, P. Werner³⁰,
M. Wessels^{58a}, J. Wetter¹⁶², K. Whalen²⁹, A. White⁸, M.J. White¹, R. White^{32b},
S. White^{123a,123b}, D. Whiteson¹⁶⁴, D. Wicke¹⁷⁶, F.J. Wickens¹³⁰, W. Wiedenmann¹⁷⁴,
M. Wielers¹³⁰, P. Wienemann²¹, C. Wiglesworth³⁶, L.A.M. Wiik-Fuchs²¹,
P.A. Wijeratne⁷⁷, A. Wildauer¹⁰⁰, M.A. Wildt^{42,ak}, H.G. Wilkens³⁰, J.Z. Will⁹⁹,
H.H. Williams¹²¹, S. Williams²⁸, C. Willis⁸⁹, S. Willocq⁸⁵, A. Wilson⁸⁸, J.A. Wilson¹⁸,
I. Wingerter-Seez⁵, F. Winklmeier¹¹⁵, B.T. Winter²¹, M. Wittgen¹⁴⁴, T. Wittig⁴³,
J. Wittkowski⁹⁹, S.J. Wollstadt⁸², M.W. Wolter³⁹, H. Wolters^{125a,125c}, B.K. Wosiek³⁹,
J. Wotschack³⁰, M.J. Woudstra⁸³, K.W. Wozniak³⁹, M. Wright⁵³, M. Wu⁵⁵, S.L. Wu¹⁷⁴,
X. Wu⁴⁹, Y. Wu⁸⁸, E. Wulf³⁵, T.R. Wyatt⁸³, B.M. Wynne⁴⁶, S. Xella³⁶, M. Xiao¹³⁷,
D. Xu^{33a}, L. Xu^{33b,al}, B. Yabsley¹⁵¹, S. Yacoob^{146b,am}, R. Yakabe⁶⁶, M. Yamada⁶⁵,
H. Yamaguchi¹⁵⁶, Y. Yamaguchi¹¹⁷, A. Yamamoto⁶⁵, K. Yamamoto⁶³, S. Yamamoto¹⁵⁶,
T. Yamamura¹⁵⁶, T. Yamanaka¹⁵⁶, K. Yamauchi¹⁰², Y. Yamazaki⁶⁶, Z. Yan²²,
H. Yang^{33e}, H. Yang¹⁷⁴, U.K. Yang⁸³, Y. Yang¹¹⁰, S. Yanush⁹², L. Yao^{33a}, W-M. Yao¹⁵,
Y. Yasu⁶⁵, E. Yatsenko⁴², K.H. Yau Wong²¹, J. Ye⁴⁰, S. Ye²⁵, A.L. Yen⁵⁷, E. Yildirim⁴²,
M. Yilmaz^{4b}, R. Yoosoofmiya¹²⁴, K. Yorita¹⁷², R. Yoshida⁶, K. Yoshihara¹⁵⁶,
C. Young¹⁴⁴, C.J.S. Young³⁰, S. Youssef²², D.R. Yu¹⁵, J. Yu⁸, J.M. Yu⁸⁸, J. Yu¹¹³,
L. Yuan⁶⁶, A. Yurkewicz¹⁰⁷, I. Yusuf^{28,an}, B. Zabinski³⁹, R. Zaidan⁶², A.M. Zaitsev^{129,aa},
A. Zaman¹⁴⁹, S. Zambito²³, L. Zanello^{133a,133b}, D. Zanzi¹⁰⁰, C. Zeitnitz¹⁷⁶, M. Zeman¹²⁷,
A. Zemla^{38a}, K. Zengel²³, O. Zenin¹²⁹, T. Ženiš^{145a}, D. Zerwas¹¹⁶, G. Zevi della Porta⁵⁷,
D. Zhang⁸⁸, F. Zhang¹⁷⁴, H. Zhang⁸⁹, J. Zhang⁶, L. Zhang¹⁵², X. Zhang^{33d}, Z. Zhang¹¹⁶,
Z. Zhao^{33b}, A. Zhemchugov⁶⁴, J. Zhong¹¹⁹, B. Zhou⁸⁸, L. Zhou³⁵, N. Zhou¹⁶⁴,
C.G. Zhu^{33d}, H. Zhu^{33a}, J. Zhu⁸⁸, Y. Zhu^{33b}, X. Zhuang^{33a}, K. Zhukov⁹⁵, A. Zibell¹⁷⁵,
D. Zieminska⁶⁰, N.I. Zimine⁶⁴, C. Zimmermann⁸², R. Zimmermann²¹, S. Zimmermann²¹,
S. Zimmermann⁴⁸, Z. Zinonos⁵⁴, M. Ziolkowski¹⁴², G. Zobernig¹⁷⁴, A. Zoccoli^{20a,20b},
M. zur Nedden¹⁶, G. Zurzolo^{103a,103b}, V. Zutshi¹⁰⁷, L. Zwalinski³⁰.

¹ Department of Physics, University of Adelaide, Adelaide, Australia

² Physics Department, SUNY Albany, Albany NY, United States of America

³ Department of Physics, University of Alberta, Edmonton AB, Canada

⁴ (a) Department of Physics, Ankara University, Ankara; (b) Department of Physics, Gazi University, Ankara; (c) Division of Physics, TOBB University of Economics and Technology, Ankara; (d) Turkish Atomic Energy Authority, Ankara, Turkey

⁵ LAPP, CNRS/IN2P3 and Université de Savoie, Annecy-le-Vieux, France

⁶ High Energy Physics Division, Argonne National Laboratory, Argonne IL, United States of America

⁷ Department of Physics, University of Arizona, Tucson AZ, United States of America

- ⁸ Department of Physics, The University of Texas at Arlington, Arlington TX, United States of America
- ⁹ Physics Department, University of Athens, Athens, Greece
- ¹⁰ Physics Department, National Technical University of Athens, Zografou, Greece
- ¹¹ Institute of Physics, Azerbaijan Academy of Sciences, Baku, Azerbaijan
- ¹² Institut de Física d'Altes Energies and Departament de Física de la Universitat Autònoma de Barcelona, Barcelona, Spain
- ¹³ ^(a) Institute of Physics, University of Belgrade, Belgrade; ^(b) Vinca Institute of Nuclear Sciences, University of Belgrade, Belgrade, Serbia
- ¹⁴ Department for Physics and Technology, University of Bergen, Bergen, Norway
- ¹⁵ Physics Division, Lawrence Berkeley National Laboratory and University of California, Berkeley CA, United States of America
- ¹⁶ Department of Physics, Humboldt University, Berlin, Germany
- ¹⁷ Albert Einstein Center for Fundamental Physics and Laboratory for High Energy Physics, University of Bern, Bern, Switzerland
- ¹⁸ School of Physics and Astronomy, University of Birmingham, Birmingham, United Kingdom
- ¹⁹ ^(a) Department of Physics, Bogazici University, Istanbul; ^(b) Department of Physics, Dogus University, Istanbul; ^(c) Department of Physics Engineering, Gaziantep University, Gaziantep, Turkey
- ²⁰ ^(a) INFN Sezione di Bologna; ^(b) Dipartimento di Fisica e Astronomia, Università di Bologna, Bologna, Italy
- ²¹ Physikalisches Institut, University of Bonn, Bonn, Germany
- ²² Department of Physics, Boston University, Boston MA, United States of America
- ²³ Department of Physics, Brandeis University, Waltham MA, United States of America
- ²⁴ ^(a) Universidade Federal do Rio De Janeiro COPPE/EE/IF, Rio de Janeiro; ^(b) Federal University of Juiz de Fora (UFJF), Juiz de Fora; ^(c) Federal University of Sao Joao del Rei (UFSJ), Sao Joao del Rei; ^(d) Instituto de Física, Universidade de Sao Paulo, Sao Paulo, Brazil
- ²⁵ Physics Department, Brookhaven National Laboratory, Upton NY, United States of America
- ²⁶ ^(a) National Institute of Physics and Nuclear Engineering, Bucharest; ^(b) National Institute for Research and Development of Isotopic and Molecular Technologies, Physics Department, Cluj Napoca; ^(c) University Politehnica Bucharest, Bucharest; ^(d) West University in Timisoara, Timisoara, Romania
- ²⁷ Departamento de Física, Universidad de Buenos Aires, Buenos Aires, Argentina
- ²⁸ Cavendish Laboratory, University of Cambridge, Cambridge, United Kingdom
- ²⁹ Department of Physics, Carleton University, Ottawa ON, Canada
- ³⁰ CERN, Geneva, Switzerland
- ³¹ Enrico Fermi Institute, University of Chicago, Chicago IL, United States of America
- ³² ^(a) Departamento de Física, Pontificia Universidad Católica de Chile, Santiago; ^(b) Departamento de Física, Universidad Técnica Federico Santa María, Valparaíso, Chile
- ³³ ^(a) Institute of High Energy Physics, Chinese Academy of Sciences, Beijing; ^(b)

Department of Modern Physics, University of Science and Technology of China, Anhui;
(^c) Department of Physics, Nanjing University, Jiangsu; (^d) School of Physics, Shandong
University, Shandong; (^e) Physics Department, Shanghai Jiao Tong University, Shanghai,
China

³⁴ Laboratoire de Physique Corpusculaire, Clermont Université and Université Blaise
Pascal and CNRS/IN2P3, Clermont-Ferrand, France

³⁵ Nevis Laboratory, Columbia University, Irvington NY, United States of America

³⁶ Niels Bohr Institute, University of Copenhagen, Kobenhavn, Denmark

³⁷ (^a) INFN Gruppo Collegato di Cosenza, Laboratori Nazionali di Frascati; (^b)

Dipartimento di Fisica, Università della Calabria, Rende, Italy

³⁸ (^a) AGH University of Science and Technology, Faculty of Physics and Applied
Computer Science, Krakow; (^b) Marian Smoluchowski Institute of Physics, Jagiellonian
University, Krakow, Poland

³⁹ The Henryk Niewodniczanski Institute of Nuclear Physics, Polish Academy of Sciences,
Krakow, Poland

⁴⁰ Physics Department, Southern Methodist University, Dallas TX, United States of
America

⁴¹ Physics Department, University of Texas at Dallas, Richardson TX, United States of
America

⁴² DESY, Hamburg and Zeuthen, Germany

⁴³ Institut für Experimentelle Physik IV, Technische Universität Dortmund, Dortmund,
Germany

⁴⁴ Institut für Kern- und Teilchenphysik, Technische Universität Dresden, Dresden,
Germany

⁴⁵ Department of Physics, Duke University, Durham NC, United States of America

⁴⁶ SUPA - School of Physics and Astronomy, University of Edinburgh, Edinburgh, United
Kingdom

⁴⁷ INFN Laboratori Nazionali di Frascati, Frascati, Italy

⁴⁸ Fakultät für Mathematik und Physik, Albert-Ludwigs-Universität, Freiburg, Germany

⁴⁹ Section de Physique, Université de Genève, Geneva, Switzerland

⁵⁰ (^a) INFN Sezione di Genova; (^b) Dipartimento di Fisica, Università di Genova, Genova,
Italy

⁵¹ (^a) E. Andronikashvili Institute of Physics, Iv. Javakhishvili Tbilisi State University,
Tbilisi; (^b) High Energy Physics Institute, Tbilisi State University, Tbilisi, Georgia

⁵² II Physikalisches Institut, Justus-Liebig-Universität Giessen, Giessen, Germany

⁵³ SUPA - School of Physics and Astronomy, University of Glasgow, Glasgow, United
Kingdom

⁵⁴ II Physikalisches Institut, Georg-August-Universität, Göttingen, Germany

⁵⁵ Laboratoire de Physique Subatomique et de Cosmologie, Université Grenoble-Alpes,
CNRS/IN2P3, Grenoble, France

⁵⁶ Department of Physics, Hampton University, Hampton VA, United States of America

⁵⁷ Laboratory for Particle Physics and Cosmology, Harvard University, Cambridge MA,
United States of America

- ⁵⁸ (a) Kirchhoff-Institut für Physik, Ruprecht-Karls-Universität Heidelberg, Heidelberg;
(b) Physikalisches Institut, Ruprecht-Karls-Universität Heidelberg, Heidelberg; (c) ZITI
Institut für technische Informatik, Ruprecht-Karls-Universität Heidelberg, Mannheim,
Germany
- ⁵⁹ Faculty of Applied Information Science, Hiroshima Institute of Technology, Hiroshima,
Japan
- ⁶⁰ Department of Physics, Indiana University, Bloomington IN, United States of America
- ⁶¹ Institut für Astro- und Teilchenphysik, Leopold-Franzens-Universität, Innsbruck,
Austria
- ⁶² University of Iowa, Iowa City IA, United States of America
- ⁶³ Department of Physics and Astronomy, Iowa State University, Ames IA, United States
of America
- ⁶⁴ Joint Institute for Nuclear Research, JINR Dubna, Dubna, Russia
- ⁶⁵ KEK, High Energy Accelerator Research Organization, Tsukuba, Japan
- ⁶⁶ Graduate School of Science, Kobe University, Kobe, Japan
- ⁶⁷ Faculty of Science, Kyoto University, Kyoto, Japan
- ⁶⁸ Kyoto University of Education, Kyoto, Japan
- ⁶⁹ Department of Physics, Kyushu University, Fukuoka, Japan
- ⁷⁰ Instituto de Física La Plata, Universidad Nacional de La Plata and CONICET, La
Plata, Argentina
- ⁷¹ Physics Department, Lancaster University, Lancaster, United Kingdom
- ⁷² (a) INFN Sezione di Lecce; (b) Dipartimento di Matematica e Fisica, Università del
Salento, Lecce, Italy
- ⁷³ Oliver Lodge Laboratory, University of Liverpool, Liverpool, United Kingdom
- ⁷⁴ Department of Physics, Jožef Stefan Institute and University of Ljubljana, Ljubljana,
Slovenia
- ⁷⁵ School of Physics and Astronomy, Queen Mary University of London, London, United
Kingdom
- ⁷⁶ Department of Physics, Royal Holloway University of London, Surrey, United Kingdom
- ⁷⁷ Department of Physics and Astronomy, University College London, London, United
Kingdom
- ⁷⁸ Louisiana Tech University, Ruston LA, United States of America
- ⁷⁹ Laboratoire de Physique Nucléaire et de Hautes Energies, UPMC and Université
Paris-Diderot and CNRS/IN2P3, Paris, France
- ⁸⁰ Fysiska institutionen, Lunds universitet, Lund, Sweden
- ⁸¹ Departamento de Física Teórica C-15, Universidad Autónoma de Madrid, Madrid,
Spain
- ⁸² Institut für Physik, Universität Mainz, Mainz, Germany
- ⁸³ School of Physics and Astronomy, University of Manchester, Manchester, United
Kingdom
- ⁸⁴ CPPM, Aix-Marseille Université and CNRS/IN2P3, Marseille, France
- ⁸⁵ Department of Physics, University of Massachusetts, Amherst MA, United States of
America

- ⁸⁶ Department of Physics, McGill University, Montreal QC, Canada
- ⁸⁷ School of Physics, University of Melbourne, Victoria, Australia
- ⁸⁸ Department of Physics, The University of Michigan, Ann Arbor MI, United States of America
- ⁸⁹ Department of Physics and Astronomy, Michigan State University, East Lansing MI, United States of America
- ⁹⁰ ^(a) INFN Sezione di Milano; ^(b) Dipartimento di Fisica, Università di Milano, Milano, Italy
- ⁹¹ B.I. Stepanov Institute of Physics, National Academy of Sciences of Belarus, Minsk, Republic of Belarus
- ⁹² National Scientific and Educational Centre for Particle and High Energy Physics, Minsk, Republic of Belarus
- ⁹³ Department of Physics, Massachusetts Institute of Technology, Cambridge MA, United States of America
- ⁹⁴ Group of Particle Physics, University of Montreal, Montreal QC, Canada
- ⁹⁵ P.N. Lebedev Institute of Physics, Academy of Sciences, Moscow, Russia
- ⁹⁶ Institute for Theoretical and Experimental Physics (ITEP), Moscow, Russia
- ⁹⁷ Moscow Engineering and Physics Institute (MEPhI), Moscow, Russia
- ⁹⁸ D.V.Skobel'tsyn Institute of Nuclear Physics, M.V.Lomonosov Moscow State University, Moscow, Russia
- ⁹⁹ Fakultät für Physik, Ludwig-Maximilians-Universität München, München, Germany
- ¹⁰⁰ Max-Planck-Institut für Physik (Werner-Heisenberg-Institut), München, Germany
- ¹⁰¹ Nagasaki Institute of Applied Science, Nagasaki, Japan
- ¹⁰² Graduate School of Science and Kobayashi-Maskawa Institute, Nagoya University, Nagoya, Japan
- ¹⁰³ ^(a) INFN Sezione di Napoli; ^(b) Dipartimento di Fisica, Università di Napoli, Napoli, Italy
- ¹⁰⁴ Department of Physics and Astronomy, University of New Mexico, Albuquerque NM, United States of America
- ¹⁰⁵ Institute for Mathematics, Astrophysics and Particle Physics, Radboud University Nijmegen/Nikhef, Nijmegen, Netherlands
- ¹⁰⁶ Nikhef National Institute for Subatomic Physics and University of Amsterdam, Amsterdam, Netherlands
- ¹⁰⁷ Department of Physics, Northern Illinois University, DeKalb IL, United States of America
- ¹⁰⁸ Budker Institute of Nuclear Physics, SB RAS, Novosibirsk, Russia
- ¹⁰⁹ Department of Physics, New York University, New York NY, United States of America
- ¹¹⁰ Ohio State University, Columbus OH, United States of America
- ¹¹¹ Faculty of Science, Okayama University, Okayama, Japan
- ¹¹² Homer L. Dodge Department of Physics and Astronomy, University of Oklahoma, Norman OK, United States of America
- ¹¹³ Department of Physics, Oklahoma State University, Stillwater OK, United States of America

- 114 Palacký University, RCPTM, Olomouc, Czech Republic
- 115 Center for High Energy Physics, University of Oregon, Eugene OR, United States of America
- 116 LAL, Université Paris-Sud and CNRS/IN2P3, Orsay, France
- 117 Graduate School of Science, Osaka University, Osaka, Japan
- 118 Department of Physics, University of Oslo, Oslo, Norway
- 119 Department of Physics, Oxford University, Oxford, United Kingdom
- 120 ^(a) INFN Sezione di Pavia; ^(b) Dipartimento di Fisica, Università di Pavia, Pavia, Italy
- 121 Department of Physics, University of Pennsylvania, Philadelphia PA, United States of America
- 122 Petersburg Nuclear Physics Institute, Gatchina, Russia
- 123 ^(a) INFN Sezione di Pisa; ^(b) Dipartimento di Fisica E. Fermi, Università di Pisa, Pisa, Italy
- 124 Department of Physics and Astronomy, University of Pittsburgh, Pittsburgh PA, United States of America
- 125 ^(a) Laboratório de Instrumentação e Física Experimental de Partículas - LIP, Lisboa; ^(b) Faculdade de Ciências, Universidade de Lisboa, Lisboa; ^(c) Department of Physics, University of Coimbra, Coimbra; ^(d) Centro de Física Nuclear da Universidade de Lisboa, Lisboa; ^(e) Departamento de Física, Universidade do Minho, Braga; ^(f) Departamento de Física Teórica y del Cosmos and CAFPE, Universidad de Granada, Granada (Spain); ^(g) Dep Física and CEFITEC of Faculdade de Ciências e Tecnologia, Universidade Nova de Lisboa, Caparica, Portugal
- 126 Institute of Physics, Academy of Sciences of the Czech Republic, Praha, Czech Republic
- 127 Czech Technical University in Prague, Praha, Czech Republic
- 128 Faculty of Mathematics and Physics, Charles University in Prague, Praha, Czech Republic
- 129 State Research Center Institute for High Energy Physics, Protvino, Russia
- 130 Particle Physics Department, Rutherford Appleton Laboratory, Didcot, United Kingdom
- 131 Physics Department, University of Regina, Regina SK, Canada
- 132 Ritsumeikan University, Kusatsu, Shiga, Japan
- 133 ^(a) INFN Sezione di Roma; ^(b) Dipartimento di Fisica, Sapienza Università di Roma, Roma, Italy
- 134 ^(a) INFN Sezione di Roma Tor Vergata; ^(b) Dipartimento di Fisica, Università di Roma Tor Vergata, Roma, Italy
- 135 ^(a) INFN Sezione di Roma Tre; ^(b) Dipartimento di Matematica e Fisica, Università Roma Tre, Roma, Italy
- 136 ^(a) Faculté des Sciences Ain Chock, Réseau Universitaire de Physique des Hautes Energies - Université Hassan II, Casablanca; ^(b) Centre National de l'Énergie des Sciences Techniques Nucleaires, Rabat; ^(c) Faculté des Sciences Semlalia, Université Cadi Ayyad, LPHEA-Marrakech; ^(d) Faculté des Sciences, Université Mohamed Premier and LPTPM, Oujda; ^(e) Faculté des sciences, Université Mohammed V-Agdal, Rabat, Morocco

- ¹³⁷ DSM/IRFU (Institut de Recherches sur les Lois Fondamentales de l'Univers), CEA Saclay (Commissariat à l'Energie Atomique et aux Energies Alternatives), Gif-sur-Yvette, France
- ¹³⁸ Santa Cruz Institute for Particle Physics, University of California Santa Cruz, Santa Cruz CA, United States of America
- ¹³⁹ Department of Physics, University of Washington, Seattle WA, United States of America
- ¹⁴⁰ Department of Physics and Astronomy, University of Sheffield, Sheffield, United Kingdom
- ¹⁴¹ Department of Physics, Shinshu University, Nagano, Japan
- ¹⁴² Fachbereich Physik, Universität Siegen, Siegen, Germany
- ¹⁴³ Department of Physics, Simon Fraser University, Burnaby BC, Canada
- ¹⁴⁴ SLAC National Accelerator Laboratory, Stanford CA, United States of America
- ¹⁴⁵ ^(a) Faculty of Mathematics, Physics & Informatics, Comenius University, Bratislava; ^(b) Department of Subnuclear Physics, Institute of Experimental Physics of the Slovak Academy of Sciences, Kosice, Slovak Republic
- ¹⁴⁶ ^(a) Department of Physics, University of Cape Town, Cape Town; ^(b) Department of Physics, University of Johannesburg, Johannesburg; ^(c) School of Physics, University of the Witwatersrand, Johannesburg, South Africa
- ¹⁴⁷ ^(a) Department of Physics, Stockholm University; ^(b) The Oskar Klein Centre, Stockholm, Sweden
- ¹⁴⁸ Physics Department, Royal Institute of Technology, Stockholm, Sweden
- ¹⁴⁹ Departments of Physics & Astronomy and Chemistry, Stony Brook University, Stony Brook NY, United States of America
- ¹⁵⁰ Department of Physics and Astronomy, University of Sussex, Brighton, United Kingdom
- ¹⁵¹ School of Physics, University of Sydney, Sydney, Australia
- ¹⁵² Institute of Physics, Academia Sinica, Taipei, Taiwan
- ¹⁵³ Department of Physics, Technion: Israel Institute of Technology, Haifa, Israel
- ¹⁵⁴ Raymond and Beverly Sackler School of Physics and Astronomy, Tel Aviv University, Tel Aviv, Israel
- ¹⁵⁵ Department of Physics, Aristotle University of Thessaloniki, Thessaloniki, Greece
- ¹⁵⁶ International Center for Elementary Particle Physics and Department of Physics, The University of Tokyo, Tokyo, Japan
- ¹⁵⁷ Graduate School of Science and Technology, Tokyo Metropolitan University, Tokyo, Japan
- ¹⁵⁸ Department of Physics, Tokyo Institute of Technology, Tokyo, Japan
- ¹⁵⁹ Department of Physics, University of Toronto, Toronto ON, Canada
- ¹⁶⁰ ^(a) TRIUMF, Vancouver BC; ^(b) Department of Physics and Astronomy, York University, Toronto ON, Canada
- ¹⁶¹ Faculty of Pure and Applied Sciences, University of Tsukuba, Tsukuba, Japan
- ¹⁶² Department of Physics and Astronomy, Tufts University, Medford MA, United States of America

- ¹⁶³ Centro de Investigaciones, Universidad Antonio Narino, Bogota, Colombia
- ¹⁶⁴ Department of Physics and Astronomy, University of California Irvine, Irvine CA, United States of America
- ¹⁶⁵ ^(a) INFN Gruppo Collegato di Udine, Sezione di Trieste, Udine; ^(b) ICTP, Trieste; ^(c) Dipartimento di Chimica, Fisica e Ambiente, Università di Udine, Udine, Italy
- ¹⁶⁶ Department of Physics, University of Illinois, Urbana IL, United States of America
- ¹⁶⁷ Department of Physics and Astronomy, University of Uppsala, Uppsala, Sweden
- ¹⁶⁸ Instituto de Física Corpuscular (IFIC) and Departamento de Física Atómica, Molecular y Nuclear and Departamento de Ingeniería Electrónica and Instituto de Microelectrónica de Barcelona (IMB-CNM), University of Valencia and CSIC, Valencia, Spain
- ¹⁶⁹ Department of Physics, University of British Columbia, Vancouver BC, Canada
- ¹⁷⁰ Department of Physics and Astronomy, University of Victoria, Victoria BC, Canada
- ¹⁷¹ Department of Physics, University of Warwick, Coventry, United Kingdom
- ¹⁷² Waseda University, Tokyo, Japan
- ¹⁷³ Department of Particle Physics, The Weizmann Institute of Science, Rehovot, Israel
- ¹⁷⁴ Department of Physics, University of Wisconsin, Madison WI, United States of America
- ¹⁷⁵ Fakultät für Physik und Astronomie, Julius-Maximilians-Universität, Würzburg, Germany
- ¹⁷⁶ Fachbereich C Physik, Bergische Universität Wuppertal, Wuppertal, Germany
- ¹⁷⁷ Department of Physics, Yale University, New Haven CT, United States of America
- ¹⁷⁸ Yerevan Physics Institute, Yerevan, Armenia
- ¹⁷⁹ Centre de Calcul de l'Institut National de Physique Nucléaire et de Physique des Particules (IN2P3), Villeurbanne, France
- ^a Also at Department of Physics, King's College London, London, United Kingdom
- ^b Also at Institute of Physics, Azerbaijan Academy of Sciences, Baku, Azerbaijan
- ^c Also at Particle Physics Department, Rutherford Appleton Laboratory, Didcot, United Kingdom
- ^d Also at TRIUMF, Vancouver BC, Canada
- ^e Also at Department of Physics, California State University, Fresno CA, United States of America
- ^f Also at Tomsk State University, Tomsk, Russia
- ^g Also at CPPM, Aix-Marseille Université and CNRS/IN2P3, Marseille, France
- ^h Also at Università di Napoli Parthenope, Napoli, Italy
- ⁱ Also at Institute of Particle Physics (IPP), Canada
- ^j Also at Department of Physics, St. Petersburg State Polytechnical University, St. Petersburg, Russia
- ^k Also at Chinese University of Hong Kong, China
- ^l Also at Department of Financial and Management Engineering, University of the Aegean, Chios, Greece
- ^m Also at Louisiana Tech University, Ruston LA, United States of America
- ⁿ Also at Institutio Catalana de Recerca i Estudis Avancats, ICREA, Barcelona, Spain

- ^o Also at Department of Physics, The University of Texas at Austin, Austin TX, United States of America
- ^p Also at Institute of Theoretical Physics, Ilia State University, Tbilisi, Georgia
- ^q Also at CERN, Geneva, Switzerland
- ^r Also at Ochadai Academic Production, Ochanomizu University, Tokyo, Japan
- ^s Also at Manhattan College, New York NY, United States of America
- ^t Also at Novosibirsk State University, Novosibirsk, Russia
- ^u Also at Institute of Physics, Academia Sinica, Taipei, Taiwan
- ^v Also at LAL, Université Paris-Sud and CNRS/IN2P3, Orsay, France
- ^w Also at Academia Sinica Grid Computing, Institute of Physics, Academia Sinica, Taipei, Taiwan
- ^x Also at Laboratoire de Physique Nucléaire et de Hautes Energies, UPMC and Université Paris-Diderot and CNRS/IN2P3, Paris, France
- ^y Also at School of Physical Sciences, National Institute of Science Education and Research, Bhubaneswar, India
- ^z Also at Dipartimento di Fisica, Sapienza Università di Roma, Roma, Italy
- ^{aa} Also at Moscow Institute of Physics and Technology State University, Dolgoprudny, Russia
- ^{ab} Also at Section de Physique, Université de Genève, Geneva, Switzerland
- ^{ac} Also at International School for Advanced Studies (SISSA), Trieste, Italy
- ^{ad} Also at Department of Physics and Astronomy, University of South Carolina, Columbia SC, United States of America
- ^{ae} Also at School of Physics and Engineering, Sun Yat-sen University, Guangzhou, China
- ^{af} Also at Faculty of Physics, M.V.Lomonosov Moscow State University, Moscow, Russia
- ^{ag} Also at Moscow Engineering and Physics Institute (MEPhI), Moscow, Russia
- ^{ah} Also at Institute for Particle and Nuclear Physics, Wigner Research Centre for Physics, Budapest, Hungary
- ^{ai} Also at Department of Physics, Oxford University, Oxford, United Kingdom
- ^{aj} Also at Department of Physics, Nanjing University, Jiangsu, China
- ^{ak} Also at Institut für Experimentalphysik, Universität Hamburg, Hamburg, Germany
- ^{al} Also at Department of Physics, The University of Michigan, Ann Arbor MI, United States of America
- ^{am} Also at Discipline of Physics, University of KwaZulu-Natal, Durban, South Africa
- ^{an} Also at University of Malaya, Department of Physics, Kuala Lumpur, Malaysia
- * Deceased